Role of PI4Kalpha1 complex in plasma membrane identity and development in Arabidopsis thaliana

Lise Noack

Numéro National de Thèse : **2020LYSEN066**

THESE de DOCTORAT DE L'UNIVERSITE DE LYON

opérée par
l'Ecole Normale Supérieure de Lyon

Ecole Doctorale N° 340
Biologie Moléculaire, Intégrative et Cellulaire

Discipline : Sciences de la Vie et de la Santé

Soutenue publiquement le 11/12/2020, par :
Lise NOACK

Rôle du complexe AtPI4Kalpha1 dans l'établissement de l'identité de la membrane plasmique et le développement chez *Arabidopsis thaliana*

Devant le jury composé de :

SIMON PLAS, Françoise	DR INRA	INRA Dijon	Rapporteure
SCHAAF, Gabriel	Professeur	INRES Bonn	Rapporteur
BERNARD, Amelie	CR CNRS	INRA Bordeaux Aquitaine	Examinatrice
ISCHEBECK, Till	Professeur	Albrecht-von-Haller-Institute	Examinateur
HAMANT, Olivier	DR INRA	ENS de Lyon	Examinateur
JAILLAIS, Yvon	DR CNRS	ENS de Lyon	Directeur de thèse

Résumé de la thèse

Rôle du complexe AtPI4Kalpha1 dans l'établissement de l'identité de la membrane plasmique et le développement chez *Arabidopsis thaliana*

Les cellules sont composées de compartiments délimités par une membrane tel que le cytosol, le réticulum endoplasmique, l'appareil de Golgi, le noyau, les plastes, etc. Chaque compartiment a ses propres caractéristiques physicochimiques ce qui permet de nombreuses réactions chimiques dans une même cellule. Pour permettre à chaque protéine associée aux membranes d'être localisée au bon compartiment, chaque membrane a une identité qui lui ait propre. Elle se définit par ses caractéristiques physiques (courbure, électrostatique, densité lipidique) et chimiques (nature des lipides membranaires). Cependant, les compartiments d'une cellule échangent du matériel en permanence. Une question fondamentale de la biologie cellulaire est de comprendre comment l'identité des membranes est maintenue malgré le flux constant d'échanges de protéines et de lipides lors des transports vésiculaires et non-vésiculaires.

Les phosphoinositides (PIPs) sont des lipides anioniques présents en faible quantité dans les membranes. Cinq espèces de PIP existent chez les plantes. Chaque PIP est localisé dans un ou plusieurs compartiments cellulaires et sa concentration varie entre les compartiments. Parmis les PIPs, il a été montré que le PI4P est localisé à la membrane plasmique et dans des compartiments intracellulaires qui correspondent au Golgi/trans-Golgi Network (TGN). Chez les plantes, le PI4P est majoritairement trouvé à la membrane plasmique, contrairement au animaux ou aux levures chez qui le PI4P se trouve principalement au niveau du TGN. Ainsi le gradient de PI4P le long de la voie d'endocytose est inversé chez les plantes par rapport aux autres organismes eucaryotes. Chez les plantes, l'accumulation de PI4P à la membrane plasmique confère un champ électrostatique important qui à son tour recrute des protéines spécifiquement à cette membrane.

Comment le gradient de PI4P est établi et maintenu chez les plantes ?

Le génome d'Arabidopsis code pour 3 protéines capables de produire du PI4P à partir de phosphoninositol : PI4Kα1, PI4Kβ1 et PI4Kβ2. PI4Kβ1 et PI4Kβ2 sont présent au TGN. Nous avons montré que PI4Kα1 se localise à la membrane plasmique. Par ailleurs, PI4Kα1 est la sous-unité catalytique d'un complexe comprenant 3 autres sous-unités : NO POLLEN GERMINATION (NPG), EFR3OF PLANT (EFOP) et HYCCIN. L'interaction de PI4Kα1 avec les autres sous unité du complexe lui permet d'être ciblé à la membrane plasmique grâce à une ancre lipidique (palmytoylation) au niveau de la partie C-terminal de EFOP. Les orthologues de PI4Kα1, Stt4 chez la levure et PI4KIIIα chez les animaux, sont localisés à la membrane plasmique par des complexes protéiques similaires à PI4Kα1, démontrant une conservation des mécanismes de production des PIP chez les eucaryotes.

La présence de PI4Kα1 au niveau de la membrane plasmique est vitale au bon développement de la plante. En effet, l'absence ou la délocalisation de PI4Kα1 ou d'un des membres du complexe entraine une létalité de la plante au niveau du grain de pollen ou de l'embryon. De la même manière une sous expression de PI4Kα1 révèle de grave défaut de développement. Ainsi PI4Kα1 est essentiel à l'identité de la membrane plasmique et par conséquent au développement de la plante.

Abbreviations

5PTase: 5-Phosphatase
ABA: Abscisic acid
ALA: AMINOPHOSPHOLIPID FLIPPASE
ALIS: ALA interacting β-subunits
ALPS: Amphipathic lipid packing sensor
AM: Arbuscular mycorrhizal
AP: ADAPTOR PROTEIN
Arf: ADP-ribosylation factor
ARM: ARMADILLO
ATG: AuTophaGy-related Protein
ATP: Adenosine triphosphate
BAR: Bib-Amphyphisin-Rsv
BKI1: BRI1 KINASE INHIBITOR 1
CASP: CASPARIAN STRIP MEMBRANE DOMAIN PROTEIN
CCP: Clathrin-coated pit
CCV: Clathrin-coated vesicle
CLASP: CYTOPLASMIC LINKER ASSOCIATED PROTEIN
CLC2: CLATHRIN LIGHT CHAIN 2
CHC: Clathrin Heavy Chain
CMP-PA: Cytidine Monophosphoryl-Phosphatidic Acid
COW: CAN OF WORMS
CPSFL1: Chloroplast Sec14-like 1
Ct: CITRINE
CVL1: CVP2-LIKE 1
CVP2: COTYLEDON VASCULAR PATTERN 2
D6K: D6-PROTEIN KINASE
D6KL3: D6K-LIKE3
DAG: Diacylglycerol
DGK: DIACYLGLYCEROL KINASE
DGPP: Diacylglycerol pyrophosphate
DRP1: DYNAMYN RELATED PROTEIN 1
EE: Early endosomes
EFOP: EFR3 OF PLANT
EIHM: Extra invasive hyphal membrane
EPCS: ER-PM Contact Sites
ER: Endoplasmic reticulum
ESCRT: Endosomal-sorting-complex-required-for-transport
Exo70: Exocyst Complex Component 70
FAB1: FORMATION OF APLOID AND BINUCLEATE CELLS 1
FAPP1: FOUR PHOSPHATE ADAPTOR PROTEIN 1
FLS2: FLAGELIN-INSENSITIVE 2
FM4-64: N-(3-Triethylammoniumpropyl)-4-(6-(4-(Diethylamino)Phenyl)Hexatrienyl)pridiniu m dibromide
FRAP: Fluorescence recovery after photobleaching
FYVE: Fab1/YOTB/Vac1/EEA1
FYVE1/FREE1: FYVE-domain protein required for endosomal sorting 1
GAP: GTPase-activating protein
GA-TGN: Golgi-associated TGN
GDP: Guanosine diphosphate;
GEF: Guanine nucleotide exchange factor
GI-TGN: Golgi-independent TGN
Gly3P: Glycerol 3-phosphate
GPAT: Glycerol-3-phosphate acyltransferase
GTP: Guanosine triphosphate
GTPases :
HEAT: Huntingtin, elongation factor 3 (EF3), protein phosphatase 2A (PP2A), kinase TOR1
HOPS: Homotypic fusion and vacuole protein sorting
HYC: HYCCIN
INE1: INAPERTURATE POLLEN1
Ins : Inositol
IP: Immunoprecipitation
IP2 : Inositol biphosphate
IP3: Inositol triphosphate
KA1: KINASE ASSOCIATED DOMAIN 1
LBD: Lipids binding domain
LE: Late endosome
LPAAT: lyso-phosphatidic acid acyltransferase
LPP: lipid-phosphate phosphatase
Lti6b: Low temperature and salt responsive protein
MCS: Membrane Contact Site
MCTP: MULTIPLE C2 AND TRANSMEMBRANE PROTEIN
MSC: Membrane surface charge
MVB: Multi-vesicular body
NETC3: NETWORKED 3C
NLS: Nuclear
NPG: NO POLLEN GERMINATION
NPGR: NPG-related
N-WASP: Neutral Wiskott Aldrich Syndrome protein
ORP: OSBP-RELATED PROTEIN
OSBP: OXYSTEROL BINDING PROTEIN
OSH: OSBP HOMOLOGUE
P4M: SidM PI4P binding of SidM
PA: Phosphatidic acid

PAK: PA Kinase
PAM: Periarbuscular membrane
PAO: Phenylarsine oxide
PAP: Phosphatidate phosphatase
PAT: PROTEIN S-ACYL TRANSFERASE
PC: Phosphatidylcholine
PD: Plasmodesmata
PE: Phosphatidylethanolamine
PH: Pleckstrin homology
PHGAP: PH GTPase Proteins
PI: Phosphoinositol
PI(3)P: Phosphatidylinositol-(3)-phosphate
PI(4)P : Phosphatidylinositol-(4)-phosphate
PI(3,4)P2: Phosphatidylinositol-(3,4)-biphosphate
PI(4,5)P2: Phosphatidylinositol-(4,4)-biphosphate
PI(3,5)P2: Phosphatidylinositol-(3,5)-biphosphate
PI(3,4,5)P3: Phosphatidylinositol-(3,4,5)-triphosphate
PI4K: PI 4-Kinases
PIP: Phosphatidylinositol phosphate
PIP5K: PIP 5-Kinases
PIP2: Phosphatidylinositol biphosphate
PIP3: Phosphatidylinositol triphosphate
PIS: PHOSPHATIDYLINOSITOL SYNTHASE
PLC: PHOSPHOLIPASE C
PLD: PHOSPHOLIPASE D
PM: Plasma membrane
PS: Phosphatidylserine
PSS1: PHOSPHATIDYLSERINE SYNTHASE 1
PTEN: PHOPHATASE AND TENSIN Homolog
PUB13: PLANT-U-BOX 13
PX: PHOX Homology
REM: REMORIN
RHD4: ROOT HAIR DEFECTIVE MUTANT 4
RNA: Ribonucleic acid
ROP: Rho-of-Plant
SA: Salicylic Acid
SAC: SUPPRESSOR OF ACTIN
SEM: Scanning Electron Microscopy
SFH: Sec Fourteen Homologs
SH3P: SRC-HOMOLOGY3-CONTAINING-PROTEIN
SNAP: Soluble NSF attachment proteins
SNARE: SNAP Receptor
SNX1: SORTING NEXIN 1
SRI: Short Rhyzoid
SV: Secretory vesicle
SYT: SYNAPTOTAGMINE
TGN: trans-Golgi Network
TIRF: Total internal reflection fluorescence microscopy
TPR: Tetratricopeptide repeat
TTC7: TPR PROTEIN 7
UBQ10: ubiquitous promoter 10
VAN3: VASCULAR NETWORK 3
VAMP: vesicle-associated membrane protein
VAP: VAMP Associated 1328 Protein
VPS33: VACUOLAR PROTEIN SORTING 33
VTI11: Vesicle transport v-SNARE 11
WASH: WASP and SCAR Homolog

Preamble

My thesis is divided in three main parts: Introduction, Results, Discussion and Perspectives. The introduction is composed of two reviews, which have been published during my thesis. The first one is a general review on the role of anionic lipids in plants published in *Annual Review*. I wrote the manuscript and designed the figures. The second review is focus on the role of phosphoinositides in endomembrane trafficking in plant cells and is published in *Current Opinion in Plant Biology*. Yvon Jaillais and myself wrote the manuscript. Yvon Jaillais made the figures. The context of the thesis is explained before the results. The results are presented, as a manuscript is order to be submitted later on and are followed by a general discussion. Finally, I contribute to two papers that can be found in annexes. The first one is a method article written in collaboration with the team of Martin Potocky and published in *Methods in Molecular Biology* can be found in annexes. The second one is a research article published in *Developmental Cell*. My contribution to this paper was to study the role of the +ALPS motif of PI4Kbeta 1 in its localization at the *trans*-Golgi Network.

Table of Content

Part 1
INTRODUCTION

Review 1:

Noack LC, Jaillais Y. Functions of Anionic Lipids in Plants. Annu Rev Plant Biol. 2020 Apr 29;71:71-102. doi: 10.1146/annurev-arplant-081519-035910. PMID: 32442391. https://doi.org/10.1146/annurev-arplant-081519-035910

Review 2:

Noack LC, Jaillais Y. Precision targeting by phosphoinositides: how PIs direct endomembrane trafficking in plants. Curr Opin Plant Biol. 2017 Dec;40:22-33. doi: 10.1016/j.pbi.2017.06.017. Epub 2017 Jul 19. PMID: 28734137. https://doi.org/10.1016/j.pbi.2017.06.017

Part 2
RESULTS

Context of the thesis

Previously in the lab, the work of Mathilde Simon and Matthieu Platre established the membrane surface charge (MCS) as a major mechanism to recruit membrane-associated proteins at the plasma membrane. The MCS of the plasma membrane relies on anionic lipids including PI4P. Their work shows that PI4P is accumulated at the plasma membrane in plant cell, which is crucial for maintenance of MCS.

My thesis work is in continuity with these founding. We try to determine the molecular actors responsible for the accumulation of PI4P at the plasma membrane. Three PI4Kinases are known in *Arabidopsis*. Among the candidates, two PI4Kinases were already largely described: PI4Kβ1 and PI4Kβ2. These PI4Kinases localized at the trans-Golgi Network/Early Endosomes. The range of phenotype display by the *pi4kβ1β2* double mutant is rather mild. Furthermore, preliminary results from Matthieu Platre indicate that the PI4P sensor PH^{FAPP1} still labelled the plasma membrane in *pi4kβ1β2* mutant. Altogether, these data suggest that PI4Kβ1 and PI4Kβ2 alone could not trigger the accumulation of PI4P at the plasma membrane. Thus, we turned to the other candidate: PI4Kα1. The aim of my thesis was to characterize this enzyme and to determine in which extent it was responsible of the accumulation of PI4P at the plasma membrane.

Contribution:
I produced the reporter lines for the different subunits of the PI4Kα1 complex, the CrisPr lines and the artificial microRNA lines. I isolated and characterized the T-DNA mutant lines and obtained the double and triple mutants. I performed all the experiments except for the following ones. Invitrogen performed the yeast-two-hybrid screen that was financed from Marie Cécile Caillaud grant. Laia Armengot and I performed the yeast-two-hybrid assay. Frédéric Delolme and Adeline Page at the Protein Science Facility, IBCP, Lyon, made the mass spectrometry experiment. Vincent Bayle prepared and imaged the samples for the transmission electron microscopy. Frédérique Rozier performed the immunolocalization of PI4Kα1 in roots. Adiilah Mamode Cassim performed the membrane and microsome purification. Adiilah Mamode Cassim, Sebastien Mongrand and I performed the western blot on these samples. Yvon Jaillais and I conceived the study and designed the experiments. I wrote the manuscript.

AtPI4Kalpha1 belongs to a 4-subunit protein complex localized into nanodomains at the plasma membrane

Noack LC, Bayle V, Armengot L, Rozier F, Mamode-Cassim A, Caillaud MC, Mongrand S, Jaillais Y.

Abstract:

Each cell is made of different compartments with its own membrane identity that allows proper localization of proteins. Phosphoinositides participate to the acquisition of this identity through their spatiotemporal enrichment to different cell compartments. In Arabidopsis thaliana, PI4P accumulates at the plasma membrane driving its high electrostatic potential, thereby facilitating interactions with polybasic regions on proteins. So far the molecular actors responsible of the accumulation of PI4P at the plasma membrane have not been described. Here, we characterized *PI4Kα1* mutants and showed that *pi4kα1* loss-of-function leads to pollen grain lethality and distortion in the allele transmission via the female gametophyte, while its knockdown displayed strong developmental phenotypes. Using yeast two hybrid screening and mass spectrometry, we identified that PI4Kα1 is part of an heterotetrameric complex composed of NO POLLEN GERMINATION (NPG), EFR3 OF PLANTS (EFOP) and HYCCIN (HYC). The interaction between PI4Kα1 and the structural subunits of the complex is essential to target PI4Kα1 at the plasma membrane. In addition, we showed that PI4Kα1 complex is anchored in immobile and predefined subdomains of the plasma membrane. This work opens new perspectives on the role of the PI4Kα1 complex in plasma membrane suborganization.

Introduction

Eukaryotic cells are composed of several membrane-surrounded compartments. Each compartment has a unique physicochemical environment delimited by a membrane with a specific biochemical and biophysical identity. The membrane identity includes the nature of the lipids, the curvature, the electrostaticity and the density of lipids at the membrane. The identity of each membrane allows the proper localization of membrane-associated proteins.

Phosphoinositides are rare anionic lipids present in membranes. Five types of phosphoinositides exist in plants - PI3P, PI4P, PI5P, PI(4,5)P_2 and PI(3,5)P_2 - depending of the number and the position of phosphates around the inositol ring. They accumulate differently at the plasma membrane and in intracellular compartments and interact with proteins through stereo-specific or electrostatic interactions (Barbosa et al., 2016; Lemmon, 2008; Simon et al., 2016). Recent work uncovered that PI4P concentrates according to an inverted gradient by comparison to their yeast and animal counterpart (Hammond et al., 2009, 2014; Levine and Munro, 1998, 2002; Roy and Levine, 2004; Simon et al., 2016). Indeed, in yeast, the major PI4P pool is in the Golgi/trans-Golgi Network (TGN) compartments while a minor pool is present at the plasma membrane (Roy and Levine, 2004). In animal cells, the plasma membrane and the Golgi/TGN PI4P pools appear equivalent (Hammond et al., 2014). The plasma membrane pool of PI4P is produced by the PI4-Kinases (PI4K) Stt4p in yeast and its homolog PI4KIIIα in animal (Audhya and Emr, 2002; Audhya et al., 2000; Balla et al., 2005; Nakatsu et al., 2012; Roy and Levine, 2004). In yeast, the PI4K Pik1p produces the PI4P pool at the TGN (Audhya et al., 2000; Roy and Levine, 2004; Strahl et al., 2005). In yeast, *stt4* and *pik1* mutants are lethal. The two pools are necessary and at least partially independent (Roy and Levine, 2004). Indeed, the TGN pool of PI4P cannot counterbalance for the plasma membrane

pool and vice versa. In animal, three PI4K isoforms, PI4KIIIβ/PI4KIIα/PI4KIIβ, are responsible for synthetizing PI4P at the Golgi/TGN and in endosomes (Balla et al., 2002; Wang et al., 2003; Wei et al., 2002). Similar to yeast, PI4KIIIα loss-of-function mutant is embryo lethal in mammals (Nakatsu et al., 2012). In PI4KIIIα conditional mutants, the pool of PI4P disappears from the plasma membrane while the TGN structures seems to remain untouched suggesting that the two pools could be independent (Nakatsu et al., 2012).

By contrast, in plants, PI4P massively accumulates at the plasma membrane and is present in fewer amounts at the TGN (Simon et al., 2014, 2016; Vermeer et al., 2009). This PI4P accumulation at the cell surface drives the plasma membrane electrostatic field, which in turn recruits a host of signalling proteins to this compartment (Barbosa et al., 2016; Platre et al., 2018; Simon et al., 2016). Moreover the plant TGN is the place of vesicular secretion but is also involved in endocytic sorting and recycling, which might imply regulatory mechanisms of lipid exchanges or membrane identity maintenance between the plasma membrane and the TGN.

The Arabidopsis genome encodes for four PI4-kinases: PI4Kα1, PI4Kα2, PI4Kβ1 and PI4Kβ2 (Szumlanski and Nielsen, 2010). PI4Kβ1 and PI4Kβ2 have first been described to localize to the Trans-Golgi Network/Early Endosomes (TGN/EE) in pollen tube (Preuss et al., 2006). This localization has been later on validated by electron tomography and confocal microscopy in root cells (Kang et al., 2011; Lin et al., 2019). *pi4kβ1β2* double mutant displays mild growth phenotype including tip growth phenotype with bulged root hairs and cell plate defects which suggest defective secretory pathway (Antignani et al., 2015; Delage et al., 2012; Kang et al., 2011; Lin et al., 2019; Preuss et al., 2006; Šašek et al., 2014). In addition, *pi4kβ1β2* present fewer and misshaped secretory vesicles in the TGN (Kang et al., 2011). If the role of PI4Kβ1 and

PI4Kβ2 at the TGN is still not fully understood, it appears clear that a functional characterization of PI4Kα1 and PI4Kα2 is needed to progress in our understanding of PI4P distribution in the cells and how PI4P is impacting vesicular trafficking between the TGN and the plasma membrane. Due to the absence of sequence corresponding to PI4Kα2 in Expressed sequence tags libraries PI4Kα2 is considered as a pseudogene (Mueller-Roeber and Pical, 2002). Very little work has been done on PI4Kα1. The catalytic activity of PI4Kα1 has been characterized *in vitro* (Stevenson-Paulik et al., 2003). Besides, PI4Kα1 is inhibiting chloroplast division (Okazaki et al., 2015). Furthermore, it is required for the accumulation of PI4P in chloroplasts, suggesting that indeed it is able to produce PI4P *in vivo* (Okazaki et al., 2015). PI4Kα1 was suggested to localize at the plasma membrane (Okazaki et al., 2015). Thus, it is a prime candidate for producing PI4P at the plasma membrane.

Here, we show that *pi4kα1* loss-of-function leads to full male sterility. Mutant pollen grains collapse and display an abnormal cell wall. We uncovered that PI4Kα1 belongs to a 4-subunit complex. Knockout of any subunits mimics *pi4kα1* pollen lethality. In addition, *PI4Kα1* knock down gives rise to dwarf plants exhibiting pleiotropic phenotype. Using fluorescent protein tagging, immunolocalization and subcellular fractionation, we confirmed the presence of PI4Kα1 complex at the plasma membrane. Moreover, we established that the 4 subunits of the complex are essential for *PI4Kα1* function. By using mutant variants and chimeric constructs, we show that the function of this complex is to target PI4Kα1 to the plasma membrane via lipid anchors. Furthermore, we observed that this heterotetrameric complex is not homogenously present on the plasma membrane but is enriched in nanodomains. Although all the subunits of the complex are peripheral proteins and lack a transmembrane domain, they show very little lateral mobility at the plasma membrane. These results suggest that

PI4P is not produced homogeneously at the plasma membrane but rather in distinct hotspots at the cell surface. Thus, the targeting of this lipid kinase by a multiprotein scaffold allows its precise spatiotemporal recruitment in order to maintain the proper electrostatic landscape of plant cell membranes or might reflect a specific function of PI4P at the plasma membrane independent of the maintenance of the electrostatic field.

Results

pi4kα1 mutants are pollen lethal

In order to study the function of *PI4Kα1*, we characterized two T-DNA alleles. The first allele (*pi4kα1-1; GK*_502D11) presented an insertion in the first exon, while the second insertion (*pi4kα1-2;* FLAG_275H12) was located in the 20th intron **(Figure 1, A)**. T-DNAs of the first and second allele possess a sulfadiazine and glufosinate resistant gene, respectively. We failed to obtain homozygous plants for both alleles. The segregations obtained after self-fertilization of heterozygous plants were 38% of sulfadiazine resistant seedlings for *pi4kα1-1* and 9% of glufosinate resistant seedlings for *pi4kα1-2* **(Table 1)**. Because there were less than 50% of resistant plants in the progeny of self-fertilized *pi4kα1* alleles, these segregations indicated likely gametophyte lethality, which might explain the absence of homozygous *pi4kα1* mutant. To address whether *pi4kα1* could be female and/or male gametophyte lethal, we performed reciprocal crosses, using *pi4kα1+/-* and wild-type as either male or female. For both alleles, we recovered 0% resistant plants when *pi4kα1+/-* was used as the male indicating no transmission of the mutation via the pollen and thus complete male sterility **(Table 2)**. When *pi4kα1*+/- was used as female, we obtained 39% and 9% of resistant plants for each allele **(Table 2)**. This result shows that the *pi4kα1* mutation did not fully impaired the transmission

through the female gametophyte but led to a partial distortion of the segregation. Ovules were cleared but did not reveal major defects in their development **(data not shown)**.

We hypothesized that the genetic background could explain the difference of segregation rate observed between the two alleles. Indeed, *pi4kα1-1* is in Col0 background while the second allele is in WS background. However, six backcrosses of *pi4kα1-2* in Col0 did not change the segregation distortion of this allele **(Table 2)**. The position of the insertion might explain this difference. Indeed, the T-DNA insertion in *pi4kα1-2* is far from the start codon **(Figure 1, A)**. It is possible that transcription occurs on the beginning of the gene sequence leading to a truncated mRNA and a truncated protein without a functional kinase domain. Such protein could act as a dominant negative notably in the female gametophyte, explaining the stronger phenotype.

At this stage, we could not experimentally determine the cause that lead to stronger female gametophyte lethality in *pi4kα1-2* compared to *pi4kα1-1*. We thus decided to focus on the male sterility phenotype, which is shared by both alleles and we used the *pi4kα1-1* allele, since the position of the insertion was more likely to lead to true knockout.

		Seggregation				
Gene	**Allele**	**Cross**		**% of resistant plants**	**% expected**	**n**
		Female	**Male**			
PI4Kα1	*pi4kα1-1*	*pi4kα1-1 +/-*	*pi4kα1-1 +/-*	38,2	75	418
	pi4kα1-2	*pi4kα1-2 +/-*	*pi4kα1-2 +/-*	9,4	75	359
NPG1	*npg1-1*	*npg1-1 +/-*	*npg1-1 +/-*	50,3	75	296
	npg1-2	*npg1-2 +/-*	*npg1-2 +/-*	32	75	504
HYC1	*hyc1*	*hyc1 +/-*	*hyc1 +/-*	38,2	75	128
HYC2	*hyc2-2*	*hyc2-2 +/-*	*hyc2-2 +/-*	59,9	75	133
	hyc2-3	*NO RESISTANCE*				

Table 1.

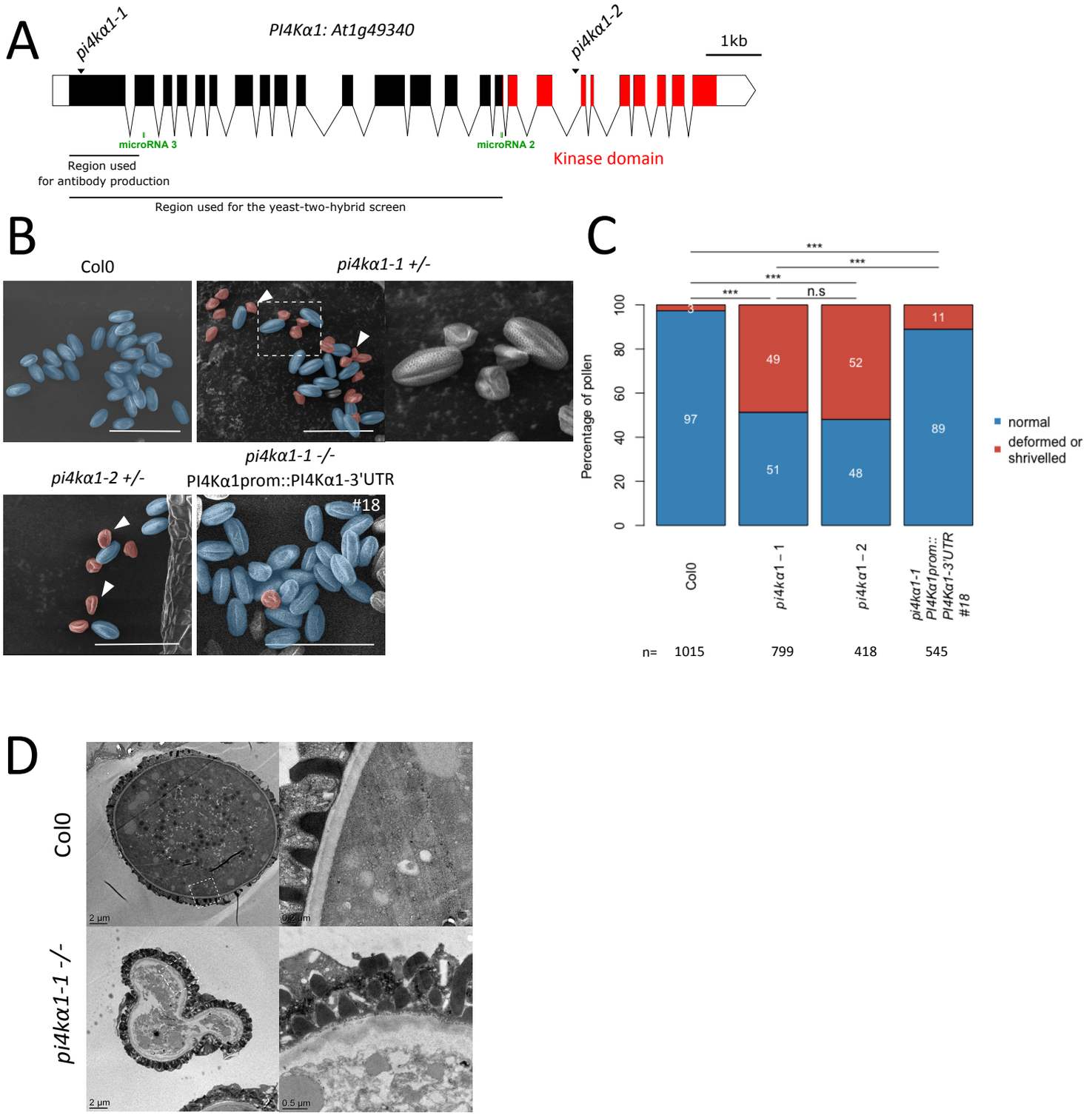

Figure 1. (A) Schematic representation of *PI4Kα1* (*At1g49340*) gene. Boxes and lines represent exons and introns, respectively. The sequence corresponding to the kinase domain is shown in red. The T-DNA positions of the alleles *pi4kα1-1* and *pi4kα1-2* are indicated. The sequence targeted by the artificial microRNA 2 and 3 are indicated in green. The parts of the protein used for the yeast-two-hybrid screen and for antibody production are also shown. **(B)** Scanning electron microscope micrograph of pollen grains from Col0, self-fertilized *pi4kα1-1* heterozygous plants, self-fertilized *pi4kα1-2* heterozygous plants, and self-fertilized *pi4kα1-1* homozygous plants expressing *PI4Kα1prom::PI4Kα1-3'UTR* (insertion n°18). Shrivelled pollen grains are coloured in red and normal pollen grains are coloured in blue. A close-up is shown for *pi4kα1-1* pollen on the right. Scale bar: 50µm **(C)** Quantification of the % of normal (in blue) versus deformed/shrivelled (in red) pollen grains from Col0, self-fertilized *pi4kα1-1* heterozygous plants, self-fertilized *pi4kα1-2* heterozygous plants, and self-fertilized *pi4kα1-1* homozygous plants expressing *PI4Kα1prom::PI4Kα1-3'UTR* (insertion n°18). n indicates the number of pollens counted for each genotype. Statistics used chi-square test. n.s, non-significant; ***, p<0.001. **(D)** Observation of Col0 and *pi4kα1-1* shrivelled pollen grains by transmission electronic microscopy. The right panel shows a close–up of the region indicated on the left panel.

Reciprocal Crosses						
Gene	Allele	Cross		% of resistant plants	% expected	n
		Female	Male			
PI4Kα1	*pi4kα1-1*	*pi4kα1-1 +/-*	Col0	39	50	424
		Col0	*pi4kα1-1 +/-*	0	50	268
	pi4kα1-2	*pi4kα1-2 +/-*	Col0	9,3	50	106
		Col0	*pi4kα1-2 +/-*	0	50	293
NPG1	*npg1-1*	*npg1-1 +/-*	Col0	40,6	50	214
		Col0	*npg1-1 +/-*	0	50	163
	npg1-2	*npg1-2 +/-*	Col0	30,8	50	26
		Col0	*npg1-2 +/-*	0	50	111
HYC1	*hyc1*	*hyc1 +/-*	Col0	47	50	185
		Col0	*hyc1 +/-*	0	50	58
HYC2	*hyc2-2*	*hyc2-2 +/-*	Col0	29,6	50	54
		Col0	*hyc2-2 +/-*	29,8	50	47
	hyc2-3	*NO RESISTANCE*				
EFOP3 EFOP4	*efop3-1 efop4-2*	*efop3-1 +/- efop4-2-/-*	Col0	55,7	50	97
		Col0	*efop3-1 +/- efop4-2-/-*	2,2	50	45
	efop3-2 efop4-2	*efop3-2 +/- efop4-2-/-*	Col0	32,4	50	68
		Col0	*efop3-2 +/- efop4-2-/-*	0	50	31
	efop3-1 efop4-4	*efop3-1 +/- efop4-4-/-*	Col0	48,1	50	27
		Col0	*efop3-1 +/- efop4-4-/-*	ND	50	ND
	efop3-2 efop4-4	*efop3-2 +/- efop4-4-/-*	Col0	50	50	12
		Col0	*efop3-2 +/- efop4-4-/-*	0	50	6

Table 2.

Next, we observed *pi4kα1* pollen grains using scanning electron microscopy (SEM) to test whether they showed morphological defects **(Figure 1, B)**. For both alleles, half of the pollen grains were shrivelled and likely not able to germinate, explaining the pollen lethality **(Figure 1, B and C)**. However, using alexander staining, we observe that the *pi4kα1-1* pollens were still alive **(Supplemental 1, B).** DAPI staining also revealed the

presence of the vegetative nucleus and the two sperm cell nuclei indicating that meiosis likely occurred normally **(Supplemental 1, C)**. Further analysis by transmission electron microscopy showed that the *pi4kα1-1* pollen grains displayed an abnormally thick cell wall **(Figure 1, D)**. Using calcofluor staining, we identified shrivelled pollen grains with abnormal accumulation of callose **(Supplemental 1, D)**. However, it was not the case of all shrivelled pollen grains, as others seem to have a normal callose deposition.

The reintroduction of a copy of *PI4Kα1* under the control of its own promoter in *pi4kα1-1* background fully complemented the *pi4kα1-1* lethality as shown by the possibility to obtain homozygous mutant plants **(**three independent complemented lines, see **Supplemental 1, A)**. In addition, self-fertilized *pi4kα1-1-/-; PI4Kα1prom::PI4Kα1* plants showed a low number of shrivelled pollen grains, comparable to control plants, indicating that a wild-type copy of *PI4Kα1* is required for transmission through the male gametophyte and normal pollen morphology **(Figure 1, B and C)**. Together, these results show that *PI4Kα1* is an essential gene for pollen development.

PI4Kα1 interacts with NO POLLEN GERMINATION proteins

To better understand the phenotype observed for *pi4kα1* knockout plants, we screened for PI4Kα1 protein partners. We performed a yeast-two-hybrid screen with the N-terminal part of PI4Kα1 (1-1468 aa). We recovered 267 in frame clones, which corresponded to 48 different proteins. Among them, the screen revealed interactions between PI4Kα1 and the three members of a proteins family called NO POLLEN GERMINATION (NPG): NPG1, NPG-Related 1 (NPGR1) and NPGR2. In the screen, we retrieved 39 clones (7 independent clones) for NPG1, 32 clones (6 independent clones) for NPGR1 and 2 clones (1 independent clone) for NPGR2. The clones from the NPG

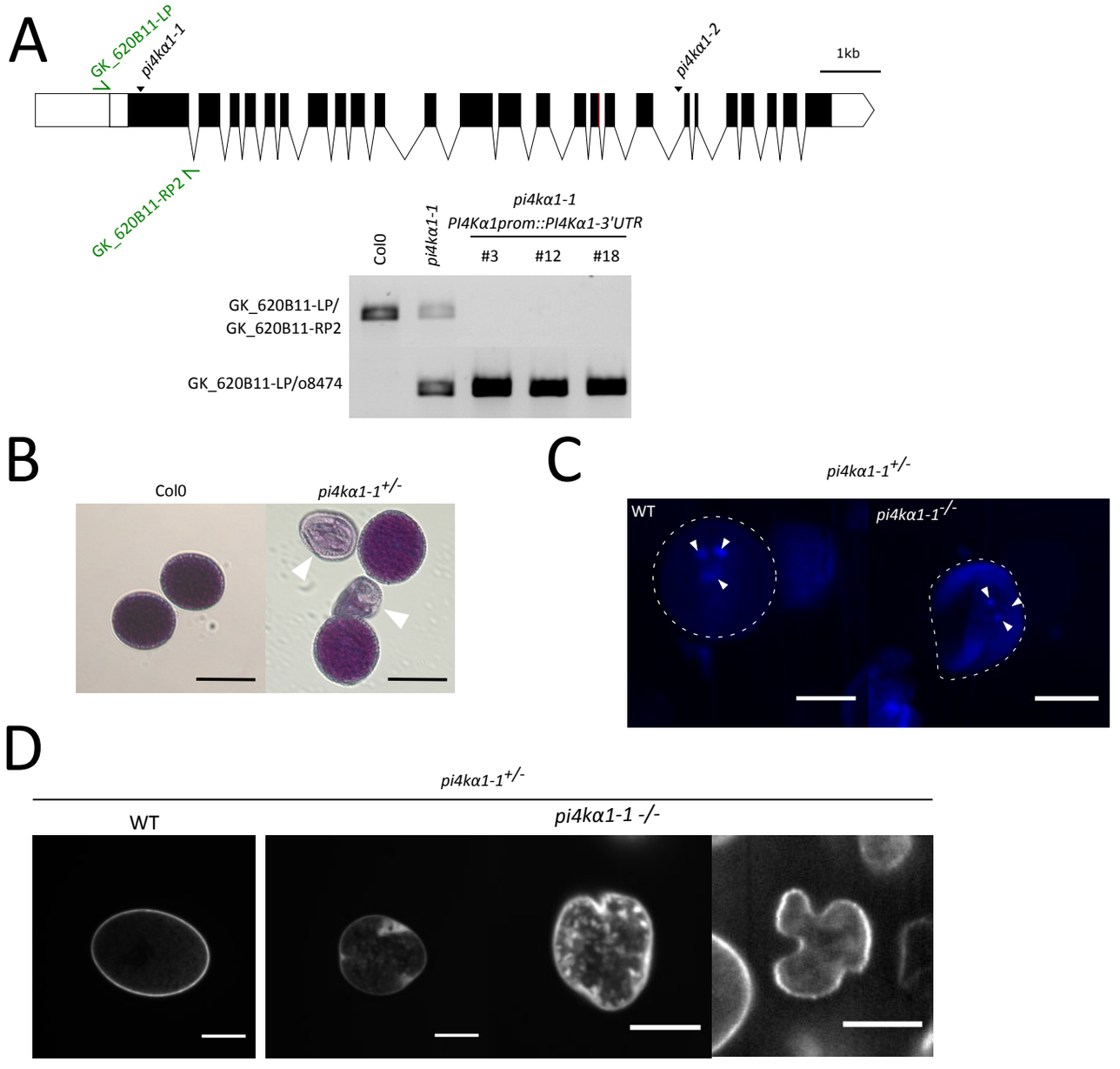

Supplemental 1. (A) Genotyping of Col0, *pi4kα1-1* heterozygous plants, and *pi4kα1-1* homozygous plants expressing *PI4Kα1prom::PI4Kα1-3'UTR* (insertion n°3, 12 and 18). The upper panel show the amplification of the gene sequence. The lower panel shows the amplification of the T-DNA border. **(B)** Alexander staining of pollen grains from Col0 and self-fertilized *pi4kα1-1* heterozygous plants. Shrivelled pollen grains are indicated with white arrowheads. Scale bars: 20µm. **(C)** DAPI staining of pollen grains from self-fertilized *pi4kα1-1* heterozygous plants with normal (WT, left) and shrivelled (*pi4kα1-1 -/-*, right) shape. Nuclei are indicated with white arrowheads. Scale bars: 10µm. **(D)** Calcofluor staining of *pi4kα1-1* normal (WT, left) and shrivelled (*pi4kα1-1 -/-*, right) pollen grains. Scale bar: 10µm.

family corresponded to about 30% of the total clone obtained from the screen, suggesting that they were over-represented.

NPG proteins contain tetratricopeptide repeats (TPR) motifs that are protein-protein interaction motifs. In the yeast-two-hybrid screen, the selected interaction domain identified for NPG1, NPGR1 and NPGR2 correspond to the C-terminal part of the proteins (aa 444-704 for NPG1; 501-694 for NPGR1 and 414-739 for NPGR2). This is also the part of the sequence that contains the highest density of TPR motifs suggesting that the interaction between PI4Kα1 and NPGs could be mediated by the C-terminal TPR motifs.

Because all three members of the NPG family interacted with PI4Kα1 in yeast-two hybrids, and given their high degree of identity and similar architecture, we decided to focus on one member of the family to confirm the interaction *in planta*. We guided this choice based on the RNAseq expression data compiled on eFP browser (https://bar.utoronto.ca/efp/cgi-bin/efpWeb.cgi). We chose NPGR2, as it is the family member with the highest and more widespread expression. Indeed, NPG1 was predicted to be specifically expressed in the pollen, while NPGR1 expression matched that of NPGR2 but was predicted to be much weaker.

To confirm the interaction between NPGR2 and PI4Kα1, we produced stable transgenic lines expressing *UBQ10::NPGR2-mCITRINE*. We raised antibodies against the native PI4Kα1 (residues 1 to 344 of PI4Kα1). In western blot the antibody recognize PI4Kα1 around the expected size (225kDa) and the tagged version of PI4Kα1 with mCITRINE and 2xmCHERRY slightly higher **(Supplemental 2, A)**. We immunoprecipitated NPGR2-mCITRINE or the plasma membrane protein Lti6B-CITRINE as control using anti-GFP antibodies and probed whether it could co-immunoprecipitate PI4Kα1, using our native antibody. We efficiently immunoprecipitated NPGR2-mCITRINE or Lti6b-GFP, but

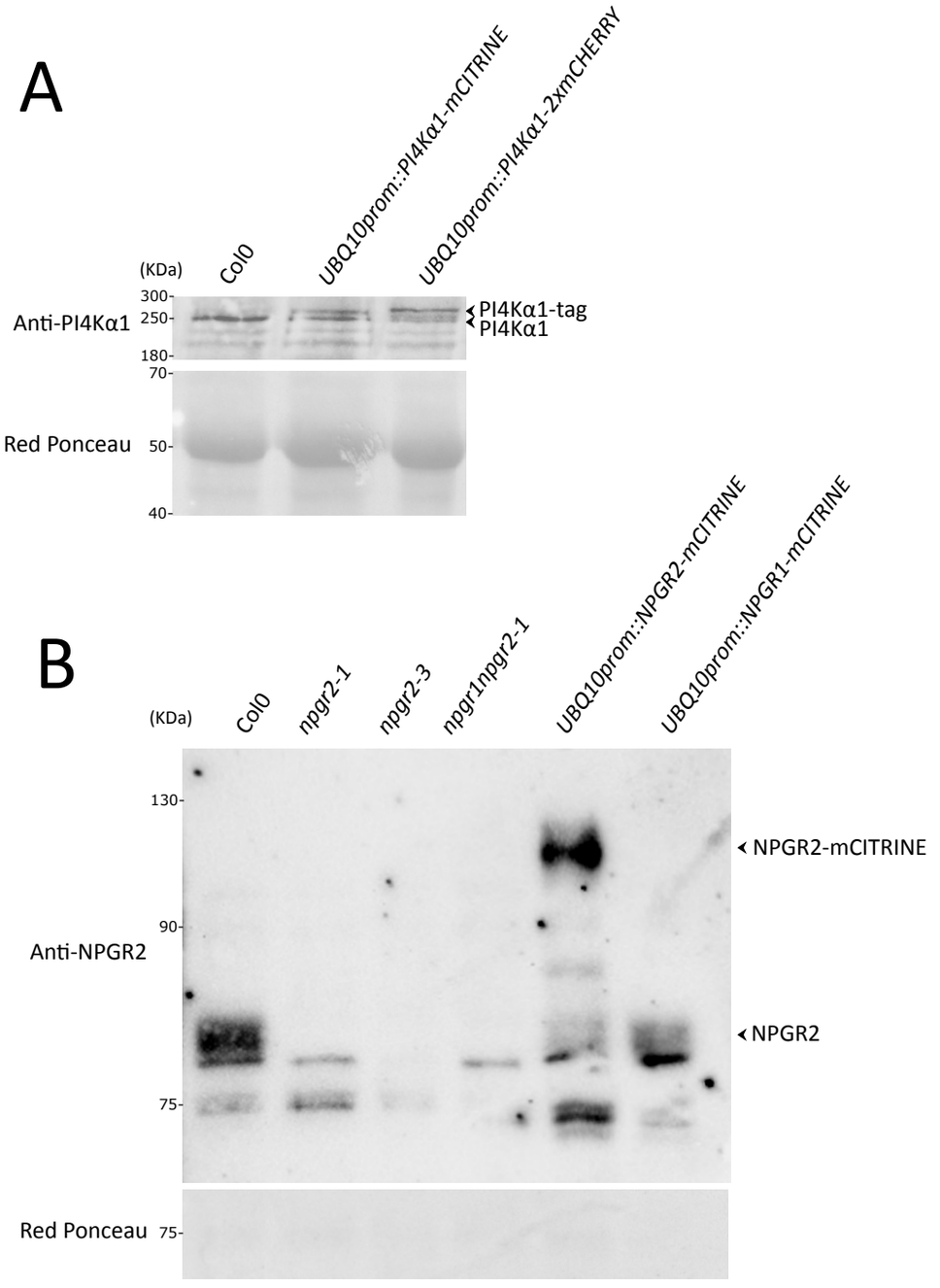

Supplemental 2. (A) Western blot anti-PI4Kα1 on total proteins extract of Col0 seedlings, seedling expressing *UBQ10prom::PI4Kα1-mCITRINE* and seedling expressing *UBQ10prom::PI4Kα1-2xmCHERRY*. Red ponceau shows similar protein loading in every well. **(B)** Western blot anti-NPGR2 on total proteins extract of Col0, *npgr2-1*, *npgr2-3, npgr1npgr2-1* seedlings, seedling expressing *UBQ10prom::NPGR2-mCITRINE* and seedling expressing *UBQ10prom::NPGR1-mCITRINE*. Red ponceau shows similar protein loading in every well.

PI4Kα1 was only co-immunoprecipitated with NPGR2-mCITRINE **(Figure 2, A)**. Together, these experiments suggest that PI4Kα1 can interact in yeast with the C-terminus of all the three members of the NPG family and is at least found in complex with NPGR2 *in planta*.

NPG proteins interact with HYCCIN proteins

Next, we asked whether the PI4Kα1 complex could include additional subunits. To this end, we used the lines expressing mCITRINE-PI4Kα1 and NPGR2-mCITRINE to perform immunoprecipitation (IP) followed by mass spectrometry analyses. Two lines expressing myristoylation-2xmCITRINE and mCITRINE-NES-mCITRINE were also used as controls for plasma membrane and cytosolic protein, respectively. In the NPGR2 IP, we found PI4Kα1, further confirming that these two proteins are present in the same complex in plants. Only one common protein was found in both NPGR2 and PI4Kα1 IPs but excluded from the two controls **(Figure 2, B)**. This protein is encoded by the *At5g64090* locus and contains an HYCCIN domain. The genome of *Arabidopsis* encodes for only two proteins with an HYCCIN domain, which we called HYCCIN1 (HYC1, *At5g21050*) and HYCCIN2 (HYC2, *At5g64090*).

HYC2 is broadly expressed, while *HYC1* expression is restricted to pollen according to eFP browser data set. Thus, we chose to confirm whether HYC2 is present in the PI4Kα1/NPGR2 sporophytic complex. To this end, we raised a *UBQ10::HYC2-mCITRINE* expressing lines and successfully isolated antibodies raised against NPGR2 (residues 1 to 273 of NPGR2). The expected size of NPGR2 is 82kDa. The antibody recognized a band between 75kDa and 90kDa that is not present in *npgr2-1* or *npgr2-3* knock out mutants or *npgr1npr2-1* double mutant **(Supplemental 2, B)**. Moreover, the antibody recognized NPGR2-mCITRINE around 110kDa but did not recognize NPGR1-mCITRINE indicating

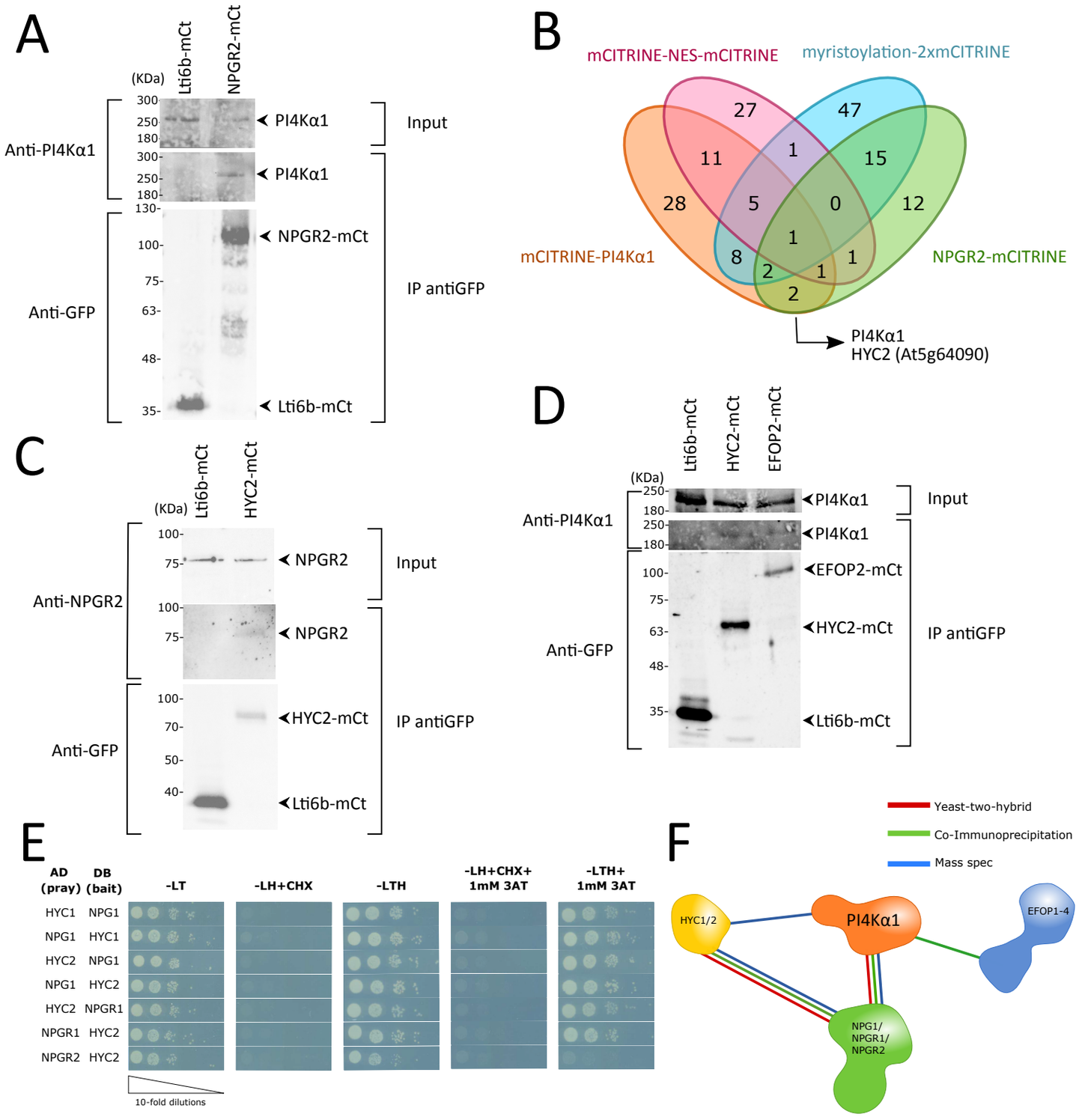

Figure 2. (A) Co-immunoprecipitation of PI4Kα1 with NPGR2. *Arabidopsis* transgenic plants overexpressing NPGR2-mCITRINE (NPGR2-mCt) or Lti6b-mCITRINE (Lti6b-mCt) were used for immunoprecipitation using anti-GFP beads. The immunoblots used anti-PI4Kα1 (upper panel) and anti-GFP (lower panel). **(B)** Venn diagram of the proteins identified by mass spectrometry from immunoprecipitation of mCITRINE-PI4Kα1, NPGR2-mCITRINE, mCITRINE-NES-mCITRINE and myristoylation-2x-mCITRINE. **(C)** Co-immunoprecipitation of NPGR2 with HYC2. *Arabidopsis* transgenic plants overexpressing HYC2-mCITRINE (HYC2-mCt) or Lti6b-mCITRINE were used for immunoprecipitation using anti-GFP beads. The immunoblots used anti-GFP (lower panel) and anti-NPGR2 (upper panel). **(D)** Co-immunoprecipitation of PI4Kα1 with EFOP2 and HYC2. *Arabidopsis* transgenic plants overexpressing EFOP2-mCITRINE (EFOP2-mCt), HYC2-mCITRINE or Lti6b-mCITRINE were used for immunoprecipitation using anti-GFP beads. The immunoblots used anti-PI4Kα1 (upper panel) and anti-GFP (lower panel). **(E)** Yeast-two hybrid assay of HYC1 with NPG1; and HYC2 with NPG1, NPGR1 and NPGR2. The indicated combinations of interactions between HYCCIN and NPG proteins were assessed by growth on plates with yeast growth media lacking Leu, Trp, and His (-LTH). Yeast growth on plates lacking Leu and Trp (-LT) shows the presence of the bait and prey vectors. The absence of growth when cycloheximide was added (+CHX) shows the absence of auto-activation of the DB vectors. The addition of 3-Amino-1,2,4-Triazol (+3AT) shows the strength of the interaction. **(F)** Summary of the experiments showing interactions between PI4Kα1, NPG, HYC and EFOP2 proteins.

that the antibody is specific of NPGR2 **(Supplemental 2, B)**. We found that NPGR2 co-immunoprecipitated with HYC2-mCITRINE, while the Lti6b-mCITRINE did not **(Figure 2, C)**. Similarly, PI4Kα1 also co-immunoprecipitated with HYC2-mCITRINE but not with Lti6b-mCITRINE **(Figure 2, D)**. Next, we used yeast-two hybrids to check whether the two HYCCIN family members may directly interact with PI4Kα1/NPGs **(Figure 2, E)**. We found that the two isoforms that are pollen specific, HYC1 and NPG1 interacted in yeast. Likewise, HYC2 interacted with NPG1, NPGR1 and NPGR2 in yeast. Together, our results indicate that HYCCIN family members likely directly interact with NPG proteins, and that HYC2 is present in complex with PI4Kα1/NPGR2 in the *Arabidopsis* sporophyte, while HYC1/NPG1/PI4Kα1 could form a similar complex in the male gametophyte.

EFOPs proteins are part of the PI4Kα1-NPG-HYC complex

HYC domain containing proteins are also found in metazoan. In human cells, one of the members of the HYCCIN family, FAM126, has been shown to be part of a complex containing PI4KIIIα (Baskin et al., 2016; Dornan et al., 2018). FAM126 directly interacts with a protein called TETRATRICOPEPTIDE REPEAT PROTEIN 7 (TTC7), which bridges PI4KIIIα, FAM126 and a third protein called EFR3 (Baskin et al., 2016; Dornan et al., 2018; Lees et al., 2017; Wu et al., 2014). While no HYCCIN containing protein are found in yeast, the plasma membrane PI4-Kinase, Stt4 is also anchored to the plasma membrane by a complex containing Ypp1, which like NPG1 contains TPR motives, and Efr3 (Baird et al., 2008; Nakatsu et al., 2012; Wu et al., 2014).

Based on these information, we hypothesized that NPGs and HYCs in plants could be functional homologs of TTC7/Ypp1 and FAM126 in *Arabidopsis*, respectively. We thus wondered whether EFR3 homologs could exist in *Arabidopsis* using blast and sequence alignments. We found four potential candidates that we named EFR3 OF PLANT

(EFOPs): EFOP1 (*At5g21080*), EFOP2 (*At2g41830*), EFOP3 (*At1g05960*) and EFOP4 (*At5g26850*).

Yeast Efr3p is a rod-shaped protein made of ARMADILLO- (ARM) and HEAT-like repeats. ARM and HEAT repeats are difficult to distinguished bioinformaticaly, but all four EFOP proteins belongs to the ARM repeat super family, which includes both ARM and HEAT repeat containing proteins (Wu et al., 2014). In *marchantia polymorpha*, both *MpPI4Kα1* (the homolog of *PI4Kα1)* and *MpSRI4* the homolog of *EFOP2* display short rhizoids, suggesting that they could act in the same pathway and/or protein complex (Honkanen et al., 2016). In addition, based on RNAseq data, EFOP2 have a rather large pattern of expression. Thus, we decided to concentrate on EFOP2 to test whether it is indeed present in the sporophytic PI4Kα1/NPGR2/HYC2 complex. To this end, we raised *UBQ10prom::EFOP2-mCITRINE* transgenic lines and immoprecipitated EFOP2-mCITRINE and Lti6b-mCITRINE using an anti-GFP antibody. We found that PI4Kα1 co-immunoprecipitated with EFOP2-mCITRINE while it did not with Lti6b-mCITRINE **(Figure 2, D)**, suggesting that EFOP2 may belong to the PI4Kα1/NPGR2/HYC2 complex. The summary of these interactions suggests that PI4Kα1 is part of an heterotetrameric complex in which NPG proteins act as a scaffold that bridges EFOP, HYC and PI4Kα1 proteins together **(Figure 2, F)**.

Disturbing subunits of PI4Kα1 complex mimics pi4kα1 pollen phenotypes

Next, we took a genetic approach to confirm whether NPG, HYC and EFOP family members indeed may function together with PI4Kα1 during gametophyte development. To this end, we isolated single mutants for all the genes encoding for a subunit of the PI4Kα1 complex **(Table 3)**.

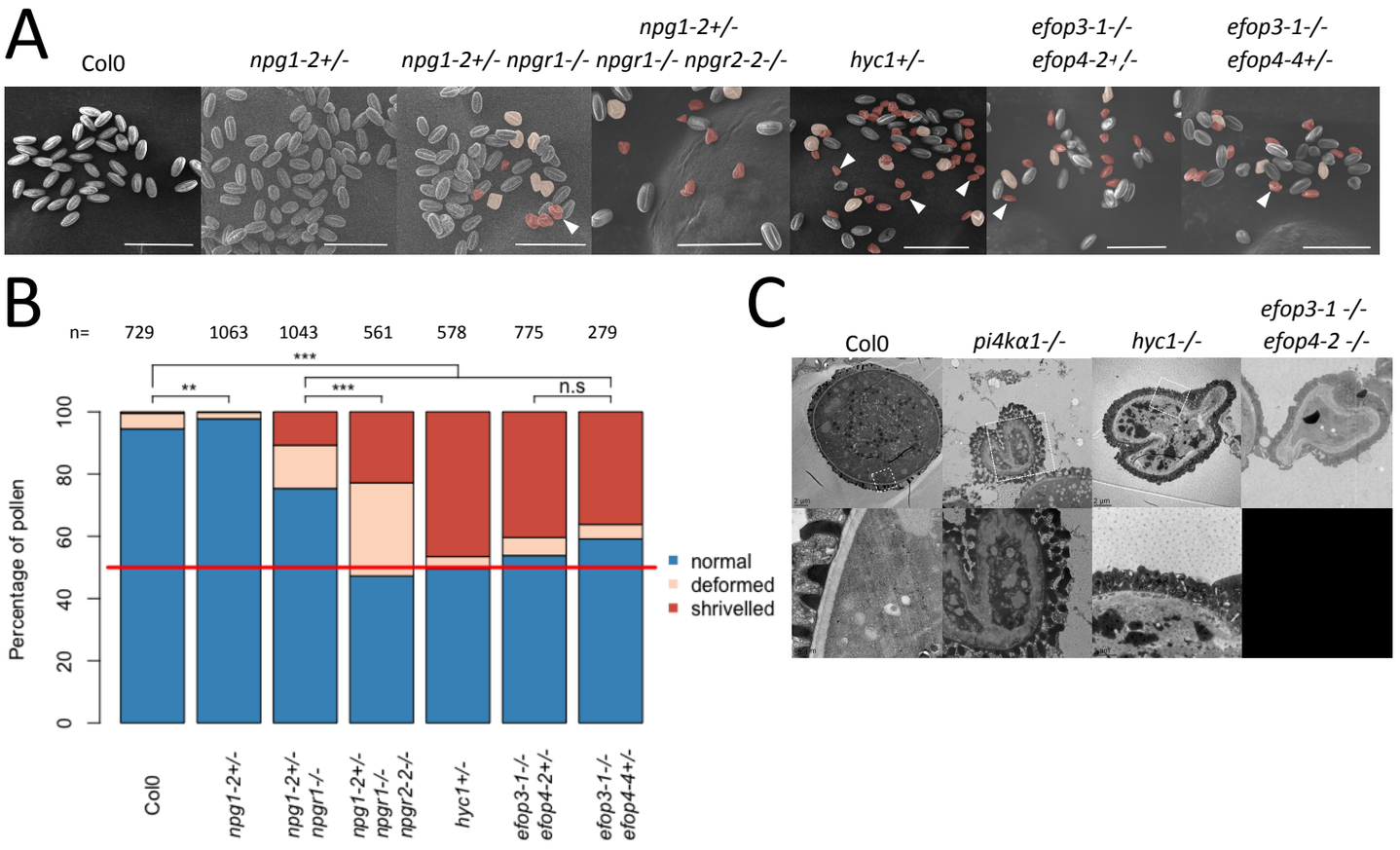

Figure 3. (A) Pollen grains observed at the scanning electron microscope of self-fertilized Col0, *npg1-2 +/-*, *npg1-2+/- npgr1-/-*, *npg1-2+/- npgr1-/- npgr2-2-/-*, *hyc1+/-, efop3-1-/-efop4-2+/-* and *efop3-1-/-efop4-2+/-* plants. Deformed pollens and shrivelled pollens are colored in red and orange, respectively. Scale bar: 50µm **(B)** Quantification of the % of normal (in blue), deformed (in orange) and shrivelled (in red) pollen grains from self-fertilized Col0, *npg1-2 +/-, npg1-2+/- npgr1-/-, npg1-2+/- npgr1-/- npgr2-2-/-, hyc1+/-, efop3-1-/-efop4-2+/-* and *efop3-1-/-efop4-2+/-* plants. n indicates the number of pollens counted for each genotype. Statistics used chi-square test. n.s, non-significant; ***, p<0.001. **(C)** Observation of pollen grains from self-fertilized Col0, *pi4kα1-1, hyc1* and *efop3-1-/-efop4-2+/-* by transmission electron microscopy. The lower panel shows a close–up of the region indicated on the upper panel.

The npg1 mutant was previously published as not able to germinate, giving its name NO POLLEN GERMINATION to the family (Golovkin and Reddy, 2003). We reproduced this result by characterizing two new T-DNA mutant alleles of *NPG1*. The self-progeny of *npg1-1+/-* and *npg1-2+/-* had segregation rate of 50,3% and 32% resistant seedlings, respectively, indicating gamete lethality **(Table 1)**. Reciprocal crosses confirmed their male sterility phenotype, with 0% of transmission of the mutation through the pollen, while the female gametophyte might be affected only for the second allele with a weak distortion of the segregation rate **(Table 2)**. However, the observation of *npg1-1* and *npg1-2* pollen grains by SEM did not show any morphological defect, unlike *pi4kα1* pollens **(Figure 3, A-B; Supplemental 3, A-B)**. The reintroduction of *NPG1* fused with mCITRINE under the control of its own promoter complemented the male sterility in *npg1-2* background, leading to *npg1-2* homozygous plants **(Supplemental 3, C)**. Similarly, the expression of NPGR2 fused to the mCITRINE under the control of the *NPG1* promoter also complemented *npg1-2* male sterility. These experiments indicate that NPGR2 can substitute for NPG1 function in pollen and that both NPG1-mCITRINE and NPGR2-mCITRINE fusion are fully functional **(Supplemental 3, C)**.

Supplemental 3. (A) Pollen grains observed at the scanning electronic microscope of self-fertilized *npg1-1+/-, npg1-1+/- npgr1-/-, npgr1-1-/- npgr2-1-/-, npgr1-1-/- npgr2-2-/-, hyc1-/-* expressing *HYC1prom::HYC1-mCITR*INE*, efop2-1-/- efop3-1-/-, efop2-1-/- efop3-2-/-, efop2-2-/- efop3-1-/-, efop2-2-/- efop3-2-/-, efop3-1+/- efop4-2-/-, efop3-2-/- efop4-2+/-, efop3-2+/- efop4-2-/-, efop3-2-/- efop4-4+/-,* and *efop3-2+/- efop4-4-/-* plants. Scale bars: 50µm **(B)** Quantification of the % of normal (in blue), deformed (in orange) and shrivelled (in red) pollen grains of all the indicated genotypes. ND is indicated when no quantification of this genotype is available. n indicates the number of pollen grains counted. **(C)** Genotyping of Col0, *npg1-2* heterozygous plants and *npg1-2* homozygous plants complemented with *NPG1prom::NPG1-mCITRINE* (insertion n° 2, 3, 5, 9, 10 and 12) and *NPG1prom::NPGR2-mCITRINE* (insertion n° 19 and 20). The upper panel shows the amplification of the gene sequence. The lower panel shows the amplification of the T-DNA border. **(D)** Genotyping of Col0, *hyc1* heterozygous plants and *hyc1* homozygous plants complemented with *HYC1prom::HYC1-mCITRINE* (insertion n° 2). The upper panel shows the amplification of the gene sequence. The lower panel shows the amplification of the T-DNA border.

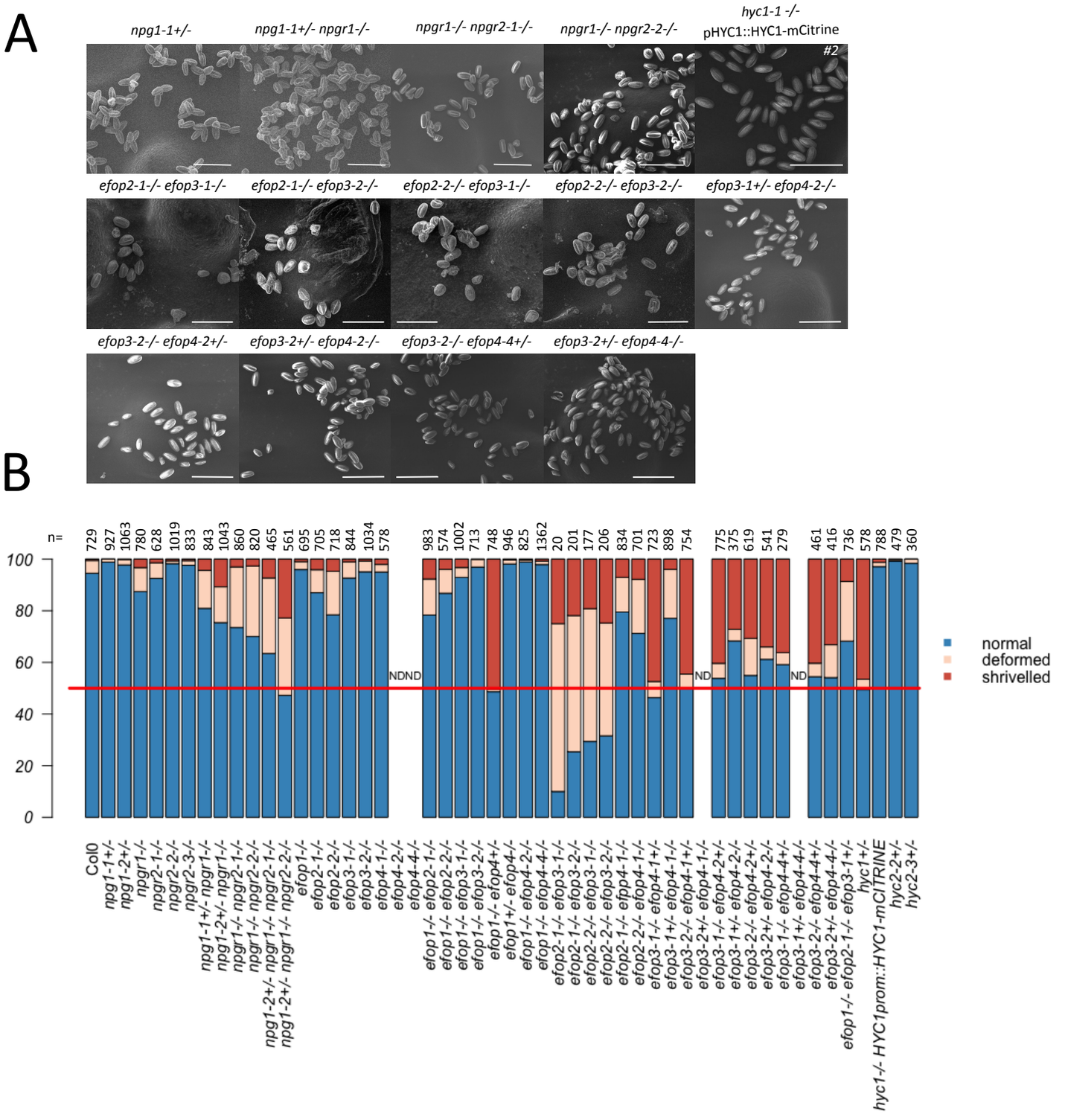
A
npg1-1+/-
npg1-1+/- npgr1-/-
npgr1-/- npgr2-1-/-
npgr1-/- npgr2-2-/-
hyc1-1 -/-
pHYC1::HYC1-mCitrine
#2
efop2-1-/- efop3-1-/-
efop2-1-/- efop3-2-/-
efop2-2-/- efop3-1-/-
efop2-2-/- efop3-2-/-
efop3-1+/- efop4-2-/-
efop3-2-/- efop4-2+/-
efop3+2-/- efop4-2-/-
efop2-2-/- efop4-4+/-
efop3+2+/- efop4-4-/-
B
n=
729 927 1063 780 628 1019 833 843 1043 860 820 465 561 695 705 718 844 1034 578
983 574 1002 713 748 946 825 1362 20 201 177 206 834 701 723 898 754
775 375 619 541 279
461 416 736 578 788 479 360
100
80
60
40
20
0
Percentage of pollen
ND
normal
deformed
shrivelled
Col0
npg1-1+/-
npg1-2+/-
npgr1-/-
npgr2-1-/-
npgr2-2-/-
npgr2-3-/-
npg1-1+/- npgr1-/-
npg1-2+/- npgr1-/-
npgr1-/- npgr2-1-/-
npgr1-/- npgr2-2-/-
npg1-2+/- npgr1-/- npgr2-1-/-
npg1-2+/- npgr1-/- npgr2-2-/-
efop1-1-/-
efop2-1-/-
efop2-2-/-
efop3-1-/-
efop3-2-/-
efop4-1-/-
efop4-2-/-
efop4-4-/-
efop1-/- efop2-1-/-
efop1-/- efop2-2-/-
efop1-/- efop3-1-/-
efop1-/- efop3-2-/-
efop1+/- efop4+/-
efop1+/- efop4-2-/-
efop1-/- efop4-4-/-
efop2-1-/- efop3-1-/-
efop2-1-/- efop3-2-/-
efop2-2-/- efop3-1-/-
efop2-2-/- efop3-2-/-
efop2-1-/- efpp4-1-/-
efop2-2-/- efop4-1-/-
efop3-1-/- efop4-1+/-
efop3-1+/- efop4-1-/-
efop3-2-/- efop4-1-/-
efop3-2+/- efop4-1-/-
efop3-1-/- efop4-2+/-
efop3-1+/- efop4-2-/-
efop3-2-/- efop4-2+/-
efop3-2+/- efop4-2-/-
efop3-1-/- efop4-4+/-
efop3-1+/- efop4-4-/-
efop3-2-/- efop4-4+/-
efop3-2+/- efop4-4-/-
efop1-/- efop2-1-/- efop3-1+/-
hyc1+/-
hyc1-/- HYC1prom::HYC1-mCITRINE
hyc2-2+/-
hyc2-3+/-
C
Col0
npg1-2+/-
npg1-2+/-
NPG1prom::NPG1-mCITRINE
#2
#3
#5
#9
#10
#12
npg1-2+/-
NPG1prom::NPGR2-mCITRINE
#19
#20
GK_480D08-LP/
GK_480D08-RP2
GK_480D08-LP/
o8474
D
Col0
hyc1+/-
hyc1-/-
HYC1prom::HYC1-mCITRINE
GK_767H11-LP/
GK_767H11-RP
GK_767H11-LP/
o8474
GK_767H11-RP/
o8474

Because, NPGR2 can substitute for NPG1 in pollen, we speculated that a certain degree of functional redundancy between NPG1, NPGR1 and NPGR2 or compensatory effects during pollen development could lead to the weaker phenotype of *npg1* pollen compared to *pi4kα1* pollen and thus explain why *npg1* pollen did not present morphological defect by SEM. To test this hypothesis we generated higher order mutant combination within the *NPG* family **(Table 3)**. The *npg1-2+/- npgr1-/-* mutant combination presented about 10% of *pi4kα1*-like shrivelled pollen grains while *npgr1npgr2-1* and *npgr1npgr2-2* double homozygous mutants displayed about 25% of deformed (but not shrivelled) pollen grains **(Figure 3, A- B; Supplemental 3, A-B)**. Finally, the *npg1-2+/-npgr1-/-npgr2-1-/-* and *npg1-2+/-npgr1-/-npgr2-2-/-* displayed about 35 and 50% of deformed and shrivelled pollen grains, respectively. These data indicate that combinations of *npg* mutants partially mimic *pi4kα1* pollen phenotype.

Next, we addressed the loss-of-function phenotypes of *HYCCIN* family members. The self-progeny of a *hyc1+/-* single mutant presented a segregation rate around 50% indicating a gametophytic lethality **(Table 1)**. As *HYC1* expression is restricted to pollen, we were expecting that the segregation bias was caused by defects of the male gametophyte. As anticipated, reciprocal crosses showed male sterility while the T-DNA transmission through the female gametophyte was not affected **(Table 2)**. Observation of *hyc1+/-* pollen grains by SEM revealed that half of the pollen grains were shrivelled **(Figure 3, A and B)**. In addition, transmission electron microscopy also showed a thickening of the cell wall of the *hyc1* mutant pollen grains, which was similar to the phenotype observed for *pi4kα1-1* **(Figure 3, C)**. Finally, the male sterility, as well as the pollen morphological defects, were complemented by the reintroduction of *HYC1prom::HYC1-mCITRINE* **(Supplemental 3, A-B and D)**. All together, these data

show that *hyc1* knockout phenotype fully mimic *pi4kα1* knockout regarding pollen development.

None of the *efop* single mutant presented any pollen morphological defects or distortion of segregation, likely because of redundancy between the four members of this family **(Supplemental 3, B)**. We thus generated all the possible combinations of double mutants **(Supplemental 3, B; Table 3)**. We were able to obtain *efop2efop3* double homozygous mutants, suggesting no strong synthetic lethality. However, they presented from 19% to 25% of shrivelled pollen grains, resembling those of the *pi4kα1* and *hyc1* mutants, and from 43% to 65% of deformed pollens (resembling those of *npgr1npgr2* double mutants). Thus, depending on the alleles, these double mutant combinations presented from 70% to 90% of abnormal pollens **(Supplemental 3, A and B)**. In addition, it was not possible to generate *efop3efop4* double homozygous mutant no matter the alleles used. Indeed, reciprocal crosses indicated 0% of transmission of *efop3* mutant allele when *efop3+/-efop4-/-* plants were used as male, revealing that *efop3efop4* pollens were lethal **(Table 2)**. SEM showed that about 45% of the pollen grains present abnormal morphology **(Figure 3, A and B; Supplemental 3, A and B)**. Finally, observation of *efop3-1efop4-2* shrivelled pollen grain by transmission microscopy revealed a thick cell wall similar to the phenotype observed for *pi4kα1-1* and *hyc1*. *efop2efop3* and *efop3efop4* double mutants mimic partially and fully *pi4kα1* and *hyc1* pollen phenotypes, respectively. Altogether, our genetic analyses indicate that all the protein classes in the putative PI4Kα1 complex are essential for the male gametophyte in Arabidopsis and that certain mutant combinations in the *NPG*, *HYC* or *EFOP* families either fully (*hyc1+/-, efop3+/-efop4-/-)* or partially (*npg1+/-, npg1+/-npgr1-/-, npgr1-/-npgr2-/-, npg1-2+/-npgr1-/-npgr2-2-/-, efop2efop3-/-*) mimic the *pi4kα1* phenotype. Thus, these proteins likely act as a single protein complex in plants.

Disturbing the PI4Kα1 complex results in various sporophytic phenotypes

The pollen lethality of *pi4kα1* knockout did not allow us to further study the role of PI4Kα1 in plant development. To bypass this issue, we developed a knockdown strategy using a total of 4 independent artificial microRNAs targeted against *PI4Kα1*. Plants expressing ubiquitously the artificial microRNAs number 2 and 3 showed strong developmental defects with dark green curly leaves, dwarfism and sterility in some cases **(Figure 4, A).** As the two microRNAs are independent and present similar phenotype, those defects are likely due to the specific knockdown of *PI4Kα1.* In addition, combinations of *npg* mutants present growth defect phenotypes. Indeed, *npgr1npgr2-2* double mutant present a mild growth phenotype **(data not shown)** while *npg1+/-npgr1-/-npgr2-2-/-* is dwarf **(Figure 4, B)**. This suggests that PI4Kα1 complex is essential not only for pollen development but also for many developmental and physiological processes. Because PI4P powers the electrostatic property of the plant plasma membrane and thus is a key determinant of its identity, this result is consistent with the idea that PI4Kα1 could be involved in PI4P production at the plasma membrane, which we expect to be essential.

While *HYC1* is specifically expressed in pollen and is male sterile, *HYC2* is predicted to be expressed in the sporophyte. We characterized two T-DNA alleles corresponding to two putative *hyc2* loss-of-function mutants. The segregation rate of *hyc2-2* heterozygous plants was of 60% **(Table 1)**. Moreover, it was not possible to retrieve homozygous plants in the progeny of both *hyc2-2* and *hyc2-3*. Reciprocal crosses indicated a transmission of the allele through the male and the female gametophytes even if a weak distortion could be observed in both cases **(Table 2)**. Siliques from *hyc2-2* and *hyc2-3* heterozygous plants presented around 25% to 30% of aborted seeds **(Figure 4, C and D; Supplemental 4, A)**. Observations of the embryo after clearing showed that in those

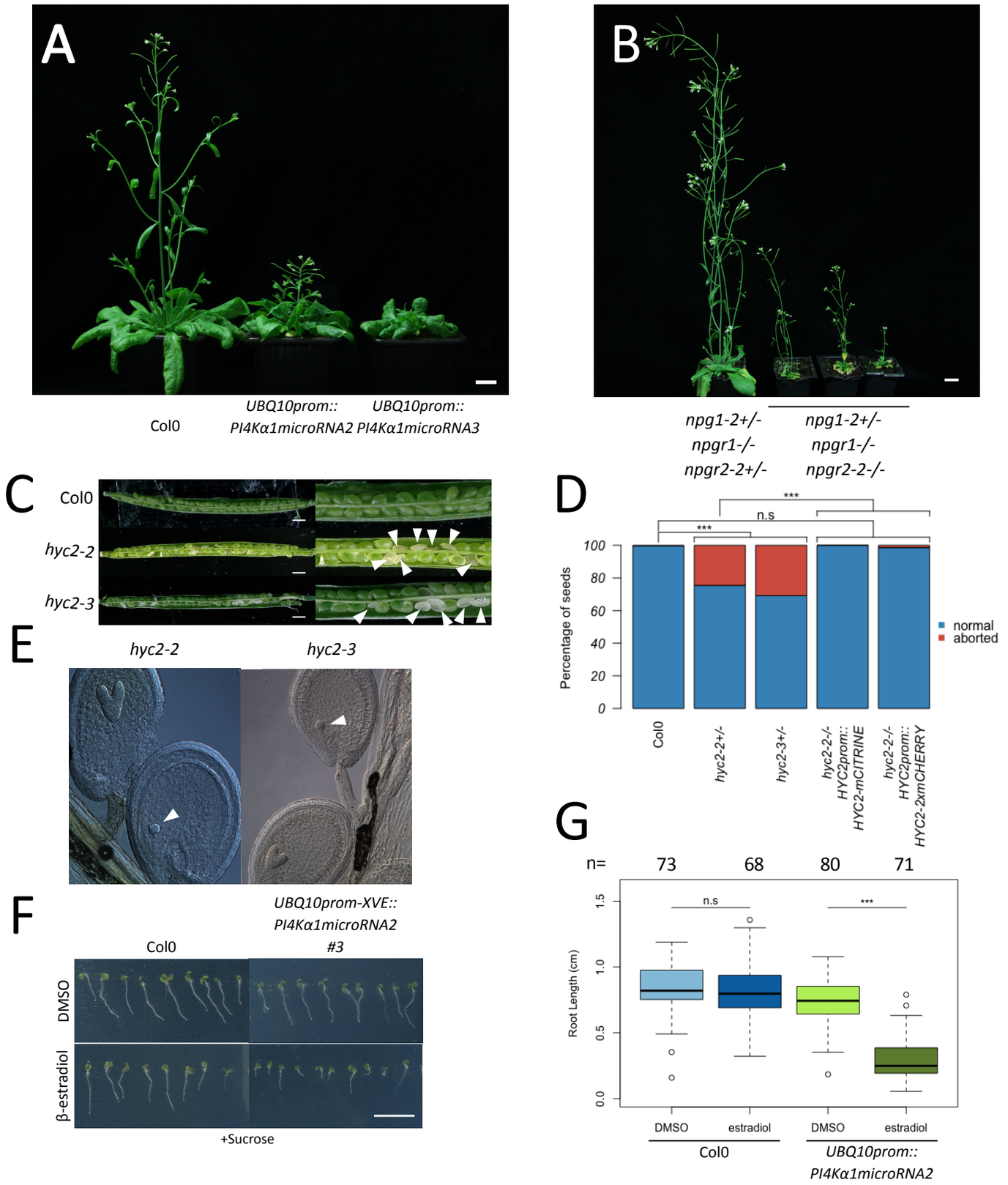

Figure 4.(A) 38 days-old Col0 and plants expressing the *microRNA2* and *microRNA3* against *PI4Kα1*. Scale bar: 2cm **(B)** 30 days-old *npg1-2+/- npgr1-/- npgr2-2-/+* and *npg1-2+/- npgr1-/- npgr2-2-/-* plants. Scale bar: 2cm. **(C)** Opened siliques of self-fertilized Col0, *hyc2-2* and *hyc2-3* heterozygous mutant plants. White arrowheads indicate aborted seeds. **(D)** % of aborted seeds in Col0, *hyc2-2+/-, hyc2-3+/-, hyc2-2-/- HYC2prom::HYC2-mCITRINE* (insertion n°10), and *hyc2-2-/- HYC2prom::HYC2-2xmCHERRY* (insertion n°11) siliques. The number of seed counted is superior at 250 for each genotype. Statistics used chi-square test. n.s, non-significant; ***, p<0.001. **(E)** Cleared seeds from *hyc2-2* and *hyc2-3* heterozygous mutant plants. White arrowheads indicate globular embryo that have stopped their development. **(F)** 5 days-old seedlings of Col0 and seedlings expressing the inducible *microRNA2* against *PI4Kα1* on non-inducible (DMSO) and inducible medium (β-estradiol) supplemented with sucrose. Scale bars: 1cm **(G)** Measurement of the primary root length of 5 days-old seedlings of Col0 and seedlings expressing the inducible *microRNA2* against *PI4Kα1* on non-inducible (DMSO) and inducible medium (β-estradiol). n indicates the number of seedlings measured. Statistics were done using Wilcoxon test. n.s, non-significant; ***, p<0.001.

siliques, some embryo stopped their development at the globular stage before degenerating while the rest of the embryos pursued their development normally **(Figure 4, E)**. This phenotype was lost and homozygous plants were obtained when HYC2-mCITRINE or HYC2-2xmCHERRY were reintroduced under the control of the *HYC2* promoter **(Figure 4, D; Supplemental 4, A and B)**. Thus, the loss of HYC2 leads to embryo lethality at the globular stage, suggesting that HYC1 is essential for the male gametophyte, while HYC2 is essential for the sporophyte. These results are consistent with the idea that the four-subunit PI4Kα1 complex is essential in plants.

The ubiquitous expression of the PI4Kα1 microRNA lines 2 and 3 leads to phenotypes with variable strength. However most of the plants died or were sterile which made

Supplemental 4. (A) Opened siliques of self-fertilized *hyc2-2* heterozygous mutant plants and self-fertilized hyc2-2 homozygous plants complemented by the expression of *HYC2prom::HYC2-mCITRINE* (insertion n°9, 10 and 17) and *HYC2prom::HYC2-2xmCHERRY* (insertion n°11, 18 and 24). White arrowheads indicate aborted seeds. **(B)** Genotyping of Col0, *hyc2-2* heterozygous plants and *hyc2-2* homozygous plants complemented with *HYC2prom::HYC2-mCITRINE* (insertion n°9, 10, 13 and 17) and *HYC2prom::HYC2-2xmCHERRY* (insertion n° 11, 18 and 24). The upper panel shows the amplification of the gene sequence. The lower panel shows the amplification of the T-DNA border. **(C)** PI4Kα1 protein levels of 9 days-old Col0 seedlings and seedlings expressing the inducible microRNA2 against *PI4Kα1* on non-inducible (DMSO) and inducible medium (β-estradiol) for two independent insertions (3 and 6). Western blot is performed using an anti-PI4Kα1 antibody and an anti-tubuline α (anti-Tub α) as control. The relative density of signal adjusted to the Col0 DMSO condition is indicated. **(D)** 9 days-old seedlings of Col0 and seedlings expressing the inducible microRNA2 against *PI4Kα1* on non-inducible (DMSO) and inducible medium (β-estradiol) supplemented with sucrose for two independent insertions (3 and 6). Scale bars: 1cm **(E)** Measurement of the primary root length of 9 days-old seedlings of Col0 and seedlings expressing the inducible microRNA2 against *PI4Kα1* on non-inducible (DMSO) and inducible medium (β-estradiol) for two independent insertions (3 and 6). n indicates the number of seedlings measured. Statistics were done using Wilcoxon test. **(F)** 11 days-old Col0 seedlings or expressing the inducible microRNA2 against *PI4Kα1* on non-inducible (DMSO) and inducible medium (β-estradiol) without sucrose for two independent insertions (3 and 6). The red arrows indicate plants with bleached cotyledons. Close-up of seedlings expressing the inducible microRNA2 against *PI4Kα1* are shown on the right panel. Scale bar: 1cm **(G)** Percentage of seedlings presenting bleached cotyledons of 11 days-old Col0 seedlings or expressing the inducible microRNA2 against *PI4Kα1* on non-inducible (DMSO) and inducible medium (5µM β-estradiol) for two independent insertions (3 and 6). n indicates the number of seedlings measured.

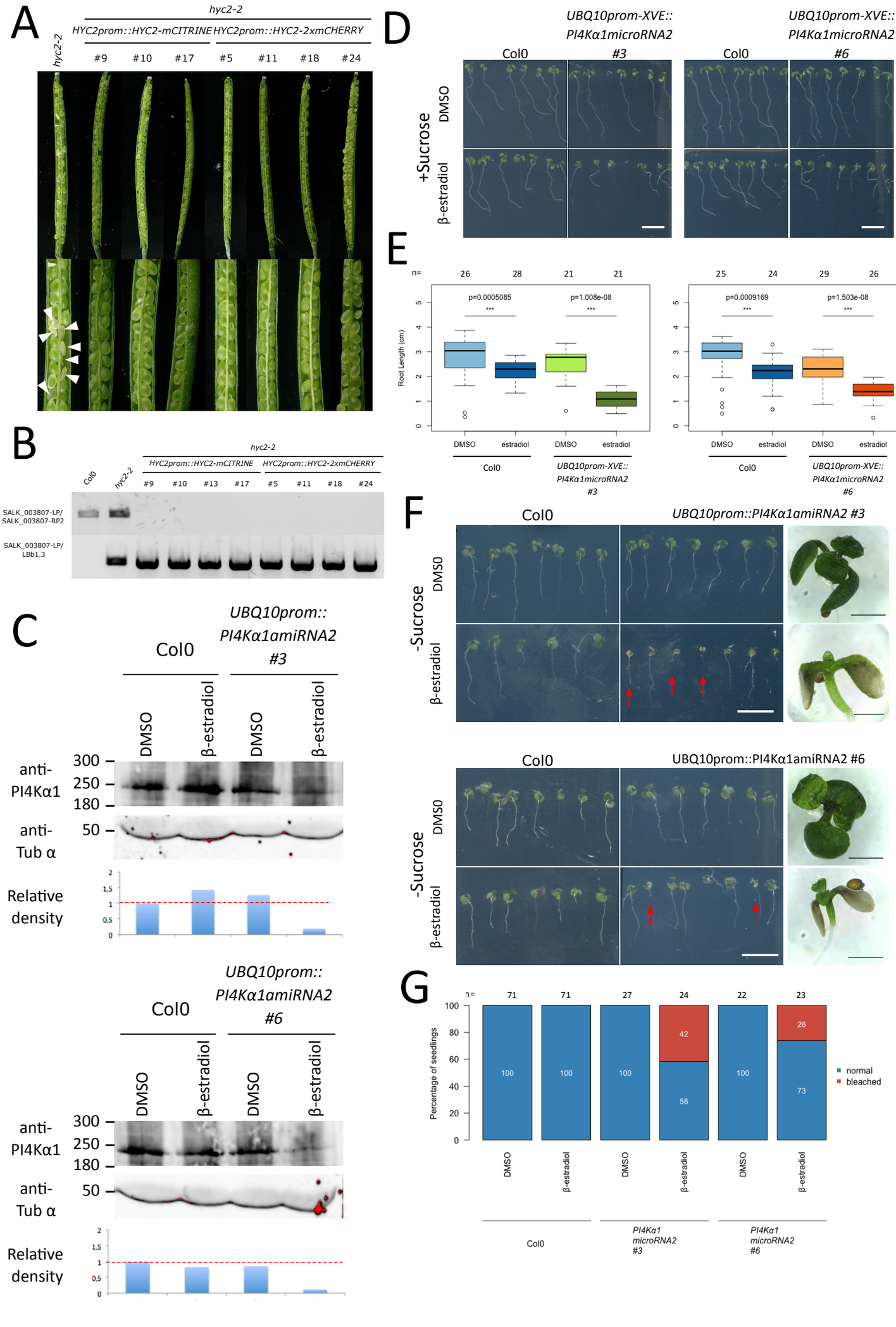
A
hyc2-2
HYC2prom::HYC2-mCITRINE HYC2prom::HYC2-2xmCHERRY
hyc2-2
#9 #10 #17 #5 #11 #18 #24
B
hyc2-2
HYC2prom::HYC2-mCITRINE HYC2prom::HYC2-2xmCHERRY
Col0 hyc2-2
#9 #10 #13 #17 #5 #11 #18 #24
SALK_003807-LP/ SALK_003807-RP2
SALK_003807-LP/ LBb1.3
C
Col0
UBQ10prom:: PI4Kα1amiRNA2 #3
DMSO β-estradiol DMSO β-estradiol
anti- PI4Kα1
300 250 180
anti- Tub α
50
Relative density
2 1,5 1 0,5 0
Col0
UBQ10prom:: PI4Kα1amiRNA2 #6
DMSO β-estradiol DMSO β-estradiol
anti- PI4Kα1
300 250 180
anti- Tub α
50
Relative density
2 1,5 1 0,5 0
D
UBQ10prom-XVE:: PI4Kα1microRNA2 #3
UBQ10prom-XVE:: PI4Kα1microRNA2 #6
Col0 Col0
+Sucrose
DMSO
β-estradiol
E
n= 26 28 21 21
p=0.0005085 *** p=1.008e-08 ***
Root Length (cm)
0 1 2 3 4 5
DMSO estradiol DMSO estradiol
Col0
UBQ10prom-XVE:: PI4Kα1microRNA2 #3
n= 25 24 29 26
p=0.0009169 *** p=1.503e-08 ***
DMSO estradiol DMSO estradiol
Col0
UBQ10prom-XVE:: PI4Kα1microRNA2 #6
F
Col0
UBQ10prom::PI4Kα1amiRNA2 #3
-Sucrose
DMSO
β-estradiol
Col0
UBQ10prom::PI4Kα1amiRNA2 #6
-Sucrose
DMSO
β-estradiol
G
n= 71 71 27 24 22 23
Percentage of seedlings
0 20 40 60 80 100
100 100 100 42 58 100 26 73
normal
bleached
DMSO β-estradiol DMSO β-estradiol DMSO β-estradiol
Col0
PI4Kα1 microRNA2 #3
PI4Kα1 microRNA2 #6

those lines difficult to work with. To avoid this problem and in order to use *PI4Kα1* knockdown for more precise analysis during plant development, we put the artificial microRNA2, which had the strongest phenotype when constitutively expressed, under the control of a β-estradiol-inducible ubiquitous promoter (*UBQ10-XVE*) (Siligato et al., 2016). Induction of the expression of *artificial microRNA2* led to a decrease in the amount of PI4Kα1 proteins **(Supplemental 4, C)**. The corresponding seedlings presented shorter primary root when grown on a medium containing sucrose **(Figure 4, F and G; Supplemental 4, D and E)**. In low sucrose medium only, upon induction, the seedlings presented small bleached cotyledons in some cases suggesting a photoautrotrophic phenotype **(Supplemental 4, F and G)**. These lines can now be used as a tool to study the effect of a knockdown of PI4Kα1 on diverse cellular and developmental processes.

*PI4Kα*1 complex is associated with the plasma membrane

To address PI4Kα1 subcellular localization, we first raised stable transgenic lines expressing PI4Kα1 tagged with the yellow fluorescent protein mCITRINE at either its N- or C-terminal ends and the red fluorescent protein 2xmCHERRY at the C-terminal end under the control of either its own promoter or the *UBQ10* promoter. Consistent with the hypothesis that PI4Kα1 acts at the plasma membrane, the three constructs mCITRINE-PI4Kα1, PI4Kα1-mCITRINE, and PI4Kα1-2xmCHERRY localized at the plasma membrane and in the cytosol **(Figure 5, A)**. However, the introduction *PI4Kα1::PI4Kα1-mCITRINE*, *PI4Kα1::mCITRINE-PI4Kα1* or *PI4Kα1::PI4Kα1-2xmCHERRY* constructs in the *pi4kα1-1+/-* mutant background did not complement the pollen lethality and we never recovered *pi4kα1-1-/-* plants **(data not shown)**. We used the same *PI4Kα1* promoter used for the rescue experiment with the untagged *PI4Kα1* **(Figure 1, B and C;**

Supplemental 1, A), suggesting that PI4Kα1 fused with a fluorescent protein is non-functional. Expression of PI4Kα1 fused to smaller tags (i.e. PI4Kα1-6xHA or Flag-PI4Kα1) also failed to complement *pi4kα1-1* **(data not shown)**.

To confirm the localization obtained with mCITRINE fusion, we used the antibodies against the native PI4Kα1 and performed whole mount immunolocalization in roots. Similar to the mCITRINE-PI4Kα1 and PI4Kα1-mCITRINE fusions, we observed again a signal at the plasma membrane **(Figure 5, B)**. We also noticed signal in the cytosol and in nuclei **(Figure 5, B)**. To further confirm the preferential association of PI4Kα1 with the plasma membrane, we used cellular fractionation of whole seedling and compared the signal obtained on a purified plasma membrane or whole microsomal fractions. We confirmed the presence of proteins in the two fractions using an antibody against V-type ATPase. The purity of the plasma membrane fraction was evaluated with antibodies against PIP1,2 aquaporin, a known plasma membrane resident protein **(Figure 5, C)**. When loading the same amount of protein in each fraction, this experiment revealed the presence of a band around 225kDa, corresponding to PI4Kα1, in the plasma membrane fraction but not, or barely visible, in the total microsomal fraction **(Figure 5, C)**. Together, fluorescent fusion, immunolocalization and cellular fractionation show that PI4Kα1 is associated with the plasma membrane.

We next address the subcellular localization of NPG, HYC and EFOP proteins at the plasma membrane. NPG1 was previously found to be an extracellular protein in pollen grains (Shin et al., 2014). In our hand, NPG1-mCITRINE, NPGR1-mCITRINE and NPGR2-mCITRINE all localized at the periphery of the cell in root meristem **(Figure 5, A)**. To distinguish between the plasma membrane and cell wall, we co-expressed NPGR2-mCITRINE with Lti6b-mCHERRY. We observed that the two signals perfectly colocalized indicating that NPGR2 is present at the plasma membrane **(Figure 5, D)**. Furthermore,

we performed plasmolysis of the epidermal root cell by addition of sorbitol. In this context, the plasma membrane detaches from the cell wall. We observed that the signal of NPGR2-mCITRINE remains at the plasma membrane and is not present in the cell wall **(Figure 5, E)**. Moreover, in western blot using an anti-NPGR2 antibody, NPGR2 was found enriched in the plasma membrane fraction compared to the microsomal fractions **(Figure 5, C)**.

Similarly, HYC1-mCITRINE, HYC2-mCITRINE, EFOP1-mCITRINE, EFOP2-mCITRINE and EFOP3-mCITRINE expressed under the control of the *UBQ10* promoter were found at the plasma membrane **(Figure 5, A and D)**. In addition to the plasma membrane localization, we noticed that EFOP1 and EFOP2 were associated with intracellular compartments, which were more prominently labelled for EFOP1 than EFOP2. Also, NPG1 and HYC1 were highly soluble in the cytosol. As HYC1 and NPG1 are normally mainly expressed in pollens, they might need each other to localized at the plasma membrane. This could explain why when we overexpressed them alone in root epidermal cells, we see most of the proteins in the cytosol.

Figure 5. (**A)** Confocal images of PI4Kα1, PI4Kα1, NPG1, NPGR1, NPGR2, HYC1, HYC2, EFOP1, EFOP2 and EFOP3 fused to mCITRINE (mCt) ou mCHERRY under the control of the *UBQ10* promoter in root epidermal cells. Scale bars: 10µm. **(B)** Confocal images of PI4Kα1 using an anti-PI4Kα1 antibody in epidermal root cells on WT seedlings. Control background without primary antibody is shown. Scale bar: 10µm. **(C)** Western blot using anti-PI4Kα1, anti-NPGR2, anti Anti-V-type ATPase, and anti-PIP1,2 aquaporin antibodies on plasma membrane and microsomal fractions from WT seedlings. **(D)** Confocal images of seedlings co-expressing Lti6b-2xmCHERRY (under the control of the *2x35S* promoter), NPGR2-mCITRINE, HYC2-mCITRINE or EFOP2-mCITRINE (under the control of the *UBQ10* promoter). The graphics on the left represent the intensity of each signal across the cell along the white line. The graphics in the middle represent the intensity of each signal along the membrane indicated with a white arrow. Matching signals are indicated with black arrows. The linear regression and the adjusted R square for each signal are indicated. The graphics on the right represent the residual in y between the signal along the membrane and the linear regression. **(E)** Confocal images of PI4Kα1-mCt, mCt-PI4Kα1, NPGR2-mCt, HYC2-mCt, EFOP2-mCt under the control of the *UBQ10* promoter in root epidermal cells in control (MES) and during plasmolysis (MES+Sorbitol). Scale bars: 10µm. **(F)** Confocal images of seedlings co-expressing Lti6b-2xmCHERRY (under the control of the *2x35S* promoter), NPGR2-mCITRINE or EFOP2-mCITRINE (under the control of the *UBQ10* promoter). The graphics represent the intensity of each signal across the cell along the white line. Matching signals are indicated with black arrows.

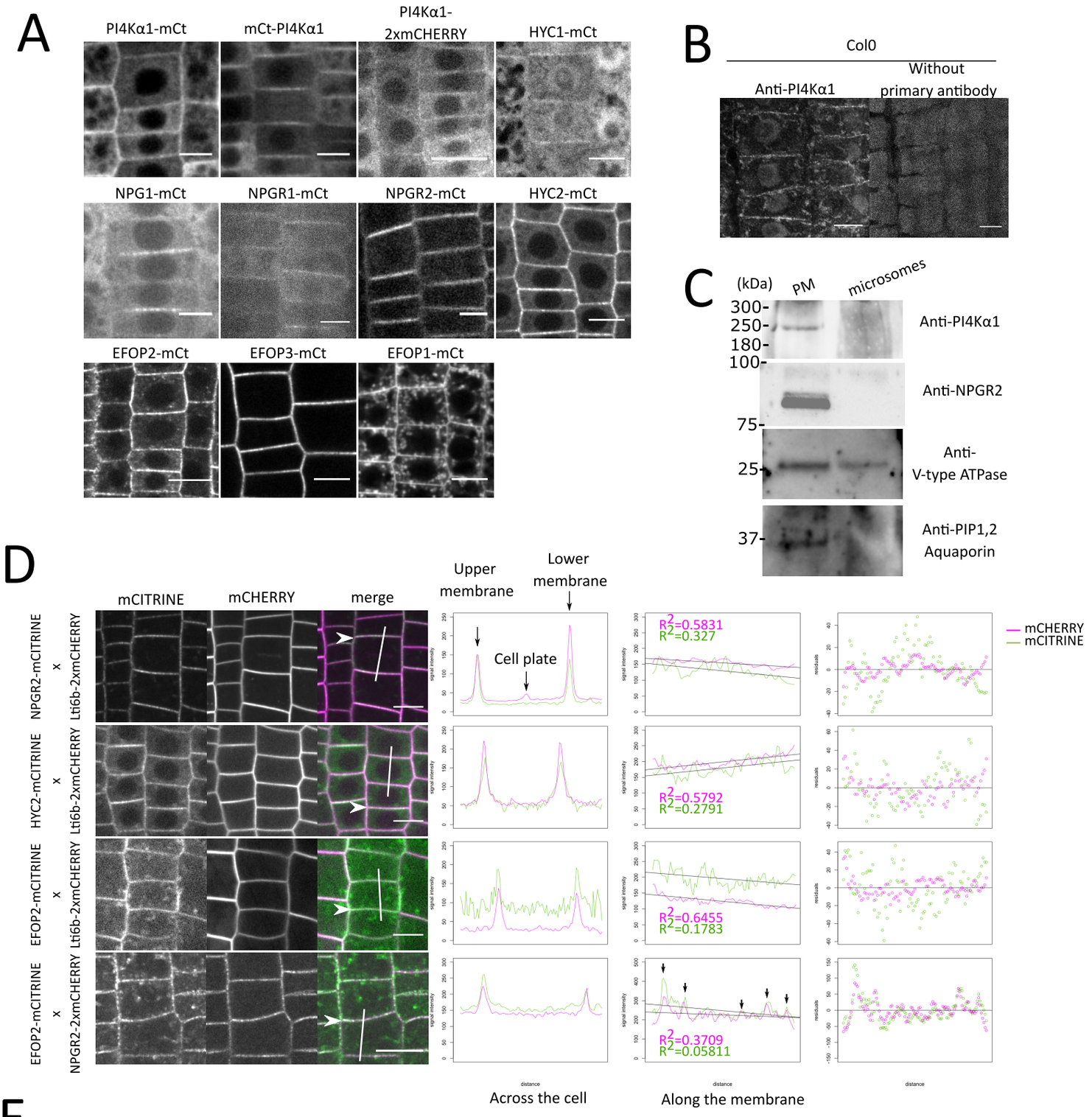
A
PI4Kα1-mCt
mCt-PI4Kα1
PI4Kα1-2xmCHERRY
HYC1-mCt
NPG1-mCt
NPGR1-mCt
NPGR2-mCt
HYC2-mCt
EFOP2-mCt
EFOP3-mCt
EFOP1-mCt
B
Col0
Anti-PI4Kα1
Without primary antibody
C
(kDa)
PM
microsomes
300-
250-
180-
100-
75-
25-
37-
Anti-PI4Kα1
Anti-NPGR2
Anti-V-type ATPase
Anti-PIP1,2 Aquaporin
D
mCITRINE
mCHERRY
merge
Upper membrane
Lower membrane
Cell plate
NPGR2-mCITRINE x Lti6b-2xmCHERRY
HYC2-mCITRINE x Lti6b-2xmCHERRY
EFOP2-mCITRINE x Lti6b-2xmCHERRY
EFOP2-mCITRINE x NPGR2-2xmCHERRY
R2=0.5831
R2=0.327
R2=0.5792
R2=0.2791
R2=0.6455
R2=0.1783
R2=0.3709
R2=0.05811
mCHERRY
mCITRINE
Across the cell
Along the membrane
E
MES
MES+Sobitol
PI4Ka1-mCt
mCt-PI4Ka1
NPGR2-mCt
HYC2-mCt
EFOP2-mCt
F
mCITRINE
mCHERRY
merge
EFOP2-mCITRINE x Lti6b-2xmCHERRY
EFOP2-mCITRINE x NPGR2-2xmCHERRY

Upon plasmolysis, PI4Kα1-mCITRINE, mCITRINE-PI4Kα1, HYC2-mCITRINE and EFOP2-mCITRINE signals are found inside the cell and absent from the cell wall. EFOP2 remained associated with the plasma membrane while PI4Kα1 and HYC2 seem to delocalize to internal compartments **(Figure 5, E)**.

In any case, all the protein classes in the putative PI4Kα1 complex were associated to some extent with the plasma membrane.

PI4Kα1 complex is present in plasma membrane nanodomains

Using confocal microscopy, we noticed that for several of the translational reporters of the PI4Kα1 complex, the signal at the plasma membrane was not continuous, raising the question of a possible subcompartimentalization of the proteins. This is notably the case for PI4Kα1-mCITRINE, NPG1-mCITRINE, NPGR2-mCITRINE, HYC2-mCITRINE, EFOP2-mCITRINE, and EFOP3-mCITRINE **(Figure 5, A, D and F)**. Using plant co-expressing Lti6b-mCt and NPGR2-mCt, HYC2-mCt or EFOP2-mCt, we observed that NPGR2-mCt, HYC2-mCt and EFOP2-mCt signals along the plasma membrane is less homogeneous than Lti6b, forming patches of high intensity **(Figure 5, D)**. We calculated the linear regression of each signal along the membrane and observed that the R square of NPGR2-mCt, HYC2-mCt and EFOP2-mCt are always smaller than the one of Lti6b-mCt indicating a higher dispersion of the intensity. In addition, plants co-expressing NPGR2-2xmCHERRY and EFOP2-mCITRINE show similar intensity pattern with signals that partially localize along the plasma membrane **(Figure 5, D).** Similarly, when we observe the plasma membrane in tangential NPGR2-2xmCHERRY and EFOP2-mCITRINE nanodomains partially colocalize **(Figure 5, F)**. As control, EFOP2-mCITRINE containing domain did not colocalized with the mostly uniformed localization of Lti6b-mCITRINE **(Figure 5, D and F)**.

PI4Kα1 complex plasma membrane subdomains are static

We investigate the lateral dynamics of the PI4Kα1 complex at plasma membrane. To do so, we used fluorescence recovery after photobleaching (FRAP). We observed that after bleaching, the signal of NPGR2-mCt, HYC2-mCt and EFOP2-mCt were not recover after 2 min of acquisition **(Figure 6, A-C)**. In comparison, PI4P sensor recovers in less than a minute after bleaching, indicating a higher mobility for PI4P sensors than for the PI4Kα1 complex. Using TIRF microscopy, we confirmed that NPGR2-mCt, HYC2-mCt and EFOP2-mCt signals were not diffusing laterally **(Figure 6, D)**. Additionally, we observed that NPGR2-mCt, HYC2-mCt and EFOP2-mCt disappear and come back at the same location on the plasma membrane. These observations suggest that fixed cluster containing the PI4Kα1 complex are present on the plasma membrane.

EFOP localize at the plasma membrane via a lipid anchor

None of the four subunits of the PI4Kα complex is a transmembrane protein. Moreover, the PI4Kα1 complex displays a peculiar clustering at the plasma membrane. We next decided to investigate the mechanism by which the PI4Kα1 complex is targeted at the plasma membrane. The *efop3-1efop4-4* and *efop3-2efop4-4* mutants showed the same pollen lethality phenotype than the *efop3-1efop4-2* and *efop3-2efop4-2* mutant **(Figure 4, A and B, Supplemental 4, A and B)**. However, *efop4-2* leads to a very small-truncated protein (42 aa) while the *efop4-4* allele leads to a small in frame deletion of 19 residues in the N-terminal part of the protein **(Figure 7, A)**.

The residues corresponding to this deletion are well conserved among the four EFOPs and include both a cysteine-rich motif, which could be S-acylated, and a polybasic region, which could contact anionic lipids at the plasma membrane **(Figure 7, A)**. We

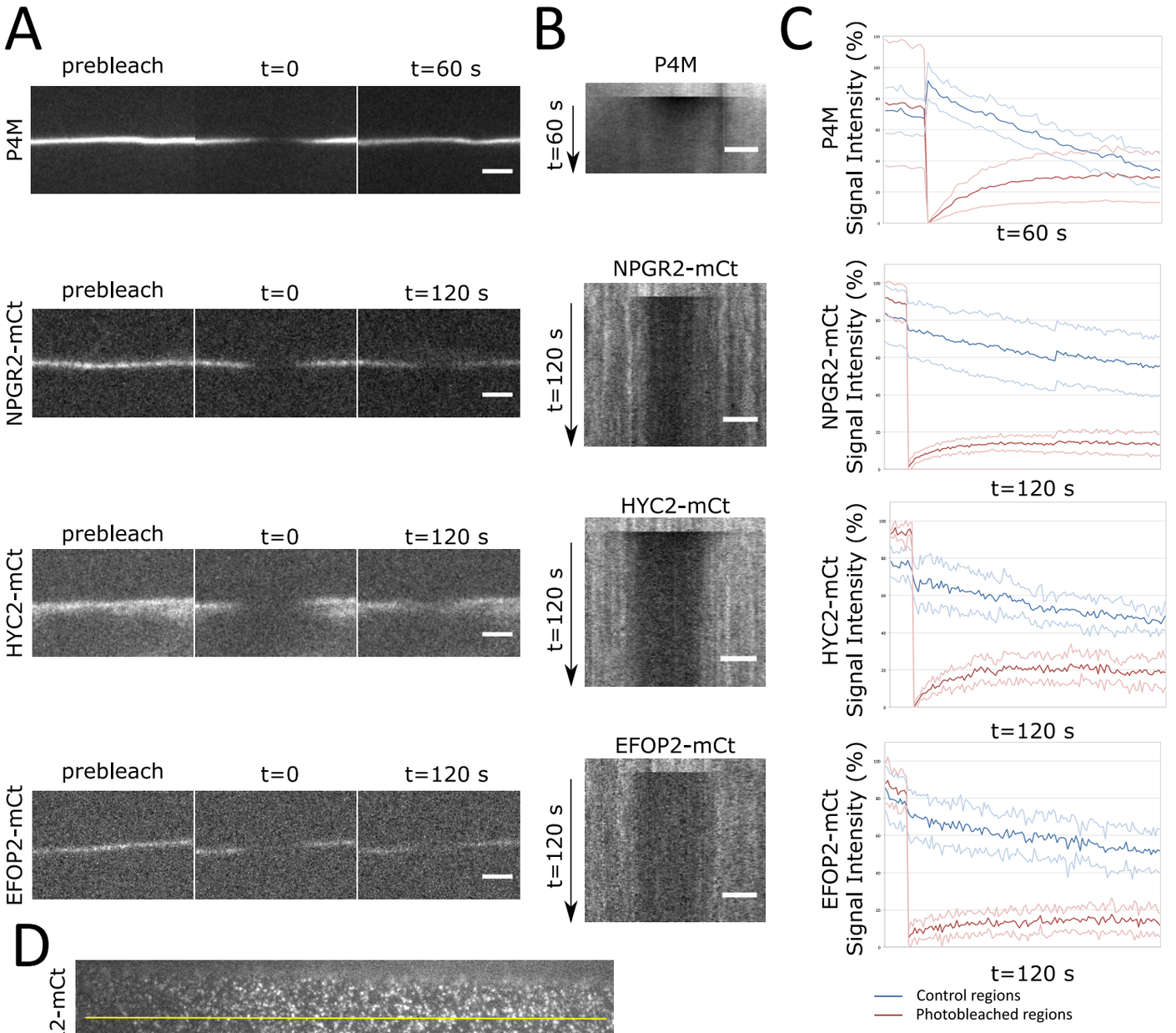

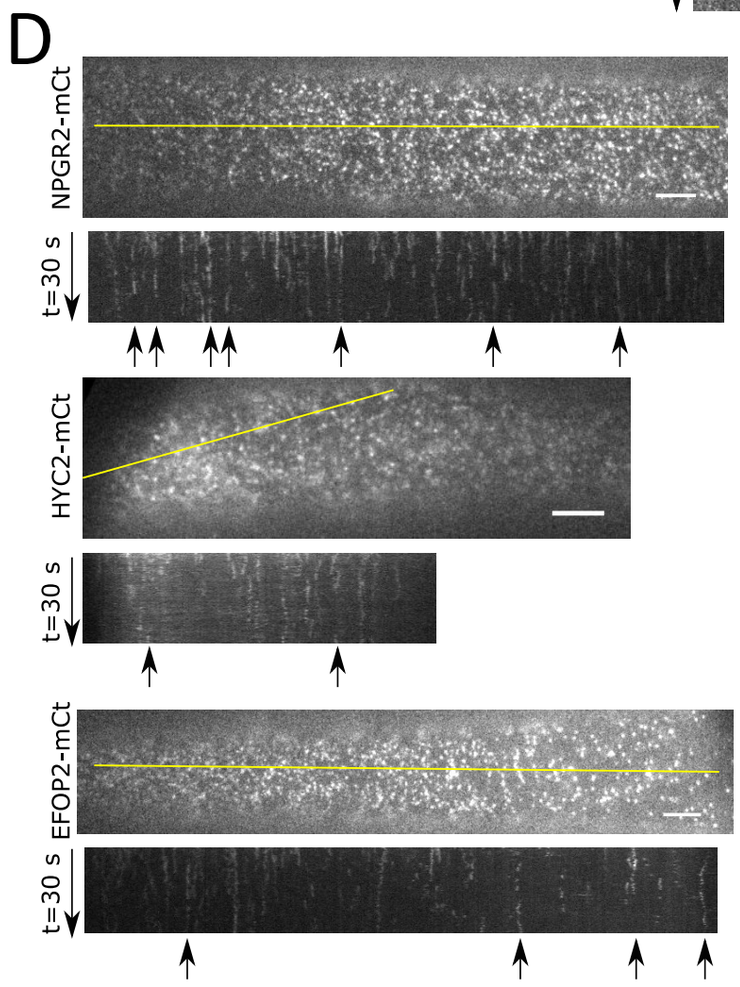

Figure 6. (A) Confocal images of P4M, NPGR2-mCt, HYC2-mCt and EFOP2-mCt before photobleaching (prebleach) and at the time indicated after photobleaching. Scale bars: 2µm. **(B)** Kymographs along the membrane for the time laps in (A). Scale bars: 2µm. **(C)** Graphics presenting the signal intensity over time for the photobleached (in red) and for control regions (in blue) on the same cells. The light colour curves represent the standard deviation. The number of zones measured is 5, 30, 5 and 26 for P4M, NPGR2-mCt, HYC2-mCt and EFOP2-mCt, respectively. **(D)** Confocal images of TIRF microscopy at t=0s for NPGR2-mCt, HYC2-mCt and EFOP2-mCt. The kymographs over 30s corresponding to the yellow lines are shown. Black arrows indicate position were the signal reappeared. Scale bars: 5µm.

thus tested the potential role of those two elements in the recruitment of the PI4Kα1 complex at the plasma membrane.

First, we evaluated the role of the polybasic patch in the N-terminus of EFOP proteins. Indeed this region could be involved in targeting the entire PI4Kα1 complex to the plasma membrane through electrostatic interactions with anionic lipids, notably PI4P. In EFOP2, this region goes from the aa 27 to the aa 39 and contains 7 positively charged residues. We mutated all lysines/arginines into neutral glutamines and generated a *UBQ10prom::EFOP2-7Q-mCITRINE* construct. We observed that EFOP2-7Q-mCITRINE was soluble when transiently expressed in *Nicotiana benthamiana* leaf cells while wild-type EFOP2-mCITRINE was localized to the plasma membrane indicating that polybasic patch in EFOP2 could be essential for plasma membrane targeting **(Figure 7, B)**. We next introduced the *UBQ10prom::EFOP2-7Q-mCITRINE* construct in *Arabidopsis* epidermal root cells. However we did not retrieve any lines with a detectable fluorescent signal. It is likely that *EFOP2-7Q-mCITRINE* is unstable either because of miss folding or because EFOP2 needs to be associated with membrane to remain stable when expressed in *Arabidopsis*. Finally, we directly investigated the role of PI4P in the recruitment of the PI4Kα1 complex, by using PAO, a PI4K inhibitor. In this condition, the PI4P sensor is detached from the plasma membrane and relocalized in the cytosol **(Figure 7, C)**. However, neither NPGR2-mCt, HYC2-mCt nor EFOP2-mCt were mislocalized upon PAO treatment. Furthermore, the dotty pattern on the plasma membrane remained. Thus, PI4P might not be involved in the targeting of the PI4Kα1 complex at the plasma membrane or the depletion of PI4P is not sufficient to delocalize PI4Kα1 complex. In any case, this indicates that the presence of the PI4Kα1 complex at the plasma membrane relies on another mechanism.

We then investigated the role of the Cys-rich motif, which was deleted in the *efop4-4* allele. This motif is known to be a potential site of S-Acylation; a lipid posttranslational modification that can anchor protein to the plasma membrane (Zaballa and Goot, 2018). Indeed, according to the SwissPalm database this motif is predicted as S-acetylated with a high (in blue) or medium level of confidence (in orange) **(Figure 7, A)**. Confirming this hypothesis, all four *Arabidopsis* EFOP proteins were found to be S-Acylated in a recent proteomic study (Kumar et al., 2020). Notably, all Cys-residues (underlined in Figure 7, A) within the Cys-rich region of EFOP3 and EFOP4 were found to be S-acylated with high confidence *in planta* (Kumar et al., 2020). To experimentally test the importance of such lipid modification in EFOP localization, we mutated the two conserved cysteines (C20 and C23) into serine and generated a *UBQ10prom::EFOP2-CC-mCITRINE* construct. Similar to EFOP2-7Q-mCITRINE, we observed that EFOP2-CC-mCITRINE was soluble when transiently expressed in *Nicotiana benthamiana* leaf cells **(Figure 7, B)**. Next, we transformed the *UBQ10prom::EFOP2-CC-mCITRINE* construct into *Arabidopsis* and found that EFOP2-CC-mCITRINE was not localized at the plasma membrane of root meristematic cells and instead accumulated in intracellular structures **(Figure 7, B)**. All together, this data suggest that EFOP2 is likely targeted to the plant plasma membrane using lipid anchoring.

The EFOP/NPG/HYC complex localizes PI4Kα1 in the cell

We then asked if EFOP proteins were sufficient to determine the localization of PI4Kα1 in the cell. Taking advantage of the EFOP2-CC construct that localized in intracellular structures, we introgressed NPGR2-2xmCHERRY or PI4Kα1-2xmCHERRY in plants expressing EFOP2-CC-mCITRINE and analyzed if EFOP2-CC was able to recruit NPGR2 or PI4Kα1 in those intracellular structures. We observed a weak signal of NPGR2

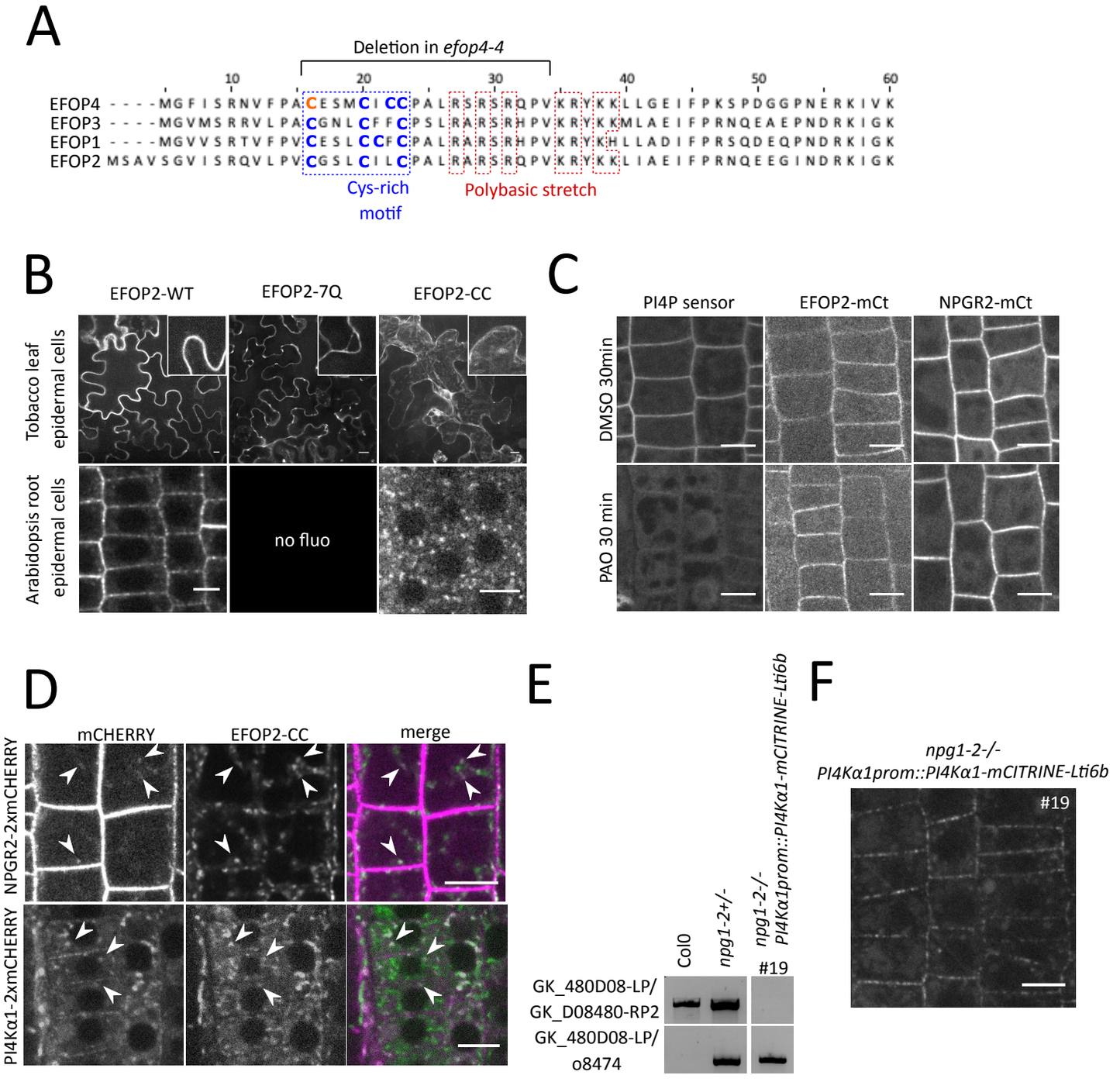

Figure 7. (A) N-terminal sequence alignment of EFOPs proteins. The conserved cys-rich motif (in blue) and polybasic patch (in red) are indicated, as well as, the deletion in *efop4-4* CrisPr allele. The bold cysteines are predicted as S-acetylated on the SwissPalm database with high (blue) and medium (orange) confidence level. **(B)** Confocal images of EFOP2-mCITRINE (wild type), EFOP2-7Q-mCITRINE and EFOP2-CC-mCITRINE in N. benthamiana leaf epidermal cells and Arabidopsis root epidermal cells. Scale bar: 10µm. **(C)** Confocal images of a PI4P sensor (PH domain of FAPP1 carrying the mutation E50A), EFOP2-mCITRINE (EFOP2-mCt) and NPGR2-mCITRINE (NPGR2-mCt) treated for 30min with 30µM PAO or the equivalent volume of DMSO. Scale bars: 10µm **(D)** Confocal images of Arabidopsis root epidermal cells co-expressing EFOP2-CC-mCITRINE and NPGR2-2xmCHERRY or PI4Kα1-2xmCHERRY. White arrows indicate internal structures where the two signals co-localize. Scale bar: 10µm. **(E)** Genotyping of Col0, *npg1-2* heterozygous plants and *npg1-2* homozygous plants complemented with *PI4Kα1prom::PI4Kα1-mCITRINE-Lti6b* (insertion n°19). The upper panel shows the amplification of the gene sequence. The lower panel shows the amplification of the T-DNA border. **(F)** Confocal images of *PI4Kα1::PI4Kα1-mCITRINE-Lti6b* in *npg1-2-/-* background (insertion n°19).

labelling intracellular compartments that partially colocalize with EFOP2-CC-containing structures. Similarly, PI4Kα1 was not only at the plasma membrane and soluble in the cytosol but also associated with the EFOP2-CC-containing structures **(Figure 7, D)**. This showed that EFOP is able to recruit NPGR2 and PI4Kα1 in different compartments of the cell.

Because NPG proteins likely bridges PI4Kα1 to the membrane-binding EFOP subunits, we reasoned that they should contribute to the targeting of PI4Kα1 at the plasma membrane. To test this hypothesis, we generated a fusion between PI4Kα1-mCITRINE and the transmembrane protein Lti6b in order to artificially target PI4Kα1 at the plasma membrane and thus bypass the role of the NPG/HYC/EFOP complex. We transformed the *npg1-2* mutant with the *PI4Kα1prom::PI4Kα1-mC*ITRINE-*Lti6b* construct, and found a line able to complement the *npg1-2* mutant **(Figure 7, E)**. This indicates that *npg1* pollen lethality is likely due to the absence of PI4Kα1 at the plasma membrane during pollen development. In these plants, PI4Kα1-mCITRINE-Lti6b is located in clusters at the plasma membrane while Lti6b is known as being rather homogenously localized at the plasma membrane **(Figure 5, D and 7, G)**. The chimeric PI4Kα1-mCITRINE-Lti6b proteins might be restricted in clusters by other factors, which indicates that the subcompartimentalization of PI4Kα1 complex might not be an intrinsic property of the complex but rather come from interactions between PI4Kα1 and other lipids or proteins. Furthermore, it might indicate that the subcompartimentalization of PI4Kα1 complex is an essential feature for the proper function of the complex.

Discussion and conclusion

PI4Kα1 complex is essential for cell survival

In this study, we showed that the loss of function of the PI4Kα1 complex lead to lethality of the male gametophyte or of the embryo in the case of the *hyc2* mutants. Furthermore, artificial microRNA strategy did not allow us to retrieve plants with very strong phenotypes. This is concordant with the idea that PI4Kα1 has a critical role for the cell function. PI4P is crucial for the plasma membrane surface charge (Platre et al., 2018; Simon et al., 2016). Thus, it is likely that the loss of the PI4Kα1 affects the membrane surface charge and lead to the mislocalization of a whole set of proteins. For instance PINOID or D6-Kinase plasma membrane localization requires PI4P and are likely delocalize in *pi4kα1* mutant (Barbosa et al., 2016; Simon et al., 2016).

PI4Kα1 complex loss-of-function might alter the general lipid homeostasis

The absence of the PI4Kα1 complex might have indirect consequences for other anionic lipids. The plasma membrane surface charge is also maintained by phosphatidylserine (PS) and phosphatidic acid (PA) in plant cell (Platre et al., 2018). However, PS is synthesized in the ER (Yamaoka et al., 2011). In yeast and animals, PS can reach the plasma membrane through vesicular trafficking and non-vesicular trafficking at ER-Plasma membrane contact site (EPCS). At these contacts, the oxysterol-binding related protein (ORP) family mediates PS exchanges against PI4P (Chung et al., 2015a; Moser von Filseck et al., 2015; Wu et al., 2018). This requires a gradient of PI4P between the plasma membrane and the ER membrane. This mechanism has not been described in plants, however similar contacts between the ER and the plasma membrane exist and the ORP family is conserved. We can speculate that alike exchanges of lipids are found in

plants and would be perturbed in the absence of the PI4Kα1 complex at the plasma membrane affecting the pool of PS.

PI4P is also the only precursor of $PI(4,5)P_2$ in plants (Gerth et al., 2017). $PI(4,5)P_2$ has an essential role at the plasma membrane as it is involved in the regulation of endocytosis, exocytosis, and protein recycling. We do not know exactly if in the absence of the PI4Kα1 complex at the plasma membrane, $PI(4,5)P_2$ can still be produced from TGN/EE PI4P for instance or if vesicular trafficking is also impaired.

The TGN/EE pools of PI4P cannot compensate for the loss of the PI4Kα1 complex

The interdependence of the TGN/EE and the plasma membrane pool of PI4P remained an open question. PI4P could be exchanged by vesicular trafficking between the two compartments. The fact that *pi4kβ1β2* double mutant and *pi4kα1* mutant display developmental phenotypes suggest that one pool of PI4P is not sufficient to compensate the loss of the other pool. However, we can imagine that small amount of PI4P is exchanged in normal condition but that the loss of the enzymes perturbed the endocytosis and exocytosis making compensatory exchange of PI4P impossible. Of note, the loss of either *pik1* and *sst4* is lethal in yeast. By contrast, only PI4Kα1 appears to be essential in plants, while the *pi4kβ1β2* double mutant has only a mild phenotype. This mirrors the strong accumulation of PI4P at the plasma membrane by comparison to the TGN in plant cells. It is thus possible that incoming PI4P from the plasma membrane to the TGN following endocytosis can somehow partially compensate for the lack of PI4P production locally at the TGN.

PI4Kα1 clusters reflect a functional unit

The PI4Kα1 complex localize at the plasma membrane in nanodomains. In yeast, Stt4 is

also found in clusters called PIK patches (Baird et al., 2008). However, the clusters of Stt4 do not correlate with clusters of PI4P that probably diffuse laterally in the membrane. Similarly in *Arabidopsis*, PI4P biosensors are not clustering at the plasma membrane. This is concordant with data *in vitro* showing that its product PI4P inhibits the catalytic activity of PI4Kα1 (Stevenson-Paulik et al., 2003). In addition, we show that these nanodomains are immobile. Do these nanodomains correspond to a functional unit? They could correspond to ER-plasma membrane contact sites. Indeed, in yeast, stt4 reside at these contacts (Omnus et al., 2018). Another hypothesis is that they could correspond to a zone of attachment between the plasma membrane and the actin cytoskeleton. Indeed, PI4Kα1 has been purified from F-actin-rich fraction from carrots and to associate with polymerized F-actin *in vitro* (Stevenson et al., 1998). Additionally, in yeast, Stt4 is necessary for a proper actin cytoskeleton organization (Audhya et al., 2000; Foti et al., 2001). The two hypotheses are not mutual exclusive. Indeed, the actin disorganization phenotype of Stt4 mutant is rescued in yeast by the knockout of Sac1, a PI4P phosphatase that reside in the ER membrane (Foti et al., 2001). Stt4 and Sac1 together control the PI4P gradient at EPCS.

A recent paper shows that $PI(4,5)P_2$ is enriched in nanodomains at the plasma membrane in pollen tubes (Fratini et al., 2020). These domains associate with PIP5K2 and stabilization of actin cytoskeleton. We can hypothesized that PI4Kα1 complex could also be targeted to these nanodomains in order to catalyse a phosphorylation cascade from PI to PI4P to $PI(4,5)P_2$. In this model, PI4Kα1 inhibition by its substrate could help to coordinate the following phosphorylation by PIP5K2.

PI4Kα1 complex targeting to the plasma membrane mechanism is conserved

Previous studies of the sequence of PI4Kα1 revealed the presence of a Plecktrin Homology (PH) domain upstream from the catalytic domain that is also conserved in yeast Stt4 and animal PI4KIIIα (Stevenson et al., 1998; Stevenson-Paulik et al., 2003; Xue et al., 1999). This PH domain was first thought to localize PI4Kα1 at the plasma membrane through interaction with anionic phospholipids. However, more recent studies on the structure of the complex in yeast and mammalian cells by cryoEM characterize this region as a N-lobe and helical domain involved in the interaction with Ypp1/TTC7 (Dornan et al., 2018; Lees et al., 2017; Wu et al., 2014). Our study also showed that PI4Kα1 plasma membrane localization is rather mediated by interactions with NPG and EFOP proteins than by a PH domain. Similarly to yeast and animal, EFOP interacts with the plasma membrane thanks to a S-acylation and/or polybasic patches on the N-terminal end (Wu et al., 2014). Several S-acylated peptides in addition to the one in the N-terminal region have been found in EFOP proteins (Kumar et al., 2020). As S-acylation is a reversible posttranslational modification, differential S-acylation could be a mechanism explaining the different localization observed for EFOP1 and EFOP2 in the cell. Another hypothesis suggest that this PH domain of PI4Kα1 could mediate interaction with actin as PI4Kα1 deleted of the PH domain is less enriched in the F-actin-rich fraction.

PI4Kα1 complex might participate in Ca^{2+} signalling

NPG proteins are annotated as calmodulin-binding protein. Indeed, NPG1 can interact with several Cam isoforms in presence of Ca^{2+} and has been suggested to play a role in Ca^{2+} dependent pollen tube germination (Golovkin and Reddy, 2003). However, Ca^{2+} is also intimately connected with phosphoinositides, membrane properties and

endomembrane trafficking (Himschoot et al., 2017). Ca^{2+} can directly bind anionic phospholipids modulating locally membrane electrostatics, preventing or promoting the recruitment of lipid binding protein, inducing the formation of $PI(4,5)P_2$ clusters and facilitating membrane fusion. As phosphoinositides can bind Ca^{2+}, diffuse in the membrane and release Ca^{2+} somewhere else, they have been suggested to buffer and modulate $Ca2^{+}$ signalling at the subcellular level. Ca^{2+} is also known to regulate many actors of endomembrane trafficking including regulators of the cytoskeleton, TPLATE complex, ANNEXINs and SYNAPTOTAGMINs. For instance, the ER-Plasma membrane tethers protein SYT1 contains C2 domains that bind Ca^{2+} and phosphoinositides (Giordano et al., 2013; Idevall-Hagren et al., 2015; Lee et al., 2019; Yamazaki et al., 2008). As previously mention, PI4Kα1 complex could localize at EPCS and participate to the Ca^{2+} signalling at this junction through calmodulin binding.

HYCCIN is an essential subunit in Arabidopsis

If EFOPs are anchoring the complex at the membrane and NPG are bridging PI4Kα1 with EFOP, the role of HYCCIN in the complex is less clear. *hyc1* and *hyc2* mutants are lethal suggesting that HYC is an essential subunit for the complex to function. In mammals, FAM126/HYC is necessary to stabilize the complex and is used as a scaffold by TTC7 to be shaped around (Dornan et al., 2018). However, knockout of FAM126A loss of function is not lethal while loss-of-function of PI4KIIIα is (Baskin et al., 2016). It is likely that FAM126B, its paralog, compensates the loss of FAM126A. Loss of FAM126A leads to a decrease in the amount of TTC7A and EFR3A protein, which are probably unstable. However, in animal cells, PI4KIIIalpha, which alone is soluble, can be recruited at the plasma membrane when co-expressed with TTC7 and EFR3 only (Chung et al., 2015b; Nakatsu et al., 2012). This suggests that FAM126 is not necessary for the complex to

form and localize at the plasma membrane. Thus, FAM126 is likely needed to stabilize the complex. In human, mutations - knockout or truncated protein or even single point mutation that retains FAM126A in the ER due to misfolding - lead to severe case of hypomyelination and congenital cataract (Baskin et al., 2016; Miyamoto et al., 2014). The presence of FAM126/HYC is required for the complex to properly function in both animal and plant while it is not conserved in yeast.

To conclude, the PI4Kα1 complex is at the heart of anionic lipid homeostasis. It is structurally conserved among eukaryotes and likely the place of many regulations. Thus, it will be highly interesting to study its dynamic during different physiological and developmental context in plants.

Material and methods

Plant Material

The Columbia (Col0) ecotype of the plant model Arabidopsis thaliana was used in this study, except *pi4kα1-2*, which is in Ws background.

In vitro culture conditions for segregations or microscopy

Seeds were surface-sterilized by addition of 4ml of HCl 37% in 100mL of bleach for four hours before plating on Murashige and Skoog (MS, Duchefa Biochemie®) media containing the appropriate antibiotic or herbicide. Basta, Kanamycin, Hygromycin and Sulfadyacin have been used at $10mg.L^{-1}$, $50mg.L^{-1}$, $30mg.L^{-1}$ and $75mg.L^{-1}$ respectively. Plates were placed under continuous white light conditions for 7 to 10 days. Resistant and sensitive seedlings were counted for segregations.

Culture condition on soil

Seeds were directly sown in soil or 7 days seedlings were transferred from in vitro plates to soil. Plants were grown at 21°C under long day condition (16 hrs light, LED 150µmol/m^2/s).

CrisPr lines

20bp target sequence upstream to a 5'-NGG -3' sequence in an exon of the gene of interest were found using the CrisPr RGEN tool (www.rgenome.net/). Primers were designed following the methods developed in Xing et al., BMC Plant Biology 2014 and Wang *et al.*, Genome Biology, 2015 **(Table 4)**.

T-DNA and CrisPr Mutant Genotyping

Leaf tissue from wild-type plants, T-DNA insertion lines and CrisPr lines were collected, frozen in liquid nitrogen and ground to powder. The powder was resuspended in the extraction buffer (200mM of Tris pH 7.5, 250mM of NaCl, 25mM of EDTA, 0.5% of SDS). DNA was precipitated with isopropanol and the DNA pellet was washed with 75% ethanol before resuspension in water.

Plants were genotyped by PCR using the GoTaq® polymerase (Promega®) and the indicated primers **(Table 5)**. PCR products were migrated on 1% agarose gel or the percentage indicated **(Table 5)**, purified using the NucleoSpin Gel and PCR Clean kit (Macherey-Nagel®) and sequenced.

Pollen observation by SEM

Pollen grains from mutant or WT flowers were placed on tape and observed using the mini SEM Hirox® 3000 at -10°C, 10kV.

Pollen inclusion and observation by TEM

For transmission electron microscopy, anthers were placed into in a fixative solution of 3.7% paraformaldehyde and 2.5% glutaraldehyde, Na2HPO4 0.1M, NaH2PO4 0.1M overnight and postfixed in 1% OsO4, Na2HPO4 0.1M, NaH2PO4 0.1M. Anthers were dehydrated through a graded ethanol series from 30% to 100% and embedded in SPURR resin. Sections were made using an ultramicrotome Leica UC7 at 70-80nm and poststained with Acetate Uranyle 5% (in Ethanol), Citrate Plomb (in NaOH). Pollen were observed using a transmission electron microscope Philips CM120.

Pollen staining

To perform Alexander staining, flowers that were about to open were dissected and anthers were put between slide and coverslip in Alexander staining solution (25% glycerol, 10% EtOH, 4% acetic acid, 0.05% acid fuchsin, 0.01% Malachite green, 0.005% phenol, 0.005% chloral hydrate, 0.005% Orange G,) for 7h at 50°C before observation under a stereomicroscope.

For DAPI staining, flowers that were about to open were dissected and their anthers were put between slide and coverslip in DAPI solution (10% DMSO, 0.1% NP-40, 50mM PIPES, 5mM EGTA, 0.01% (4',6-diamidino-2-phénylindole) DAPI) for 5min at RT before observation at the confocal microscope. DAPI was excited with a 405nm laser (80mW)

and fluorescence emission was filtered by a 447/60 nm BrightLine® single-band bandpass filter (Semrock, http://www.semrock.com/).

For calcofluor staining, flower buds were fixed in PFA 4% for 1 hour and cleared using clearsee (Kurihara et al., 2015) for 2 weeks. Callose was stain by addition of calcofluor white 0.1% for 30min and observed with confocal microscope. Calcofluor was excited with a 405nm laser (80mW) and fluorescence emission was filtered by a 447/60 nm BrightLine® single-band bandpass filter (Semrock, http://www.semrock.com/).

Seed clearing

Siliques were opened. The replums with the seeds attached were placed between slide and coverslip in clearing solution (87.5% chloral hydrate, 12.5% glycerol) for 1 hour before observation at the microscope with differential interference contrast.

Cloning of reporter lines

Coding gene or genomic gene sequences and 3'UTR sequences were cloned using Gateway® technology (Invitrogen®). Promoter sequences were cloned by Gibson Assembly method (Biolab®). The coding sequences were amplified by PCR using the high fidelity Phusion Hot Start II (Thermo Fisher Scientific®) taq polymerase and the indicated primers and template **(Table 6)**. The PCR products were purified using the NucleoSpin Gel and PCR Clean kit (Macherey-Nagel®) and recombined in the indicated vector using BP Clonase™ II Enzyme Mix (Invitrogen®) or Gibson Assembly mix (Biolab®) **(Table 6)**. Thermocompetent DH5α *E. coli* were transformed with the corresponding vectors and plate on LB (Difco™ LB Broth, Lennox, #214010, 20 g/L, 15% agar, Difco™ Bacto Agar) containing the Kanamycin at 50mg.L^{-1}. Plasmids were purified

using the Nucleospin Plasmid kit (Macherey-Nagel®) and inserts sequenced. Expression vectors containing the promoter-gene-fluorescent tag cassette or 3'UTR were obtained by using LR clonase-based three-fragment recombination system (Invitrogen®), the pB7m34GW/pH7m34GW/pK7m34GW/pS7m43GW/ pLOK180_pR7m34g destination vectors, and the corresponding entry vectors. Thermocompetent DH5α cells were transformed and selected on LB plate (Difco™ LB Broth, Lennox, #214010, 20 g/L, 15% agar, Difco™ Bacto Agar) containing 100mg.L^{-1} of Spectinomycin. Plasmids were purified using the Nucleospin Plasmid kit (Macherey-Nagel®) and inserts sequenced.

Artificial microRNA designed

Artificial microRNA were designed using Web MicroRNA Designer (http://wmd3.weigelworld.org/cgi-bin/webapp.cgi). DNA synthesis containing AttB1-AttB2 sites and the miR319a modified with the sequence of the artificial microRNA **(Table 7)** were ordered at Integrate DNA Technology® (IDT). The DNA were recombined in the pDONR 221 (Invitrogen®) using BP Clonase™ II Enzyme Mix (Invitrogen®).

Directed mutagenesis

Plasmids were amplified by PCR using the high fidelity Phusion Hot Start II (Thermo Fisher Scientific®) taq polymerase and the indicated primers carrying mutations **(Table 8)**. PCR products were digested using and cutsmart buffer (Biolab®). Thermocompetent DH5α *E. coli* were transformed with the digested PCR product and plate on LB (Difco™ LB Broth, Lennox, #214010, 20 g/L, 15% agar, Difco™ Bacto Agar) containing the

appropriate antibiotic. Plasmids were purified using the Nucleospin Plasmid kit (Macherey-Nagel®) and mutations were sequenced.

Agrobacterium transformation

Electrocompetent *A. tumefaciens* (C58pmp90) were transformed by electroporation. 1µL of DNA plasmid at a concentration of 0.25-1 µg/µl was added into 50 µL of electrocompetent agrobacterium on ice. The agrobacterium were transfered into cold 1mm wide electroporation chamber (Eurogentec, #CE00150). A pulse of 2 kV, 335 Ω, 15µF, for 5 ms was performed on the electroporation chamber using the MicropulserTM (Bio-Rad, #165-2100). 1 mL of liquid LB media was added and the bacteria were placed into a new tube and incubated at 29°C for 2-3h. The agrobacterium were selected on LB (Difco™ LB Broth, Lennox, #214010, 20 g/L, 15% agar, Difco™ Bacto Agar) or YEB (0.5% beef extract, 0.1% yeast extract, 0.5% peptone, 0.5% sucrose, 1.5% bactoagar, pH7.2) plates containing the appropriate antibiotics to select the agrobacterium strain (50mg.L-1 of Rifampicin and 20mg.L-1 of Gentamycin) and the target construct (250mg.L-1 of Spectinomycin). Plates were incubated at 29°C for 48h.

Plant Transformation

Agrobacterium were spun and resuspended in 5% sucrose and 0.02% Silwet L-77 detergent. *Arabidopsis* were transformed by floral dipping.

Transformed seedlings were selected on Murashige and Skoog (MS, Duchefa Biochemie®) media containing the appropriate antibiotic or herbicide. Basta, Kanamycin, Hygromycin and Sulfadyacin have been used at $10mg.L^{-1}$, $50mg.L^{-1}$, $30mg.L^{-1}$ and $75mg.L^{-1}$ respectively.

Artificial microRNA phenotype

Surface-sterilized seeds were plated on Murashige and Skoog (MS, Duchefa Biochemie®) media supplemented or not with sucrose (10g per L) containing 5µM β-estradiol or the equivalent volume of DMSO. Plates were vernalized 3 days before being placed under continuous white light conditions for 11 days. Plates were scanned. Root length and horizontal gravity angles were measured using ImageJ software.

Protein extraction, immunoprecipitation and western blot analysis

Leaf tissue from wild-type plants and/or transgenic lines were collected, frozen in liquid nitrogen and ground to powder. The powder was resuspended in -20°C MetOH; 1% Protease inhibitor (P9599, Sigma-Aldrich®) and incubated at -20°C for 5min. Proteins were pelleted, resuspended in -20°C acetone and incubated at -20°C for 5min. Proteins were pelleted. The pellet was dried and resuspended in Protein Extraction Reagent (C0856, Sigma-Aldrich®) supplemented with 1% Protease inhibitor (P9599, Sigma-Aldrich®). Protein extraction were then kept at -20°C.

Protein samples in 1xSDG (Tris-HCL 0.25M, 10% glycerol, 2% DTT, 2.5% SDS) supplemented with bromophenol blue were denaturated at 95°C for 5min. Samples migrated on 7,5% (for proteins over 200kDa) or 10% SDS-PAGE polyacrylamide gel at 140V with 1xTris-Glycine SDS running buffer (Euromedex®). Proteins were transferred on nitrocellulose membrane 0.45 µm in 1xTris-Glycine (Euromedex®), 20%EtOH transfer buffer at 100V for 1h. Membrane were blocked with 5% milk, 1X PBS-T (Phosphate Buffer Saline) (Dominique Dutscher®), 2% Tween® 20 for 1h. Primary antibodies **(Table 9)** were used at 1/2000[e] in 5% milk, 1X TBS, 0.1% Tween 20

overnight. Secondary antibodies were used at 1/5000e in 1X TBS, 0.1% Tween 20 for 1h. Protein revelation was done using the Clarity or Clarity Max ECL Western Blotting Substrates (Biorad®) and the Chemidoc MP imaging system (Biorad®).

For co-immunoprecipitation, leaf tissue from transgenic lines were collected, frozen in liquid nitrogen and ground to powder. Proteins fused to mCITRINE were immunoprecipitated using the pull down kit Miltenyi µMacs anti-GFP (Miltenyi Biotec®). Crude extracts were put in 1XSDG supplemented with bromophenol blue and denaturated at 95°C for 5min while IP samples were directly ready for migration on polyacrylamide gels.

Confocal Imaging setup

7 to 10 days-old seedlings were observed with an Zeiss microscope (AxioObserver Z1, Carl Zeiss Group, http://www.zeiss.com/) with a spinning disk module (CSU-W1-T3, Yokogawa, www.yokogawa.com) and a Prime 95B camera (Photometrics, https://www.photometrics.com/) using a 63x Plan-Apochromat objective (numerical aperture 1.4, oil immersion) and the appropriated laser and bandpath filter.

GFP was excited with a 488 nm laser (150mW) and fluorescence emission was filtered by a 525/50 nm BrightLine® single-band bandpass filter (Semrock, http://www.semrock.com/). mCITRINE was excited with a 515nm laser (60mW) and fluorescence emission was filtered by a 578/105 nm BrightLine® single-band bandpass filter (Semrock, http://www.semrock.com/). mCHERRY was excited with a 561nm laser (80mW) and fluorescence emission was filtered by a 609/54 nm BrightLine® single-band bandpass filter (Semrock, http://www.semrock.com/).

Immunolocalization

5 days-olds seedlings were fixed in PFA 1%, MTBS (50mM PIPES, 5mM EGTA, 5mM MgS04, pH7) for 1h. Roots were Superfrost Plus® slides (Thermo Scientific, #10149870) and dried at RT for 1h and rehydrated using MTBS + 0.1% tritonx100. Permeabilization was done using 2% Driselase (Sigma, # D9515) in MTSB for 30 min. Roots were treated with 10% dimethylsulfoxide, 3% Igepal (Sigma, #CA-630) in MTSB for 1 h. Blocking was done using 5% normal goat serum (NGS Sigma #G9023) in MTSB. Roots were incubating overnight with the primary antibody diluted at 1/100 (anti-PI4Kα1) and with secondary antibody diluted at 1/500 for 3h (anti Rat IgG, alexa Fluor 488 conjugate, InVitrogen-Molecular Probes, #A-21210). Roots were placed between slide and coverslip in Vectashield® (Vectorlabs, #H-1000-10) and observed using a confocal microscope Zeiss 800.

Microsomes and plasma membrane purification

Microsomes were purified as described in (Simon-Plas et al., 2002) and resuspended in phosphate buffer (5 mM, pH 7,8) suppelemented with sucrose (300 mM) and KCl (3 mM). PM were obtained after cell fractionation by partitioning twice in a buffered polymer two-phase system with polyethylene glycol 3350/dextran T-500 (6.6% each).

For PI4Ka1, proteins were precipitated using 5 volumes of -20°C acetone for 1 volume of protein extraction and incubated for 10min at -20°C. Proteins were pelleted. This process was repeated 2 more times. Pellet was dried and resuspended in 1xSDG supplemented with bromophenol blue. All steps were performed at 4 °C.

Yeast-two-hybrid

AD vectors (prey) and DB vectors (bait) were transformed in the Y8800 and Y8930 yeast strains, respectively. Transformed yeasts were plated on SD (0.67% yeast nitrogen base, 0.5% dextrose anhydrous, 0.01% adenine, 1.8% agar) with all amino acids except tryptophan (SD-T) for AD vectors and SD-L for DB vectors for selection.

Yeast colony transformed with AD- or DB- vectors were grown in SD-T and SD-L liquid media, 30°C, 200rpm for 48h. Mating was performed at 30°C, 200rpm, overnight using 10µl of AD and 10µl DB clones in 180µl YEPD (1% yeast extract, 2% peptone, 2% dextrose anhydrous, 0.01% adenine) liquid media. Diploid yeasts were selected by addition of 100µl of SD-LT liquid media. Yeast were grown for 48h at 30°C, 200rpm. Diploids yeasts were plates on the different selective media: SD-LT to verify the mating; SD-LTH to select the positive interactions; SD-LTH+3AT (3-Amino-1,2,4-Triazol at 1mM final) to select strong interactions only: SD-LH+CHX (cycloheximide at 10µg/mL final) to determine the autoactivated DB clones; SD-LH+CHX+3AT to determine which concentration of 3AT erase the autoactivation of DB clones.

Mass spec analysis

Mass spec analysis had been performed by the Protein Science Facility of SFR (Structure Fédérative de Recherche) Bioscience Lyon. Trypsine-digested samples were analysed by LC-MS/MS (Orbitrap, ThermoFischer Scientific®). The peptides identified were compare to UniProtKb database.

Sequence Analysis

Sequence alignments have been performed using the Muscle WS software and edited with Jalview 2.0 software. Clustal colour code has been used. Domains have been

identified using the SMART (Simple Modular Architecture Research Tool) software. Predicted lipid modification sites have been found using the GPS-Lipid software.

Plasmolysis

7 to 10 days-old seedlings were placed between side and coverslip in MES 10mM with or without 0.75M sorbitol and observed using a confocal microscope.

PAO treatment

7 to 10 days-old seedlings were incubated in liquid MS with 30µM PAO (Sigma, www.sigmaaldrich.com, PAO stock solution at 60 mM in DMSO) for 30 min before observation using a confocal microscope.

Tobacco leaf infiltration

Transformed agrobacterium were directly taken from plate with a tip and resuspended into 2 mL of infiltration media (10 mM MES, 10 mM MgCl2, 0.15 mM acetosyringone (Sigma-Aldrich®, #D134406)) by pipetting. The OD600 was measured using a spectrophotometer (Biophotometer, Eppendorf) and adjusted to 1 by adding infiltration media.

The infiltration was performed on « heart shape » tobacco leaves from 2-3 weeks old plants. Using 1 mL syringe (Terumo®, #125162229), the infiltration solution with the agrobacterium was pressed onto the abaxial side of the chosen tobacco leaf. The plants were put back to the growth chamber for 2-3 days under long day conditions.

5 mm2 regions of the leaf that surround the place where the infiltration has been made were cut. The pieces of leaf were mounted in water between slide and coverslip with the abaxial side of the leaf facing the coverslip. Using the appropriate wavelength, an

epifluorescent microscope and the smallest objective (10X), the surface of the leaf was screened to find the transformed cells. Then, the subcellular localization of the fluorescent protein was observed using a spinning confocal microscope and 63X objective.

Single Mutant

Gene	Locus	Name	T-DNA or CrisPr line	Zygosity	Phenotype observed	Detail
PI4Kα1	At1g49340	*pi4kα1-1*	GK502_D11	Heterozygous	Male sterility	Insertion in the 1st exon (208bp from ATG) of 26bp followed by two T-DNA in inverted tandem
		pi4kα1-2	FLAG_275H12	Heterozygous	Male sterility	Insertion in the 22nd intron (9087bp from ATG) of 28bp followed by one T-DNA
NPG1	At2g43040	*npg1-1*	SAIL_262_A01	Heterozygous	Male sterility	Insertion in the 3rd exon (734bp from ATG) of 22bp followed by two T-DNA in inverted tandem
		npg1-2	GK_480D08	Heterozygous	Male sterility	Insertion in the 3rd exon (1585bp from ATG) of 2bp followed by two T-DNA in inverted tandem and 16bp
NPGR1	At1g27460	*npgr1*	SALK_090514	Homozygous	None	Insertion in the 3rd exon (1152bp from ATG) of 13bp followed by two T-DNA in inverted tandem and 49bp
NPGR2	At4g28600	*npgr2-1*	CrisPr	Homozygous	None	Insertion of 1 T in the first exon at the 236 pb after the ATG leading a early codon stop and a truncated protein of 82aa
		npgr2-2		Homozygous	None	Deletion of 17 bp leading a early codon stop and a truncated protein of 76aa
HYC1	At5g21050	*hyc1*	GK_767H11	Heterozygous	Male sterility	Deletion of 10bp and insertion of two T-DNA ininverted tandem at 786bp from ATG
HYC2	At5g64090	*hyc2-2*	SALK_003807	Heterozygous	Embryo lethality	Insertion of 9bp followed by one T-DNA at 611bp from ATG
		hyc2-3	SALK_040977	Heterozygous	Embryo lethality	Deletion of 30bp and insertion of two T-DNA ininverted tandem at 705bp from ATG
EFOP1	At5g21080	*efop1*	GK_620B11	Homozygous	None	Insertion in the 9th exon (2118bp from ATG) of 11bp followed by two T-DNA in inverted tandem and 213bp
EFOP2	At2g41830	*efop2-1*	SALK_128017	Homozygous	None	Insertion in the 6th intron (1976bp from ATG) of one T-DNA
		efop2-2	GK_387B07	Homozygous	None	Insertion in the 11th intron (3829bp from ATG) of 10bp followed by two T-DNA in inverted tandem and 78bp
EFOP3	At1g05960	*efop3-1*	SALK_121262	Homozygous	None	Insertion in the 1st intron (136bp from ATG) of one T-DNA
		efop3-2	SALK_133976	Homozygous	None	Insertion in the 10th intron (2488bp from ATG) of 58bp followed by two T-DNA in inverted tandem and 28bp
EFOP4	At5g26850	*efop4-1*	SAIL_642H01	Homozygous	None	Insertion in the 5'UTR (19bp before ATG) of one T-DNA and 9bp
		efop4-2	CrisPr	Homozygous	None	Insertion of 1A in position 34 leading a early codon stop and a truncated protein of 42aa
		efop4-4		Homozygous	None	Deletion of 57bp leading to deletion of 19 aa including palmytoylation site and positive charges

Table 3.

	Gene	Locus	Name	T-DNA or CrisPr line	Zygosity	Phenotype observed
Double Mutant	NPG1 NPGR1	At2g43040 At1g27460	*npg1-1 npgr1*	SAIL_262_A01 / SALK_090514	NPG1 Heterozygous / NPGR1 Homozygous	About 10% of shrivelled pollen
			npg1-2 npgr1	GK_480D08 / SALK_090514		
	NPGR1 NPGR2	At1g27460 At4g28600	*npgr1 npgr2-1*	SALK_090514 / CrisPr	Double Homozygous	About 10% of shrivelled pollen
			npgr1 npgr2-2	SALK_090514 / CrisPr		Weak pollen phenotype / Growth phenotype
	EFOP1 EFOP2	At5g21080 At2g41830	*efop1 efop2-1*	GK_620B11 / SALK_128017	Double Homozygous	None
			efop1 efop2-2	GK_620B11 / GK_387B07		
	EFOP1 EFOP3	At5g21080 At1g05960	*efop1 efop3-1*	GK_620B11 / SALK_121262	Double Homozygous	None
			efop1 efop3-2	GK_620B11 / SALK_133976		
	EFOP1 EFOP4	At5g21080 At5g26850	*efop1 efop4-1*	GK_620B11 / SAIL_642H01	No doube homozygous	About 50% of shrivelled pollens when efop1 is homozygous and efop4-1 is heterozygous
			efop1 efop4-2	GK_620B11 / CrisPr	Double Homozygous	None
			efop1 efop4-4	GK_620B11 / CrisPr		
	EFOP2EFOP3	At2g41830 At1g05960	*efop2-1 efop3-1*	SALK_128017 / SALK_121262	Double Homozygous	From 70 to 90% of deformed or shrivelled pollen grains
			efop2-1 efop3-2	SALK_128017 / SALK_133976		
			efop2-2 efop3-1	GK_387B07 / SALK_121262		
			efop2-2 efop3-2	GK_387B07 / SALK_133976		
	EFOP2 EFOP4	At2g41830 At5g26850	*efop2-1 efop4-1*	SALK_128017 / SAIL_642H01	Double Homozygous	None
			efop2-2 efop4-1	GK_387B07 / SAIL_642H01		
	EFOP3 EFOP4	At1g05960 At5g26850	*efop3-1 efop4-1*	SALK_121262 / SAIL_642H01	No doube homozygous	About 50% of shrivelled pollens when efop3-1 is homozygous and efop4-1 is
			efop3-1 efop4-2	SALK_121262 / CrisPr		About 50% of deformed or shrivelled pollen grains
			efop3-1 efop4-4	SALK_121262 / CrisPr		
			efop3-2 efop4-1	SALK_133976 / SAIL_642H01		About 50% of shrivelled pollens when efop3-2 is homozygous and efop4-1 is
			efop3-2 efop4-2	SALK_133976 / CrisPr		About 50% of deformed or shrivelled pollen grains
			efop3-2 efop4-4	SALK_133976 / CrisPr		
Triple Mutant	NPG1 NPGR1 NPGR2	At2g43040 At1g27460 At4g28600	*npg1-2 npgr1 npgr2-1*	SAIL_262_A01 / SALK_090514 / CrisPr	NPG1 Heterozygous / NPGR1 and NPGR2 Homozygous	Dwarfism
			npg1-2 npgr1 npgr2-2	SAIL_262_A01 / SALK_090514 / CrisPr		
	EFOP1 EFOP2 EFOP3	At5g21080 At2g41830 At1g05960	*efop1 efop2-1 efop3-1*	GK-620B11 / SALK_128017 / SALK_121262	Triple homozygous	None

Table 3.(next part)

Gene mutated	Primer Name	Description	Primer Sequence (5'-3'; forward then reverse)
NPGR2	NPGR2-BsF	To obtain new Crispr lines using the egg especific promoter or 35S promoter vectors from Wang et al. Genome biology 2015. Cloning using Golden Gate reaction. Forward primer to clone a Single gRNA1 NPGR2 using pCBC-DT1T2 vector as a template. 4 primers PCR with primers NPGR2-F0 and NPGR2-R0 and NPGR2-BsR. Amplicon size around 620 bp. This primer contains de gRNA sequence and the BSAI cutting site. Original primer name in the protocol: DT1-BsF.	ATATATGGTCTCGATTGTTACGTAAATGCAACTTCTCGTT
	NPGR2-F0	To obtain new Crispr lines using the egg especific promoter or 35S promoter vectors from Wang et al. Genome biology 2015. Cloning using Golden Gate reaction. Forward primer to clone a Single gRNA1 NPGR2 using pCBC-DT1T2 vector as a template. 4 primers PCR with primers NPGR2-BsF and NPGR2-R0 and NPGR2-BsR. Amplicon size around 620 bp. This primer contains de gRNA sequence. Original primer name in the protocol: DT1-F0.	TGTTACGTAAATGCAACTTCTCGTTTTAGAGCTAGAAATAGC
	NPGR2-R0	To obtain new Crispr lines using the egg especific promoter or 35S promoter vectors from Wang et al. Genome biology 2015. Cloning using Golden Gate reaction. Reverse primer to clone a Single gRNA2 NPGR2 using pCBC-DT1T2 vector as a template. 4 primers PCR with primers NPGR2-BsF and NPGR2-F0 and NPGR2-BsR. Amplicon size around 620 bp. This primer contains de gRNA sequence. Original primer name in the protocol: DT2-R0.	AACagttatctctgcgtgagacgCAATCTCTTAGTCGACTCTAC
	NPGR2-BsR	To obtain new Crispr lines using the egg especific promoter or 35S promoter vectors from Wang et al. Genome biology 2015. Cloning using Golden Gate reaction. Reverse primer to clone a Single gRNA2 NPGR2 using pCBC-DT1T2 vector as a template. 4 primers PCR with primers NPGR2-BsF and NPGR2-F0 and NPGR2-R0. Amplicon size around 620 bp. This primer contains de gRNA sequence and the BSAI cutting site. Original primer name in the protocol: DT2-BsR.	ATTATTGGTCTCGAAACagttatctctgcgtgagacgCAA
EFOP4	EFOP4-BsFR	To obtain new Crispr lines using the egg especific promoter or 35S promoter vectors from Wang et al. Genome biology 2015. Cloning using Golden Gate reaction. Forward primer to clone a Single gRNA1 EFOP4 using pCBC-DT1T2 vector as a template. 4 primers PCR with primers EFOP4-F0 and EFOP4-R0 and EFOP4-BsR. Amplicon size around 620 bp. This primer contains de gRNA sequence and the BSAI cutting site. Original primer name in the protocol: DT1-BsF.	ATATATGGTCTCGATTGATGCACATACTCTCGCATGCGTT
	EFOP4-F0	To obtain new Crispr lines using the egg especific promoter or 35S promoter vectors from Wang et al. Genome biology 2015. Cloning using Golden Gate reaction. Forward primer to clone a Single gRNA1 EFOP4 using pCBC-DT1T2 vector as a template. 4 primers PCR with primers EFOP4-BsF and EFOP4-R0 and EFOP4-BsR. Amplicon size around 620 bp. This primer contains de gRNA sequence. Original primer name in the protocol: DT1-F0.	TGATGCACATACTCTCGCATGCGTTTTAGAGCTAGAAATAGC
	EFOP4-R0	To obtain new Crispr lines using the egg especific promoter or 35S promoter vectors from Wang et al. Genome biology 2015. Cloning using Golden Gate reaction. Reverse primer to clone a Single gRNA2 EFOP4 using pCBC-DT1T2 vector as a template. 4 primers PCR with primers EFOP4-BsF and EFOP4-F0 and EFOP4-BsR. Amplicon size around 620 bp. This primer contains de gRNA sequence. Original primer name in the protocol: DT2-R0.	AACgtcaagcgttacaagaaattCAATCTCTTAGTCGACTCTAC
	EFOP4-BsR	To obtain new Crispr lines using the egg especific promoter or 35S promoter vectors from Wang et al. Genome biology 2015. Cloning using Golden Gate reaction. Reverse primer to clone a Single gRNA2 EFOP4 using pCBC-DT1T2 vector as a template. 4 primers PCR with primers EFOP4-BsF and EFOP4-F0 and EFOP4-R0. Amplicon size around 620 bp. This primer contains de gRNA sequence and the BSAI cutting site. Original primer name in the protocol: DT2-BsR.	ATTATTGGTCTCGAAACgtcaagcgttacaagaaattCAA

Table 4.

Gene	Locus	Mutant Name	T-DNA or CrisPr line	Primer Name	Primer Sequence (5'-3'; forward then reverse)	Additional information for genotyping
PI4Kα1	At1g49340	*pi4kα1-1*	GK502_D11	GK502_D11-LP	ACCGGTTATACCGATTTGGTC	
				GK502_D11-RP2	TTGTTTCAGCAAGATATATCG	
		pi4kα1-2	FLAG_275H12	FLAG_275H12-RP	AGTCCTACCCTCCTGAACGAG	
				FLAG_275H12-LP	TCACGACATCTTTTGTCCAAAC	
NPG1	At2g43040	*npg1-1*	SAIL_262_A01	SAIL_262_A01-LP	AGTGAGAAGGGGGAAGATGAG	
				SAIL_262_A01-RP	AGTGTTCCAACGCTCAATACG	
		npg1-2	GK_480D08	GK_480D08-LP	AAGAAGTAATGCCTGGTGTGTTTA	
				GK_480D08-RP2	TGTGTTATTGTACAAGTTCTTC	
NPGR1	At1g27460	*npgr1*	SALK_090514	SALK_090514-LP	CCCTGGAATTGCTTCCTTTAC	
				SALK_090514-RP	TTTCTCTTGCGCTCGAATTAG	
NPGR2	At4g28600	*npgr2-1*	CrisPr	NPGR2-CPR-1	CTGTTCTTTCTCGAAATATG	Sequencing
				NPGR2-CPR-2	CCTTTAGACCGTCTTCTATG	
		npgr2-2		NPGR2-CPR-1	CTGTTCTTTCTCGAAATATG	Migration on 4% agarose gel
				NPGR2-CPR-3	CCTTTAGACCGTCTTCTATG	
HYC1	At5g21050	*hyc1*	GK_767H11	GABI_767H11-LP	CTTCCTCAAGCCATGACTCAC	
				GABI_767H11-RP	ACATCATCGACTTGCAGGATC	
HYC2	At5g64090	*hyc2-2*	SALK_003807	SALK_003807-LP	TGCCCCATTAGAAACAAACTG	
				SALK_003807-RP	ACTCAACTATACATCATAACC	
		hyc2-3	SALK_040977	SALK_040977-LP	TCAGACTCAATTCCCATGGAC	
				SALK_040977-RP	GAGAGGCTCTTGCGTACAATG	
EFOP1	At5g21080	*efop1*	GK_620B11	GABI_620B11_RP	GAGGATGCTAAAAACCCCAAG	
				GABI_620B11_LP	TTCGTCGTCAAAACTTTCACC	
EFOP2	At2g41830	*efop2-1*	SALK_128017	SALK_128017_RP	TGTGCCAATTAGGACTGGAAG	
				SALK_128017_LP	TTAAAACAGGGAATGCAATCG	
		efop2-2	GK_387B07	GABI387B07ch2_LP	TTCAAGCTATGGTCCATCCAG	
				GABI387B07ch2_RP	TTCAAACATAGCTCTCCCTCG	
EFOP3	At1g05960	*efop3-1*	SALK_121262	SALK_121262_RP	TTCTGGGTTTTCAGGGTTCTC	
				SALK_121262_LP	TCGACAAGAGTATTGCAACCC	
		efop3-2	SALK133976	SALK_133976_LP	AGGGCCAAGAAGATACCAAAG	
				SALK_133976_RP	CATGGGACTCATAACCACTGG	
EFOP4	At5g26850	*efop4-1*	SAIL_642H01	SAIL642H01ch5_LP	ACATTAATCGATGGAGCATCG	
				SAIL642H01ch5_RP	TTAGGGATACGGATTGGGTTC	
		efop4-2	CrisPr	EFOP4-CPR-1	GTATAGATGAGGTCTGGTTTC	Msl1 digestion and migration on 4% agarose gel
				EFOP4-CPR-2	GCAGGACAGCAAATGCACATACaCTCGCAT	
		efop4-4		EFOP4-CPR-1	GTATAGATGAGGTCTGGTTTC	Migration on 2% agarose gel
				EFOP4-CPR-3	TTAGGGATACGGATTGGGTTC	

Table 5.

Cloning of reporter lines

	Name	Sequence	Primer Sequence (5'-3'; forward then reverse)	Modifications	Template	Destination vector
Genes	PI4Kα1	Coding sequence from ATG to Stop	GGGGACAAGTTTGTACAAAAAAGCAGGCTTAACCATGGAGGCACTGACGGAGCTTTGTG	B1-Kozak sequence	cDNA from seedlings	pDONR 221
			GGGGACCACTTTGTACAAGAAAGCTGGGTACTTCTCGATGCCTTGTTGCAAATACTG	B2-stop mutated		
			GGGGACAAGTTTGTACAAAAAAGCAGGCTTAACCATGGAGGCACTGACGGAGCTTTGTG	B1-Kozak sequence		pDONR P2R-*P3*
			GGGGACCACTTTGTACAAGAAAGCTGGGTATTACTTCTCGATGCCTTGTTGCAAATACTG	B2-STOP		
			GGGGACAGCTTTCTTGTACAAAGTGGCTATGGAGGCACTGACGGAGCTTTGTGAC	B2R		
			GGGGACAACTTTGTATAATAAAGTTGCTTACTTCTCGATGCCTTGTTGCAAATACTG	B3		
	NPG1	Coding sequence from ATG to Stop	GGGGACAAGTTTGTACAAAAAAGCAGGCTTAACCATGCTCGGGAATCAATCCG	B1-Kozak sequence	cDNA from seedlings	pDONR221
			GGGGACCACTTTGTACAAGAAAGCTGGGTATTAAAGAATGGTTGAGAAGCTTTCAA	B2-stop mutated		
	NPGR1	Coding sequence from ATG to Stop	GGGGACAAGTTTGTACAAAAAAGCAGGCTTAACCATGTTGTGTGCTTGTTCAGGC	B1-Kozak sequence	cDNA from seedlings	pDONR 221
			GGGGACCACTTTGTACAAGAAAGCTGGGTATCAAATGAAACTCTGTACCGGAGC	B2-stop mutated		
	NPGR2	Coding sequence from ATG to Stop	GGGGACAAGTTTGTACAAAAAAGCAGGCTTAACCATGAAGAACAGCGAGATTAGGCC	B1-Kozak sequence	cDNA from seedlings	pDONR 221
			GGGGACCACTTTGTACAAGAAAGCTGGGTATCATCTGAATGGCTCCACTGG	B2-stop mutated		
	HYC1	Coding sequence/genomic sequence from ATG to Stop	GGGGACAAGTTTGTACAAAAAAGCAGGCTTAACCATGTCTGATTCTTCCTCAAGCCATG	B1-Kozak sequence	genomic DNA	pDONR 221
			GGGGACCACTTTGTACAAGAAAGCTGGGTAAACGGAGAGAACGGTGTCGTTTGATAGCTC	B2-stop mutated		
	HYC2	Coding sequence/genomic sequence from ATG to Stop	GGGGACAAGTTTGTACAAAAAAGCAGGCTTAACCATGGACTTCTCCGTCAAACCTTCCGG	B1-Kozak sequence	genomic DNA	pDONR 221
			GGGGACCACTTTGTACAAGAAAGCTGGGTACTTTGATGCCAGAAGAATCTCAGG	B2-stop mutated		
	ELP1	Genomic sequence from ATG to Stop	GGGGACAAGTTTGTACAAAAAAGCAGGCTTAACCATGGGGGTTGTTTCAAGAACC	B1-Kozak sequence	genomic DNA	pDONR 221
			GGGGACCACTTTGTACAAGAAAGCTGGGTACTAATCAAGAGGAACCAACGGC	B2-STOP		
	ELP2	Coding sequence from ATG to Stop	GGGGACAAGTTTGTACAAAAAAGCAGGCTTAACCATGAGCGCAGTCTCGGGTG	B1-Kozak sequence	cDNA from seedlings	pDONR 221
			GGGGACCACTTTGTACAAGAAAGCTGGGTAACAGCCAGCAGCTTTAAGGAAG	B2-stop mutated		
	ELP3	Coding sequence from ATG to Stop	GGGGACAAGTTTGTACAAAAAAGCAGGCTTAACCATGGGGGTTATGTCCAGACG	B1-Kozak sequence	cDNA from seedlings	pDONR 221
			GGGGACCACTTTGTACAAGAAAGCTGGGTATTAACACCCGGCTGCTTTC	B2-STOP		
Promoters	pPI4Kα1	1316bp upstream ATG with homology to pDONR P4-P1r	TTTGTATAGAAAAGTTGCTGTTAGGTTGATTCTCCTATCCTGGGTTTG	B4	genomic DNA	pDONR P4-P1r
			AACTTTTTTGTACAAACTTGCCTCCGATTAAACAAAAAAAACAACGTTACG	B1		
		pDONR P4-P1r with homology to pPI4Kα1	TTTTGTTTAATCGGAGGCAAGTTTGTACAAAAAAGTTGAACGAG	B4	pDONR P4-P1r	
			AGGATAGGAGAATCAACCTAACAGCAACTTTTCTATACAAAGTTGGC	B1		
	pNPG1	3983bp uspstream ATG with homology to pDONR P4-P1r	ACTTTGTATAGAAAAGTTGCTTATAGTTATGAAACTTAATGATTAGCGAGTTG	B4	genomic DNA	pDONR P4-P1r
			TTCAACTTTTTTGTACAAACTTGCTGTTCTTCACCTTTTAGACTAAACCC	B1		
		pDONR P4-P1r with homology to pNPG1	AGTCTAAAAGGTGAAGAACAGCAAGTTTGTACAAAAAAGTTGAACGAGAAACG	B4	pDONR P4-P1r	
			TCATTAAGTTTCATAACTATAAGCAACTTTTCTATACAAAGTTGGCATTATAAAAAAGC	B1		
	pNPGR1	1226bp upstream ATG with homology to pDONR P4-P1r	ACTTTGTATAGAAAAGTTGCTGGAAAGGAGAAACTAGGAGAGACGTCGCTATTTG	B4	genomic DNA	pDONR P4-P1r
			CGTTCAACTTTTTTGTACAAACTTGCCTTCTCCTCTTTCTCCTCACAAACGCGGAAATGC	B1		
		pDONR P4-P1r with homology to pNPGR1	GTGAGGAGAAAGAGGAGAAGGCAAGTTTGTACAAAAAAGTTGAACGAGAAACG	B4	pDONR P4-P1r	
			CTCTCCTAGTTTCTCCTTTCCAGCAACTTTTCTATACAAAGTTGGC	B1		
	pHYC1	1212bp upstream ATG with homology to pDONR P4-P1r	GTATAGAAAAGTTGCTGAAAAGCCAGTCAGCGTCCGATGTAGCCCG	B4	genomic DNA	pDONR P4-P1r
			TTTGTACAAACTTGCTTTGGGGAAGATGATGATCGCTTCTGAG	B1		
		pDONR P4-P1r with homology to pHYC1	GCTGACTGGCTTTTCAGCAACTTTTCTATACAAAGTTGGC	B4	pDONR P4-P1r	
			CATCATCTTCCCCAAAGCAAGTTTGTACAAAAAAGTTGAACGAG	B1		
	pHYC2	1430bp upstream ATG with homology to pDONR P4-P1r	GTATAGAAAAGTTGCTTGTGTGGGATTTTGATTCTTCTTCTC	B4	genomic DNA	pDONR P4-P1r
			TTTGTACAAACTTGCGGGAATTGAGTCTGACTTGAGAGAC	B1		
		pDONR P4-P1r with homology to pHYC2	AGTCAGACTCAATTCCCGCAAGTTTGTACAAAAAAGTTGAACGAG	B4	pDONR P4-P1r	
			TCAAAATCCCACACAAGCAACTTTTCTATACAAAGTTGGC	B1		
	pELP1	2594bp upstream ATG with homology to pDONR P4-P1r	TGTATAGAAAAGTTGCTAATCCAATGACTAGAAAAGTCTACAC	B4	genomic DNA	pDONR P4-P1r
			TACGTTTCTCGTTCAACTTTTTTGTACAAACTTGCCGATCTATCTCTCTTCC	B1		
		pDONR P4-P1r with homology to pELP1	CGAATATTCGCGGAAGAGAGATAGATCGGCAAGTTTGTACAAAAAAGTTG	B4	pDONR P4-P1r	
			GACTTTTCTAGTCATTGGATTAGCAACTTTTCTATACAAAGTTGGC	B1		
	pELP3	2411bp upstream ATG with homology to pDONR P4-P1r	TATAGAAAAGTTGCTTGCCCACACGCAGGATCGAACTACGGACCTTC	B4	genomic DNA	pDONR P4-P1r
			CAACTTTTTTGTACAAACTTGCTTTCTTCTCCGCCTAATATCC	B1		
		pDONR P4-P1r with homology to pELP3	TAGGCGGAGAAGAAAGCAAGTTTGTACAAAAAAGTTGAACGAGAAACG	B4	pDONR P4-P1r	
			CGATCCTGCGTGTGGGCAAGCAACTTTTCTATACAAAGTTGGC	B1		
3'UTR	PI4Kα1 3'UTR	395bp dowstream STOP codon	GGGGACAGCTTTCTTGTACAAAGTGGCTGAAGAAGAAGAGGGAACTTAATGATATCCG	B2R	genomic DNA	pDONR P2R-*P3*
			GGGGACAACTTTGTATAATAAAGTTGCGAATACAAATACCTCTACATGTTAATAG	B3		

Table 6.

Name	Sequence ordered	Region targetted
microRNA 2	ACAAGTTTGTACAAAAAAGCAGGCTCaaacacacgctcggacgcatattacacatgttcatacacttaa tactcgctgttttgaattgatgttttaggaatatatatgt**aga**TAATAGGTTGTGCCCCAACGT**tcaca ggtcgtgatatgattcaattagcttccgactcattcatccaaataccgagtcgccaaaattcaaa ctagactcgttaaatgaatgaatgatgcggtagacaaattggatcattgattctctttga**ACGTTG GGGCACAACCTATTA**tct**ctctttttgtattccaattttcttgattaatctttcctgcacaaaaacatg cttgatccactaagtgacatatatgctgccttcgtatatatagttctggtaaaattaacattttg ggtttatctttatttaaggcatcgccatg**ACCCAGCTTTCTTGTACAAAGTGGT	4376-4396
microRNA 3	ACAAGTTTGTACAAAAAAGCAGGCTCaaacacacgctcggacgcatattacacatgttcatacacttaa tactcgctgttttgaattgatgttttaggaatatatatgt**aga**TAAAAGTAATGCAAGCGTCGC**tc acaggtcgtgatatgattcaattagcttccgactcattcatccaaataccgagtcgccaaaattc aaactagactcgttaaatgaatgaatgatgcggtagacaaattggatcattgattctctttga**GC GACGCTTGCATTACTTTTA**tct**ctctttttgtattccaattttcttgattaatctttcctgcacaaaa acatgcttgatccactaagtgacatatatgctgccttcgtatatatagttctggtaaaattaaca ttttgggtttatctttatttaaggcatcgccatg**ACCCAGCTTTCTTGTACAAAGTGGT	1150-1170

in red: AttB1 and AttB; in black: artificial microRNA; in bold: hair pin sequence

Table 7.

Directed mutagenesis

Name	Mutation	Primer Sequence (5'-3'; forward then reverse)
EFOP1noSTOP/pDONR 221	Revertion of the STOP codon (TAG-->TTG leu) in EFOP1gwSTOP/p221	cctcttgattTgtacccagctttcttgtacaaagtt
		agctgggtacAaatcaagaggaaccaacggcttggc
EFOP3noSTOP/pDONR 221	Deletion of the stop (TAT)	gcagccgggTGTtacccagctttcttgtacaaagttgg
		gaaagctgggtaACAcccggctgctttcaagaatttatc
EFOP2-CC/pDONR 221	Site directed mutagenesis C20 and C23 to S (TGT->AGT and TGC->AGC) to mutate the palmytoylation	tgtggtagccttAgtattcttAgccctgcgcttcgtgcaaggtctagacag
		acgaagcgcagggcTaagaatacTaaggctaccacaaacaggcaaaacttgcctc
EFOP2-7Q/pDONR 221	site directed mutagenesis R29Q (AGG-->CAA) on EFOP2	attctttgccctgcgctt**CGT**gca**CAG**tct**AGA**cagcctgtgaagaggtac
		cttgtacctcttcacaggctgTCTagaCTGtgcACGaagcgcagggcaaag
	site directed mutagenesis R27Q (CGT-->CAA)and R31Q (AGA-->CAA) on EFOP2 to use on EFOP2-R29Q	attctttgccctgcgcttCAAgcaCAGtctCAAcagcctgtgaagaggtac
		cttgtacctcttcacaggctg**TTG**aga**CTG**tgc**TTG**aagcgcagggcaaag
	site directed mutagenesis K35Q (AAG-->CAG)and K38Q (AAG-->CAG) on EFOP2 to use on EFOP2-3Q	CAGtctCAAcagcctgtgCAGAGGtacCAGAAGctcattgctgagatttttcc
		aaaaatctcagcaatgagCTTCTGgtaCCTCTGcacaggctgTTGagaCTGtgc
	site directed mutagenesis R36Q (AAG-->CAG) and K39Q (AAG-->CAG) on EFOP2 to use on EFOP2-5Q	CAGtctCAAcagcctgtgCAGCAGtacCAGCAGctcattgctgagatttttcc
		aaaaatctcagcaatgagCTGCTGgtaCTGCTGcacaggctgTTGagaCTGtgc
PI4Ka1-ami2ins/pDONR 221		/5Phos/AgcccaTacAtcaagcctgtcagcttcatgctggcag
		/5Phos/caGccAatAagttcaaaggacagtccgtattcgcgg

Table 8.

	Antibody	References	Company	Host	Concentration used
Primary	anti-GFP	A-6455	ThermoFisher	Rabbit	1/2000
	anti-mCherry	ab167453	Abcam	Rabbit	1/1000
	anti-PI4Ka1	A03 rat #1	Proteogenix	Rat	1/1000
	anti-NPGR2	9094-A01 rabbit #2	Proteogenix	Rabbit	1/2000
Secondary	anti-Rat IgG, HRP conjugate	AP136P	Merck	Goat	1/5000
	anti-Rabbit IgG, HRP conjugate	W4011	Promega	Goat	1/5000

Table 9.

References

Antignani, V., Klocko, A.L., Bak, G., Chandrasekaran, S.D., Dunivin, T., and Nielsen, E. (2015). Recruitment of PLANT U-BOX13 and the PI4Kβ1/β2 Phosphatidylinositol-4 Kinases by the Small GTPase RabA4B Plays Important Roles during Salicylic Acid-Mediated Plant Defense Signaling in Arabidopsis. Plant Cell *27*, 243–261.

Audhya, A., and Emr, S.D. (2002). Stt4 PI 4-Kinase Localizes to the Plasma Membrane and Functions in the Pkc1-Mediated MAP Kinase Cascade. Developmental Cell *2*, 593–605.

Audhya, A., Foti, M., and Emr, S.D. (2000). Distinct Roles for the Yeast Phosphatidylinositol 4-Kinases, Stt4p and Pik1p, in Secretion, Cell Growth, and Organelle Membrane Dynamics. Mol Biol Cell *11*, 2673–2689.

Baird, D., Stefan, C., Audhya, A., Weys, S., and Emr, S.D. (2008). Assembly of the PtdIns 4-kinase Stt4 complex at the plasma membrane requires Ypp1 and Efr3. J Cell Biol *183*, 1061–1074.

Balla, A., Tuymetova, G., Barshishat, M., Geiszt, M., and Balla, T. (2002). Characterization of type II phosphatidylinositol 4-kinase isoforms reveals association of the enzymes with endosomal vesicular compartments. J. Biol. Chem. *277*, 20041–20050.

Balla, A., Tuymetova, G., Tsiomenko, A., Várnai, P., and Balla, T. (2005). A Plasma Membrane Pool of Phosphatidylinositol 4-Phosphate Is Generated by Phosphatidylinositol 4-Kinase Type-III Alpha: Studies with the PH Domains of the Oxysterol Binding Protein and FAPP1. MBoC *16*, 1282–1295.

Barbosa, I.C.R., Shikata, H., Zourelidou, M., Heilmann, M., Heilmann, I., and Schwechheimer, C. (2016). Phospholipid composition and a polybasic motif determine D6 PROTEIN KINASE polar association with the plasma membrane and tropic responses. Development dev.137117.

Baskin, J.M., Wu, X., Christiano, R., Oh, M.S., Schauder, C.M., Gazzerro, E., Messa, M., Baldassari, S., Assereto, S., Biancheri, R., et al. (2016). The leukodystrophy protein FAM126A/Hyccin regulates PI4P synthesis at the plasma membrane. Nat Cell Biol *18*, 132–138.

Chung, J., Torta, F., Masai, K., Lucast, L., Czapla, H., Tanner, L.B., Narayanaswamy, P., Wenk, M.R., Nakatsu, F., and De Camilli, P. (2015a). PI4P/phosphatidylserine countertransport at ORP5-and ORP8-mediated ER–plasma membrane contacts. Science *349*, 428–432.

Chung, J., Nakatsu, F., Baskin, J.M., and De Camilli, P. (2015b). Plasticity of PI4KIIIα interactions at the plasma membrane. EMBO Rep *16*, 312–320.

Delage, E., Ruelland, E., Guillas, I., Zachowski, A., and Puyaubert, J. (2012). Arabidopsis Type-III Phosphatidylinositol 4-Kinases β1 and β2 are Upstream of the Phospholipase C Pathway Triggered by Cold Exposure. Plant Cell Physiol *53*, 565–576.

Dornan, G.L., Dalwadi, U., Hamelin, D.J., Hoffmann, R.M., Yip, C.K., and Burke, J.E. (2018). Probing the Architecture, Dynamics, and Inhibition of the PI4KIIIα/TTC7/FAM126 Complex. J. Mol. Biol. *430*, 3129–3142.

Foti, M., Audhya, A., and Emr, S.D. (2001). Sac1 Lipid Phosphatase and Stt4 Phosphatidylinositol 4-Kinase Regulate a Pool of Phosphatidylinositol 4-Phosphate That Functions in the Control of the Actin Cytoskeleton and Vacuole Morphology. MBoC *12*, 2396–2411.

Fratini, M., Krishnamoorthy, P., Stenzel, I., Riechmann, M., Bacia, K., Heilmann, M., and Heilmann, I. (2020). Plasma membrane nano-organization specifies phosphoinositide effects on Rho-GTPases and actin dynamics in tobacco pollen tubes. BioRxiv 2020.08.12.248419.

Gerth, K., Lin, F., Menzel, W., Krishnamoorthy, P., Stenzel, I., Heilmann, M., and Heilmann, I. (2017). Guilt by Association: A Phenotype-Based View of the Plant Phosphoinositide Network. Annual Review of Plant Biology *68*, 349–374.

Giordano, F., Saheki, Y., Idevall-Hagren, O., Colombo, S.F., Pirruccello, M., Milosevic, I., Gracheva, E.O., Bagriantsev, S.N., Borgese, N., and De Camilli, P. (2013). PI(4,5)P(2)-dependent and Ca(2+)-regulated ER-PM interactions mediated by the extended synaptotagmins. Cell *153*, 1494–1509.

Golovkin, M., and Reddy, A.S.N. (2003). A calmodulin-binding protein from Arabidopsis has an essential role in pollen germination. Proc Natl Acad Sci U S A *100*, 10558–10563.

Hammond, G.R.V., Schiavo, G., and Irvine, R.F. (2009). Immunocytochemical techniques reveal multiple, distinct cellular pools of PtdIns4P and PtdIns(4,5)P2. Biochem J *422*, 23–35.

Hammond, G.R.V., Machner, M.P., and Balla, T. (2014). A novel probe for phosphatidylinositol 4-phosphate reveals multiple pools beyond the Golgi. J Cell Biol *205*, 113–126.

Himschoot, E., Pleskot, R., Van Damme, D., and Vanneste, S. (2017). The ins and outs of Ca2+ in plant endomembrane trafficking. Current Opinion in Plant Biology *40*, 131–137.

Honkanen, S., Jones, V.A.S., Morieri, G., Champion, C., Hetherington, A.J., Kelly, S., Proust, H., Saint-Marcoux, D., Prescott, H., and Dolan, L. (2016). The Mechanism Forming the Cell Surface of Tip-Growing Rooting Cells Is Conserved among Land Plants. Current Biology *26*, 3238–3244.

Idevall-Hagren, O., Lü, A., Xie, B., and De Camilli, P. (2015). Triggered Ca2+ influx is required for extended synaptotagmin 1-induced ER-plasma membrane tethering. EMBO J. *34*, 2291–2305.

Kang, B.-H., Nielsen, E., Preuss, M.L., Mastronarde, D., and Staehelin, L.A. (2011). Electron Tomography of RabA4b- and PI-4Kβ1-Labeled Trans Golgi Network Compartments in

Arabidopsis. Traffic *12*, 313–329.

Kumar, M., Carr, P., and Turner, S. (2020). An atlas of Arabidopsis protein S-Acylation reveals its widespread role in plant cell organisation of and function (Plant Biology).

Lee, E., Vanneste, S., Pérez-Sancho, J., Benitez-Fuente, F., Strelau, M., Macho, A.P., Botella, M.A., Friml, J., and Rosado, A. (2019). Ionic stress enhances ER–PM connectivity via phosphoinositide-associated SYT1 contact site expansion in Arabidopsis. PNAS *116*, 1420–1429.

Lees, J.A., Zhang, Y., Oh, M.S., Schauder, C.M., Yu, X., Baskin, J.M., Dobbs, K., Notarangelo, L.D., Camilli, P.D., Walz, T., et al. (2017). Architecture of the human PI4KIIIα lipid kinase complex. PNAS *114*, 13720–13725.

Lemmon, M.A. (2008). Membrane recognition by phospholipid-binding domains. Nat Rev Mol Cell Biol *9*, 99–111.

Levine, T.P., and Munro, S. (1998). The pleckstrin homology domain of oxysterol-binding protein recognises a determinant specific to Golgi membranes. Current Biology *8*, 729–739.

Levine, T.P., and Munro, S. (2002). Targeting of Golgi-Specific Pleckstrin Homology Domains Involves Both PtdIns 4-Kinase-Dependent and -Independent Components. Current Biology *12*, 695–704.

Lin, F., Krishnamoorthy, P., Schubert, V., Hause, G., Heilmann, M., and Heilmann, I. (2019). A dual role for cell plate-associated PI4Kβ in endocytosis and phragmoplast dynamics during plant somatic cytokinesis. EMBO J. *38*.

Miyamoto, Y., Torii, T., Eguchi, T., Nakamura, K., Tanoue, A., and Yamauchi, J. (2014). Hypomyelinating leukodystrophy-associated missense mutant of FAM126A/hyccin/DRCTNNB1A aggregates in the endoplasmic reticulum. J Clin Neurosci *21*, 1033–1039.

Moser von Filseck, J., F., K., L., H., L. B., P., M. R., F., and P. (2015). Phosphatidylserine transport by ORP/Osh proteins is driven by phosphatidylinositol 4-phosphate. Science *349*, 428–432.

Mueller-Roeber, B., and Pical, C. (2002). Inositol Phospholipid Metabolism in Arabidopsis. Characterized and Putative Isoforms of Inositol Phospholipid Kinase and Phosphoinositide-Specific Phospholipase C. Plant Physiol *130*, 22–46.

Nakatsu, F., Baskin, J.M., Chung, J., Tanner, L.B., Shui, G., Lee, S.Y., Pirruccello, M., Hao, M., Ingolia, N.T., Wenk, M.R., et al. (2012). PtdIns4P synthesis by PI4KIIIα at the plasma membrane and its impact on plasma membrane identity. J Cell Biol *199*, 1003–1016.

Okazaki, K., Miyagishima, S., and Wada, H. (2015). Phosphatidylinositol 4-Phosphate Negatively Regulates Chloroplast Division in Arabidopsis[OPEN]. Plant Cell *27*, 663–674.

Omnus, D.J., Cadou, A., Chung, G.H.C., Bader, J.M., and Stefan, C.J. (2018). A Cytoplasmic GOLD Protein Controls Cell Polarity. BioRxiv 379057.

Platre, M.P., Noack, L.C., Doumane, M., Bayle, V., Simon, M.L.A., Maneta-Peyret, L., Fouillen, L., Stanislas, T., Armengot, L., Pejchar, P., et al. (2018). A Combinatorial Lipid Code Shapes the Electrostatic Landscape of Plant Endomembranes. Dev. Cell *45*, 465-480.e11.

Preuss, M.L., Schmitz, A.J., Thole, J.M., Bonner, H.K.S., Otegui, M.S., and Nielsen, E. (2006). A role for the RabA4b effector protein PI-4Kβ1 in polarized expansion of root hair cells in Arabidopsis thaliana. J Cell Biol *172*, 991–998.

Roy, A., and Levine, T.P. (2004). Multiple Pools of Phosphatidylinositol 4-Phosphate Detected Using the Pleckstrin Homology Domain of Osh2p. J. Biol. Chem. *279*, 44683–44689.

Šašek, V., Janda, M., Delage, E., Puyaubert, J., Guivarc'h, A., López Maseda, E., Dobrev, P.I., Caius, J., Bóka, K., Valentová, O., et al. (2014). Constitutive salicylic acid accumulation in pi4kIIIβ1β2 Arabidopsis plants stunts rosette but not root growth. New Phytol *203*, 805–816.

Shin, S.-B., Golovkin, M., and Reddy, A.S.N. (2014). A pollen-specific calmodulin-binding protein, NPG1, interacts with putative pectate lyases. Sci Rep *4*.

Siligato, R., Wang, X., Yadav, S.R., Lehesranta, S., Ma, G., Ursache, R., Sevilem, I., Zhang, J., Gorte, M., Prasad, K., et al. (2016). MultiSite Gateway-Compatible Cell Type-Specific Gene-Inducible System for Plants1[OPEN]. Plant Physiol *170*, 627–641.

Simon, M.L.A., Platre, M.P., Assil, S., van Wijk, R., Chen, W.Y., Chory, J., Dreux, M., Munnik, T., and Jaillais, Y. (2014). A multi-colour/multi-affinity marker set to visualize phosphoinositide dynamics in Arabidopsis. Plant J *77*, 322–337.

Simon, M.L.A., Platre, M.P., Marquès-Bueno, M.M., Armengot, L., Stanislas, T., Bayle, V., Caillaud, M.-C., and Jaillais, Y. (2016). A PtdIns(4)P-driven electrostatic field controls cell membrane identity and signalling in plants. Nature Plants *2*, nplants201689.

Simon-Plas, F., Elmayan, T., and Blein, J.-P. (2002). The plasma membrane oxidase NtrbohD is responsible for AOS production in elicited tobacco cells. Plant J. *31*, 137–147.

Stevenson, J.M., Perera, I.Y., and Boss, W.F. (1998). A Phosphatidylinositol 4-Kinase Pleckstrin Homology Domain That Binds Phosphatidylinositol 4-Monophosphate. J. Biol. Chem. *273*, 22761–22767.

Stevenson-Paulik, J., Love, J., and Boss, W.F. (2003). Differential Regulation of Two Arabidopsis Type III Phosphatidylinositol 4-Kinase Isoforms. A Regulatory Role for the Pleckstrin Homology Domain. Plant Physiol *132*, 1053–1064.

Strahl, T., Hama, H., DeWald, D.B., and Thorner, J. (2005). Yeast phosphatidylinositol 4-kinase, Pik1, has essential roles at the Golgi and in the nucleus. J Cell Biol *171*, 967–979.

Szumlanski, A.L., and Nielsen, E. (2010). Phosphatidylinositol 4-Phosphate is Required for Tip Growth in Arabidopsis thaliana. In Lipid Signaling in Plants, T. Munnik, ed. (Berlin, Heidelberg: Springer), pp. 65–77.

Vermeer, J.E.M., Thole, J.M., Goedhart, J., Nielsen, E., Munnik, T., and Gadella Jr, T.W.J. (2009). Imaging phosphatidylinositol 4-phosphate dynamics in living plant cells. The Plant Journal *57*, 356–372.

Wang, Y.J., Wang, J., Sun, H.Q., Martinez, M., Sun, Y.X., Macia, E., Kirchhausen, T., Albanesi, J.P., Roth, M.G., and Yin, H.L. (2003). Phosphatidylinositol 4 Phosphate Regulates Targeting of Clathrin Adaptor AP-1 Complexes to the Golgi. Cell *114*, 299–310.

Wei, Y.J., Sun, H.Q., Yamamoto, M., Wlodarski, P., Kunii, K., Martinez, M., Barylko, B., Albanesi, J.P., and Yin, H.L. (2002). Type II phosphatidylinositol 4-kinase beta is a cytosolic and peripheral membrane protein that is recruited to the plasma membrane and activated by Rac-GTP. J. Biol. Chem. *277*, 46586–46593.

Wu, H., Carvalho, P., and Voeltz, G.K. (2018). Here, there, and everywhere: The importance of ER membrane contact sites. Science *361*, eaan5835.

Wu, X., Chi, R.J., Baskin, J.M., Lucast, L., Burd, C.G., De Camilli, P., and Reinisch, K.M. (2014). Structural Insights into Assembly and Regulation of the Plasma Membrane Phosphatidylinositol 4-Kinase Complex. Dev Cell *28*, 19–29.

Xue, H.-W., Pical, C., Brearley, C., Elge, S., and Müller-Röber, B. (1999). A Plant 126-kDa Phosphatidylinositol 4-Kinase with a Novel Repeat Structure CLONING AND FUNCTIONAL EXPRESSION IN BACULOVIRUS-INFECTED INSECT CELLS. J. Biol. Chem. *274*, 5738–5745.

Yamaoka, Y., Yu, Y., Mizoi, J., Fujiki, Y., Saito, K., Nishijima, M., Lee, Y., and Nishida, I. (2011). PHOSPHATIDYLSERINE SYNTHASE1 is required for microspore development in Arabidopsis thaliana. The Plant Journal *67*, 648–661.

Yamazaki, T., Kawamura, Y., Minami, A., and Uemura, M. (2008). Calcium-dependent freezing tolerance in Arabidopsis involves membrane resealing via synaptotagmin SYT1. Plant Cell *20*, 3389–3404.

Zaballa, M.-E., and Goot, F.G. van der (2018). The molecular era of protein S-acylation: spotlight on structure, mechanisms, and dynamics. Critical Reviews in Biochemistry and Molecular Biology *53*, 420–451.

Part 3
DISCUSSION AND PERSPECTIVES

General discussion and perspectives

I- How is the gradient of PI4P established and maintained in plant cells?

This question was the starting point of my thesis. This work led to the characterization of a new complex in plants likely involved in the plasma membrane PI4P pool. However, our understanding of the maintenance of the PI4P gradient is still limited. Here, I will discuss what we know and do not know about the dynamics of PI4P in plant cells and the molecular actors involved in the establishment of the plasma membrane PI4P pool.

1- The localization of PI4P in plants, animal and yeast

The repartition of anionic lipids in cells has been mainly investigated using genetically encoded biosensors that correspond to a lipid-binding domain fused to a fluorescent protein. Biosensors are powerful tools as they allow visualizing lipid pools *in vivo* at a subcellular scale. However, they also introduce some bias (Platre and Jaillais, 2016). First, the probe may compete with endogenous lipid-binding proteins. Thus, biosensors mainly reflect the pool of "free" lipids and we hypothesized that it corresponds to the pool of lipid able to recruit new effectors to a compartment. Secondly, lipid-binding domain interactions can rely of coincidence binding. Several membrane features such as curvature, lipid packing, and presence of another lipids or proteins at the membrane might be necessary for the interaction.

In yeast, the PH domain of Osh2 labels the Golgi. Upon depletion of PI4P at the Golgi, Osh2 reveals the presence of a pool of PI4P at the plasma membrane (Roy and Levine, 2004) **(Figure 1)**. In addition, a tandem dimer of the PH domain of Osh2 localizes both

to the Golgi and the plasma membrane, but the Golgi labelling is much stronger. Together, these data suggest that the main pool of PI4P is at the Golgi in yeast.

In animals, PI4P has been first found in the Golgi using the PH domain of FAPP1 and OSBP (Levine and Munro, 1998, 2002) **(Figure 1)**. PH^{OSBP} also labels slightly the plasma membrane. However, FAPP1 and OSBP interact with ARF1, a protein that mainly resides in Golgi/TGN (De Matteis and Godi, 2004; Levine and Munro, 2002). Direct immunolocalisation using anti-PI4P antibodies confirmed the PI4P plasma membrane pool in animal cell (Hammond et al., 2009). Later on a new PI4P sensor was developed: P4M from the protein SidM of the bacterial pathogen *Legionella pneumophila* (Hammond et al., 2014)**.** In animal cells, P4M labels the plasma membrane, the Golgi/TGN as well as Rab7-positive compartments that correspond to late endosomes/lysosomes in similar concentration suggesting that the different pools are equivalent to recruit new effectors (Hammond et al., 2014) **(Figure 1)**. However, targeted depletion of PI4P at the Golgi decreases the PI4P pool by 20% only while Wortmannin treatment depletes 80% of the total pool of PI4P and 100% of the PM pool suggesting that the PM pool might be quantitatively more important that the Golgi one (Hammond et al., 2014).

In *Arabidopsis*, the PH domain of FAPP1 and OSBP label the plasma membrane and the TGN/EE (Simon et al., 2016) **(Figure 1)**. To confirm the presence of the PI4P sensor independently of ARF1 a mutated version of the PH^{FAPP1} sensor that prevents binding to ARF1 was designed. Using this probe, the labelling of the PM was increased and the labelling of TGN/EE was decreased but remained (Simon et al., 2016). P4M almost exclusively labels the plasma membrane (Platre et al., 2018; Simon et al., 2016) **(Figure 1)**. Upon specific depletion of PM PI4P, P4M delocalized to intracellular compartments

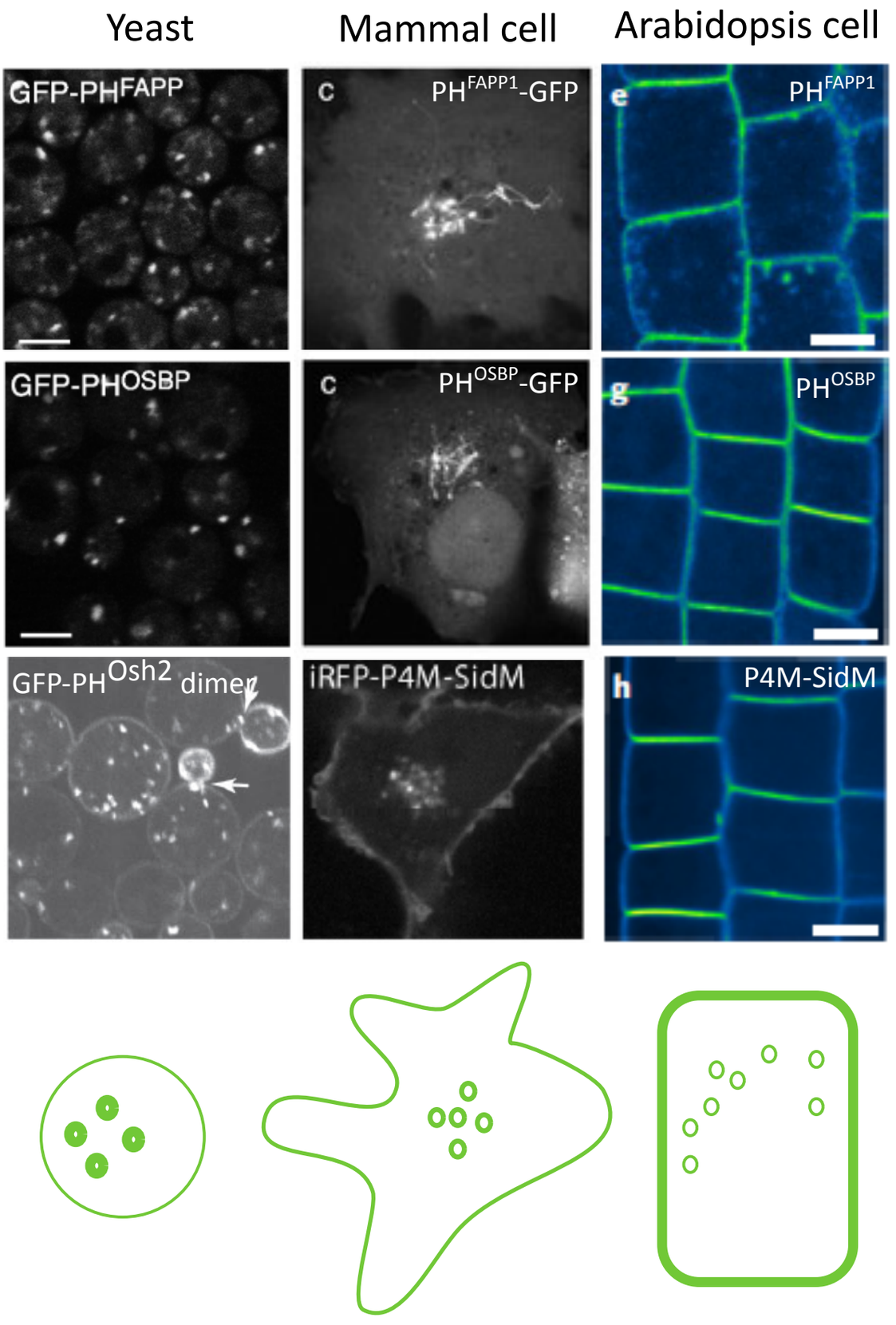

Figure 1. The pool of PI4P in yeast, animal and plant cell. Confocal images of various PI4P biosensors in yeast (on the left), mammal cells (in the middle) and plant cells (on the right) and a schematic representation of the PI4P pools in the different cells. (Balla et al., 2005; Hammond et al., 2014; Levine and Munro, 2002; Roy and Levine, 2004; Simon et al., 2016)

indicating a higher PI4P concentration at the PM than in the TGN/EE (Simon et al., 2016). So far, no PI4P has been detected in late endosomes in *Arabidopsis*.

To conclude, PI4P labels the plasma membrane in all eukaryotes. In *Arabidopsis*, PI4P massively accumulates at the plasma membrane while in yeast the main pool of PI4P is in the Golgi. In animal cells, the Golgi and the PM pools seem to have the same ability to recruit effectors. In any cases, PI4P is present in several pools. To recruit effectors at a specific compartment, the presence of PI4P must be couple with other features such as electrostatics, curvature or interaction with a protein.

Finally, the ability of PIP to be rapidly converted implies that the pools of PI4P might not be static and might change locally or broadly upon developmental and physiological events. For example, in budding yeast, the plasma membrane of the daughter cell accumulate PI4P massively (Manford et al., 2012; Omnus et al., 2016, 2020; Stefan et al., 2011). In plants, we have clues that PI4P pool change with the physiological or developmental context. In *Arabidopsis*, during colletotrichum infection the Extra Invasive Hyphal Membrane in continuity with the plasma membrane is depleted in PI4P (Shimada et al., 2019). In root, the plasma membrane pool of PI4P seems to increase in the elongation zone compare to the meristematic zone while PS behaves oppositely (Platre et al., 2019). However, the biological relevance of these observations remained to be determined. For this kind of observations, the use of several independent biosensors or other technics such as membrane fractionation of immunolocalization is important as these observations might just be the result of an increase or decrease of the sensor expression depending of the tissue. In particular, biosensors with already high expression might not be able to react to small variations of PI4P at the plasma membrane. Furthermore, in the case of depletion of PI4P at the plasma membrane, P4M is supposedly delocalized to intracellular compartments corresponding to the TGN/EE.

Thus, the measure of a ratio of intensity between the plasma membrane and the cytosol might not reflect the variation of PI4P at the PM.

2- The PI4K-kinases of *Arabidopsis*

In *Arabidopsis*, the PI4-Kinases family counts 12 members: 2 PI4Kα, 2 PI4Kβ and 8 PI4Kγ **(Figure 2)**. No PI4-kinase activity has been demonstrated for PI4Kγ (Mueller-Roeber and Pical, 2002). On the contrary, PI4Kγ3, PI4Kγ4, and PI4Kγ7 have been characterized as protein kinases (Galvão et al., 2008; Mueller-Roeber and Pical, 2002).

For PI4Kβ1 and PI4Kβ2, they have been shown to work redundantly *in vivo* (Kang et al., 2011; Lin et al., 2019; Preuss et al., 2006). The PI4-Kinase activities of PI4Kβ1 and PI4Kα1 have been characterized *in vitro* (Stevenson et al., 1998; Xue et al., 1999). *In vivo*, *PI4Kα1* knock down impairs the production of PI4P in chloroplasts (Okazaki et al., 2015).

The case of *PI4Kα2* is less clear. *PI4Kα2* has been considered as a pseudo gene as no RNA sequencing was retrieved in Expressed sequence tags libraries. PI4Kα2 is a smaller isoform of PI4Kα1 **(Figure 2)**. PI4Kα2 sequence corresponds to the 114 N-terminal aa and the 419 C-terminal aa containing the entire catalytic domain of PI4Kα1. It shares a very high percentage of similarity with PI4Kα1 (~93%) (Stevenson-Paulik et al., 2003). However, expression data are now available on eFP browser (https://bar.utoronto.ca/efp/cgi-bin/efpWeb.cgi) and peptides specific of the sequence of PI4Kα2 are found in the proteome of *Arabidopsis* (https://www.proteomicsdb.org). Moreover, the antibody used against PI4Kα1 in Stevenson-Paulik et al. recognizes a protein around 60kDa that could correspond to PI4Kα2. As a big part of the PI4Kα1 sequence is not found in PI4Kα2, it is unlikely that PI4Kα2 interacts also with NPG proteins. However, we cannot exclude that PI4Kα2 is functional and acts in other

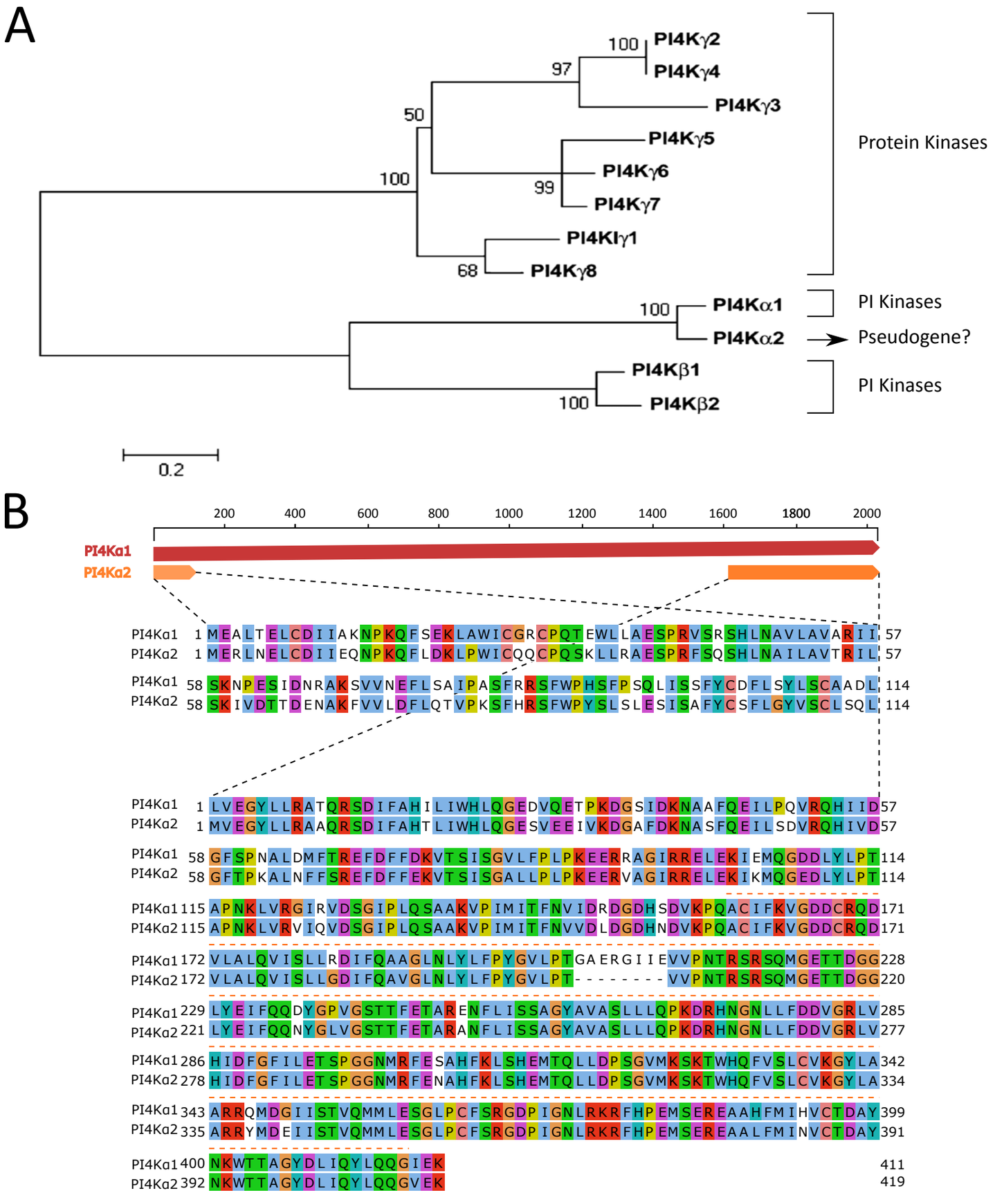

Figure 2. PI4-Kinases in Arabidopsis. (A) Unrooted phylogenetic tree of the PI4-Kinase family in Arabidopsis using the p-distance method with gaps treated by pairwise deletions and a 500 bootstrap replicate. (Adapted from Szumlanski and Nielsen, 2010). **(B)** Sequence alignment of the first 114 aa in N-terminal and the last 419 aa in C-terminal PI4Kα1 and PI4Kα2. Sequence alignments have been performed using the Muscle WS software and edited with Jalview 2.0 software. Clustal colour code has been used. The kinase catalytic domain is indicated with an orange dash line.

compartment (nucleus, plastids for instance). Using reporter lines and mutant lines, it would be interesting to determine the localization of PI4Kα2 and evaluate the effect of a loss-of-funtion of PI4Kα2.

Consequently, PI4Kα1, PI4Kβ1 and PI4Kβ2 are the only kinases known for certain to phosphorylate PI into PI4P in *Arabidopsis*.

3- The PI4P homeostasis

The PI4P homeostasis at the plasma membrane relies on several parameters including the enzyme activity, the pool of substrate and the exchange of lipids between compartments **(Figure 3 and 4)**.

- **The presence of the enzyme in the compartment**

The association of immunolocalization, confocal microscopy and electron tomography confirmed that PI4Kβ1 and 2 localize in the TGN/EE (Kang et al., 2011; Lin et al., 2019; Preuss et al., 2006). Our data confirmed that PI4Kα1 localizes at the PM (Okazaki et al., 2015) **(Results, Figure 5)**. We can speculate that each enzyme act where they localize. However, the localization of the enzyme is dynamic as it can be recruited under certain conditions. For instance, PI4Kβ1 is known to interact with different effectors: RabA4b, CBL1, PUB13 (Antignani et al., 2015; Kang et al., 2011; Preuss et al., 2006). PI4Kβ1 is targeted to the TGN by coincidence binding of RabA4b and the curved electrostatic membrane of the TGN thanks ta a +ALPS motif in C-terminal of the protein (Kang et al., 2011; Platre et al., 2018; Preuss et al., 2006). CBL1 has been suggested to recruit PI4Kβ1 upon Ca2+ stimulation (Preuss et al., 2006). Cold stress or pathogens infection have also been suggested to activate PI4Kβ1 (Antignani et al., 2015; Delage et al., 2012; Janda et al., 2014).

We show that EFOP proteins are responsible of the targeting of PI4Kα1 at the plasma membrane and that delocalizing EFOP2 is sufficient to delocalized PI4Kα1 **(Results, Figure 7)**. Our fluorescent reporters for EFOP1 and EFOP2 are also found in intracellular compartments **(Results, Figure 5)**. So, we cannot exclude that PI4Kα1 is also recruited in these compartment constitutively or upon some signals. So far, the nature of these compartments is not known. It could correspond to TGN/EE where PI4P is also found. Otherwise, it could be link to plastid membranes. Indeed, PI4P is found on the envelope of chloroplast (Gerth et al., 2017a). Recently, Golgi-derived PI4P vesicles have also been involved in mitochondria division in animal cells (Nagashima et al., 2020).

- **The regulation of catalytic activity**

Effectors, by secondary messenger, hormones, etc, can regulate the catalytic activity of the PI4-Kinases. The membrane environment can also affect the catalytic activity of the PI4Ks linking the different lipid metabolism. For example, in animal cell the production of sphingolipids at the TGN increases the membrane curvature, which results in an activation of PI4KIIIβ. Nothing is known about modulation of the PI4-kinase activity in plants *in vivo*. PI4Kα1 is inhibited by its own substrate *in vitro* but it is not the case of PI4Kβ1 (Stevenson-Paulik et al., 2003). How this data relate to the function of the enzymes *in vivo* need to be investigated. First, we could measure the amount of PI4P in plants overexpressing untagged PI4Kα1, NPG or EFOP proteins. If we do not see an accumulation of PI4P, it correlates with the fact that no phenotype could be retrieve from plant overexpressing NPG or EFOP proteins. Also overexpressing a chimeric construct in which the kinase domain of PI4Kβ1 replaces the kinase domain of PI4Kα1 should trigger the accumulation of PI4P at the plasma membrane while PI4Kα1 should not. However, this assumes that the presence of PI is not rate limiting.

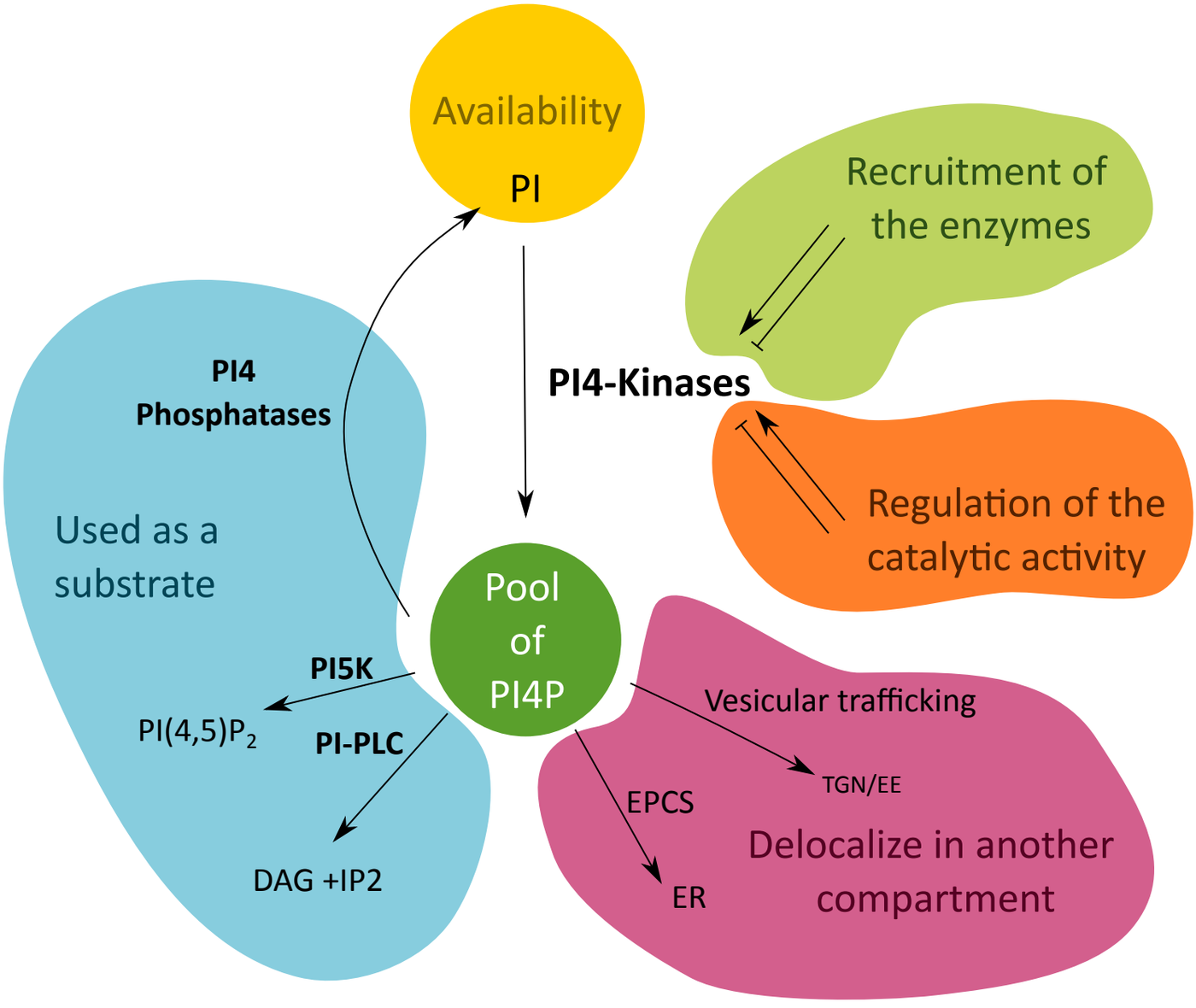

Figure 3. PI4P homeostasis in plant cell. Schematic representation of the parameters influencing the pool of PI4P in the cell. PI4, phosphatidylinositol-4-phosphate; PI5K, phosphatidylinositol-5-kinase; PI-PLC, Phosphoinositide Phospholipase C; PI, phosphoinositide; PI4P, phosphatidylinositol-4-phosphate; PI(4,5)P2, phosphatidylinositol-4,5-biphosphate; DAG, Diacylglycerol; IP2, D-myo-inositol 1,4-diphosphate; ER, endoplasmic reticulum; EPCS, ER-plasma membrane contact site; TGN/EE, trans-Golgi network/early endosomes.

- **The availability of the substrate**

A recent paper on mammalian cells monitored the distribution of PI within the cell (Zewe et al., 2020). One of the key observations was that the amount of PI available at the plasma membrane was very low compare to the amount of phosphoinositides. Moreover, depleting PI in the ER where it is first produced, induced a larger decrease in the amount of PI4P and PI(4,5)P_2 at the plasma membrane than directly depleting PI at the plasma membrane. They suggest that the delivery of PI from the ER to the plasma membrane could be a key regulatory process in the production of PI4P and PI(4,5)P_2 at the plasma membrane rather than the regulation of PIP kinase activity. Additionally, vesicular trafficking is not fast enough to explain the PI replenishment observed after depletion. They suggest that active transfer of PI at ER-PM contact sites could regulate PIP synthesis at the plasma membrane. For example, TMEM24 and Nir2 are contact site proteins known to transfer PI to the plasma membrane (Kim et al., 2015; Lees et al., 2017a; Sun et al., 2019). In plants, the enzyme producing PI, PIS1 and PIS2 localized at the ER and Golgi (Löfke et al., 2008). The distribution of PI as well as the mechanism by which it is exported from the ER (vesicular trafficking or lipid transfer enzymes) still needs to be studied. No LTP are known in plant to transfer PI at ER-PM contact sites. However, the use of monensin, a drug that inhibits vesicular trafficking does not affect the level of PI at the PM while PS, PC and PE are affected. This suggests that PI transfer from the ER to the PM must rely on another mechanism that vesicular trafficking (Moreau et al., 1994, 1998).

- **PI4P as a substrate for other pathway**

Once produced, PI4P can in turn be used as a substrate **(Introduction A, Figure 1)**. First, it can be dephosphorylated by PI4P phosphatases. No PI4P phosphatases are known at the plasma membrane. However, SAC7/RHD4 has been shown to localize in

the TGN (Thole et al., 2008). It is not clear at this time how SAC7 regulates the pool of PI4P in the TGN/EE. Secondly, PI4P can be phosphorylated by PI5-Kinases to produce PI(4,5)P_2. At the plasma membrane, several PI5-Kinases have been shown to act in a tissue specific way: PI5K1 and 2 in the phloem; PI5K3 in root hairs; PI5K6 in pollen tube for instance (Marhava et al., 2020; Stenzel et al., 2008). Third, PI4P can be degraded by PIP-specific phospholipase C to give DAG and IP2 both at the plasma membrane and in the TGN/EE. In addition to the direct enzymatic reactions involving PI4P, metabolism of other lipids can have an indirect effect on the pool of PI4P. For instance, recent data show that PI4P level at the TGN is decreased upon reduction of acyl-chain length of sphingolipid due to PI-PLC activation. This result links sphingolipids and phosphoinositides metabolism in the control of protein sorting at the TGN/EE.

- **The mobility of PI4P**

Once produce in one compartment, PI4P can eventually relocate to another compartment through vesicular trafficking and exchanges at membrane contact sites. This will be discussed in the following section.

To conclude, many black boxes still remain to fully understand how the two pools of PI4P are established, maintained and regulated in plant cells.

4- Interdependence between the two pools of PI4P

a. Exchanges through vesicular trafficking

The two PI4P compartments are at the heart of constant exchanges of material. Indeed, the plasma membrane and the TGN/EE exchange membranes through endocytosis and exocytosis. Is PI4P a part of these exchanges or the two pools behave independently?

In yeast, Stt4 produces PI4P at the plasma membrane and Pik1 in the TGN (Audhya and Emr, 2002; Audhya et al., 2000; Roy and Levine, 2004). The absence of one of the two

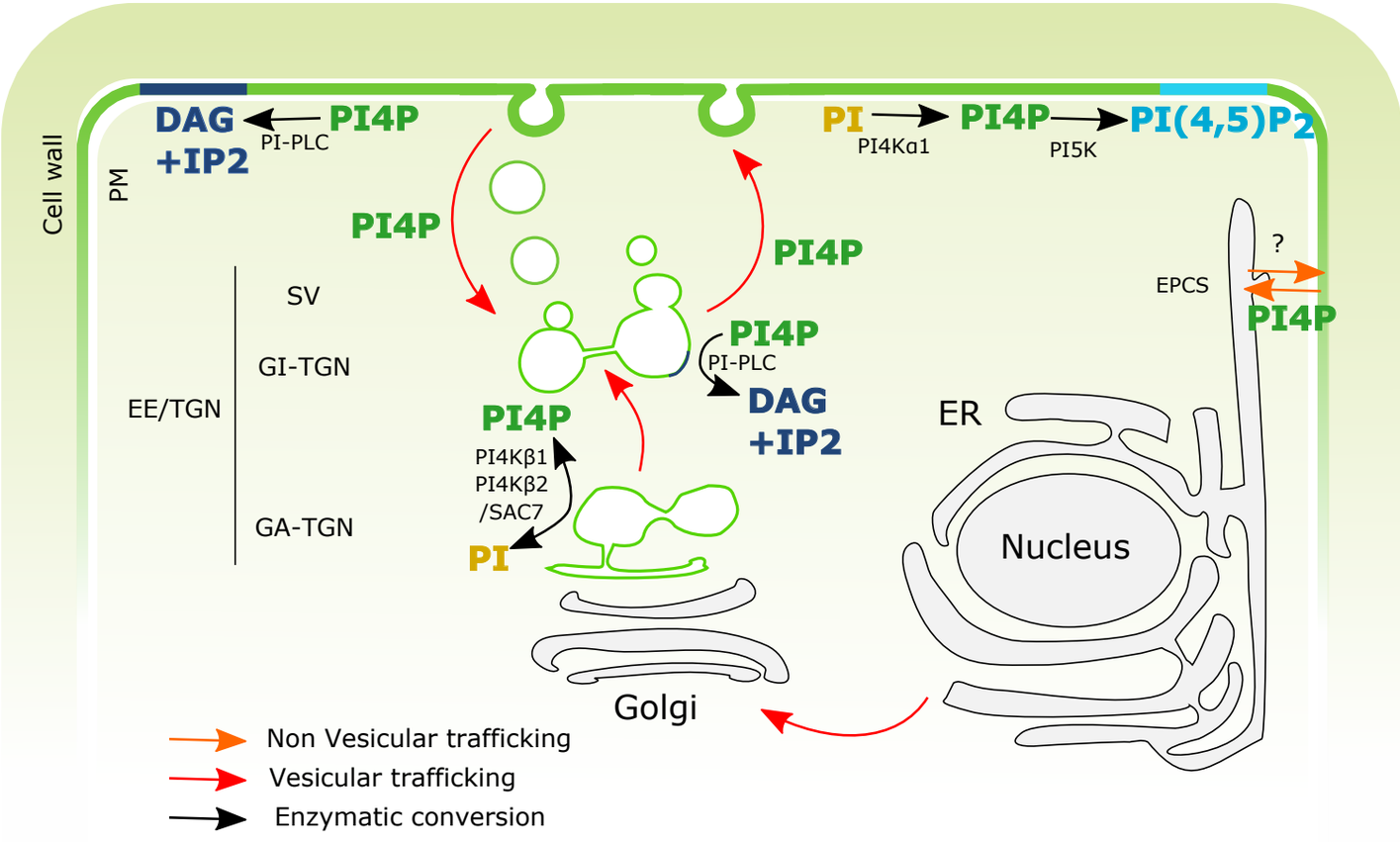

Figure 4. PI4P dynamic in plant cellRepresentation of the pools of PI4P, the exchanges between compartments and the enzymatic conversion involving PI4P in a plant cell. PI4K, phosphatidylinositol-4-kinase; PI5K, phosphatidylinositol-5-kinase; PI-PLC, Phosphoinositide Phospholipase C; SAC7, SUPPRESSOR OF ACTIN 7; PI, phosphoinositide; PI4P, phosphatidylinositol-4-phosphate; PI(4,5)P2, phosphatidylinositol-4,5-biphosphate; DAG, Diacylglycerol; IP2, D-myo-inositol 1,4-diphosphate; PM, plasma membrane; ; ER, endoplasmic reticulum; EPCS, ER-plasma membrane contact site; TGN/EE, trans-Golgi network/early endosomes; SV, secretory vesicle; GI-TGN, Golgi independent-TGN; GA-TGN, Golgi associated-TGN.

enzymes leads to death. Using temperature inducible mutant, it has been shown that in absence of Stt4 no PI4P was detected at the plasma membrane suggesting that PI4P do not traffic in big proportion from the TGN to the plasma membrane. Vice versa in the pik1 mutant, no PI4P from the plasma membrane was detected in the TGN (Roy and Levine, 2004). These data suggest that the two PI4P pools are largely independent. Similarly, in animal, PI4KIIIα localized at the plasma membrane while PI4KIIIβ, PI4KIIα and PI4KIIβ are found in the Golgi/TGN and endosomes (Balla et al., 2002, 2005; Nakatsu et al., 2012; Wang et al., 2003; Wei et al., 2002). PI4KIIα and PI4KIIβ can also act at the plasma membrane (Balla and Balla, 2006). In mammals, the loss of PI4KIIIα is embryo lethal (Nakatsu et al., 2012). In conditional mouse KO for PI4KIIIα the pool of PI4P at the plasma membrane was lost while the TGN morphology stay unchanged (Nakatsu et al., 2012). By contrast, in PI4KIIIβ, PI4KIIα and PI4KIIβ mutants, the golgi/TGN lose its structure suggesting that PI4KIIα is not functionally redundant with the other PI4-Kinase paralogs in animal (Balla and Balla, 2006; Balla et al., 2002; Wang et al., 2003). The key question is therefore how compartments maintain a specific identity despite the constant flow and exchange of proteins and lipids that happen during vesicular and non-vesicular mediated trafficking.

In *Arabidopsis*, *pi4kα1* loss-of–function is lethal **(Results, Figure 1)** which suggest that PI4Kβ1 and PI4Kβ2 cannot compensate for the pool of PI4P at the plasma membrane. By contrast, *pi4kβ1β2* double mutants present only mild phenotypes (Delage et al., 2012; Lin et al., 2019; Preuss et al., 2006; Rubilar-Hernández et al., 2019). To test the independence of the two pools in *Arabidopsis*, we must assess the localization of PI4P in *pi4kβ1β2* mutant and in PI4Kα1 complex loss of function using PI4P biosensors or membrane fractionation followed by lipidomic analyses.

Preliminary data from Matthieu Platre show that the PI4P sensor PH^{FAPP1} still localizes at the plasma membrane and at the TGN/EE in *pi4kβ1β2* mutant. As PH^{FAPP1} also interact with ARF1, this result need to be reproduced using a mutated version of PH^{FAPP1} to confirm the presence of PI4P at the TGN. Assuming PI4P remains at the TGN/EE in *pi4kβ1β2* background, PI4P from the plasma membrane might traffic to the TGN and partially compensate the loss of PI4Kβ1 and PI4Kβ2. PI4Kα1 could also delocalize at the TGN. Thus, the localization of the PI4Kα1 complex should be monitor in the *pi4kβ1β2* background. Indeed, some of the EFOPs or NPG protein seemed to also localize in intracellular compartments, that we do not know the nature. Thus, we can hypothesizes that PI4Kα1 might be able under some condition to delocalize in the TGN. Furthermore, we could evaluate increase of the strength of *pi4kβ1β2* specific phenotypes (root hair phenotype or the cell plate phenotype (Lin et al., 2019; Preuss et al., 2006) when crossed with a knock down of *PI4Kα1*.

Finally, the plant TGN might still partially function without PI4P. This might be due to compensatory effect from other anionic lipids with similar properties. It would be interesting to study the repartition of PA or PS and other PIP in *pi4kβ1β2* mutant.

b. Exchanges at membrane contact sites

In *Arabidopsis*, the ER membrane establishes contact sites with other organelles including the plasma membrane, at so-called ER-PM contact site (EPCS). These contacts are maintained by tethering proteins from the SYT, VAP or MCTP family (Bayer et al., 2017; Brault et al., 2019; Pérez-Sancho et al., 2015; Saravanan et al., 2009; Wang et al., 2016a, 2016b). All tethering proteins interact with PIP and/or PS suggesting that the lipid composition of the membrane is important for the establishment of these contacts. Moreover, recent studies show that the PIP content at EPCS is dynamic and modulated

upon stress. Indeed, ionic stress triggers the expansion of EPCS tethered by SYT1 in association with accumulation of PI(4,5)P_2 at the PM while treatment with rare earth element induces the accumulation of PI4P at those same EPCS (Lee et al., 2019, 2020). These PIP accumulations could result from a rearrangement of PI4P and PI(4,5)P_2 at the plasma membrane or from a recruitment of PIP kinases. In our study, we visualize that PI4Kα1 complex has a dotty pattern at the plasma membrane **(Results, Figure 5 and 6)**. This pattern could correspond (partially or fully) to EPCS. Thus co-localization study with EPCS markers in normal and upon stress conditions could allow us to test this possibility.

In mammals and yeast, lipid exchanges between the membrane of the ER and the plasma membrane mediated by LTP take place at EPCS. For instance, ORP can transfer PS from the ER to the plasma membrane in exchange of PI4P **(Introduction A, Figure 4)** (Wu et al., 2018). In this system PI4P serves as biofuel for the counter transport of PS. Moreover, in yeast, Stt4 has been shown to directly localize at EPCS where Osh3 transfer PI4P to the ER. This lipid exchanges have not been formally demonstrated in plants. However, most LTP are conserved, including the ORP family. Thus, non-vesicular transfer is a mechanism to take in account in the establishment of PI4P at the plasma membrane.

Finally, PI4P transfer at EPCS also requires Sac1 dephosphorylating PI4P at the ER membrane. In yeast, knock out of *sac1* rescue comes of the phenotype of *stt4* mutant (Foti et al., 2001). *Arabidopsis* genomes count three orthologs of Sac1: SAC6, SAC7/RHD4 and SAC8 (Despres et al., 2003; Thole et al., 2008). It is not clear if these proteins can have similar function in plants. Indeed, they all complement yeast *sac1* mutant and localize in the ER when express in tobacco (Despres et al., 2003). However, SAC7 functional reporter is found in the TGN when expressed in A*rabidopsis* (Thole et

al., 2008). Further work is needed to assess the localization of the sac1 orthologs in *Arabidopsis*. Additionally, *sac6*, *sac7* and *sac8* mutant crossed with *PI4Kα1* knockdown or *npg1npgr1npgr2* mutant for instance could allow us to assess the genetic interaction with *PI4Kα1*.

5- PI4P and TGN compartmentalization

SAC7, as well as PI4Kβ1 and PI4Kβ2, localize at the TGN (Thole et al., 2008). However they have opposite catalytic activities, as the first one is a PI4-Phosphatases and the seconds are PI4-Kinases. Thus it seems rather counterintuitive to find them at the same compartment. Additionally, the phospholipases PLC2 and PLC7 that used PI4P as substrate are also found in the TGN/EE and may participate to the TGN PI4P homeostasis (Ito et al., 2020).

However, the insights on the organisation of the plant TGN/EE have made a lot of progresses in the past few years. In plants, the TGN/EE is a place of sorting of proteins coming from the Golgi but also a hub for recycling proteins from the plasma membrane and degradation pathways toward the vacuoles. Recently, the TGN/EE have been decomposed into two structures: the Golgi associated TGN (GA-TGN), which stay in contact with the trans-side of the Golgi through cisternae and the Golgi-independent TGN (GI-TGN) in which cisternae are detached from the Golgi (Kang et al., 2011; Uemura et al., 2014; Viotti et al., 2010). The two types of TGN have been characterized by different morphology – the GI-TGN presents higher density of secretory vesicles (SV) and clathrin coated vesicles (CCV) – and associated to different set of proteins (Uemura et al., 2014).

PI4P participates to the electrostatic field and the curvature of the TGN/EE membranes. These are important membranes features to target peripheral proteins with polybasic

patch or specific domains such as +ALPS motifs or the BAR domains. For instance, PI4Kβ1 is targeted to the TGN through a +ALPS motif (Platre et al., 2018) **(Figure 6)**. Thus, it will be interesting to look at the distribution of PI4P, as well as, the enzymes known at the TGN to act on the pool of PI4P in the TGN/EE taking in account the recent insights on the TGN organisation. So far, PI4Kβ1 and its protein partner RabA4b have been shown to localize in GA-TGN, GI-TGN and SV (Kang et al., 2011).

pi4kβ1β2 mutant and sac7/rhd4 mutant show disturbed tip growth in root hairs, suggesting problems in secretion or endocytosis as those two mechanisms are necessary for tip growth (Preuss et al., 2006; Thole et al., 2008). In addition, cell plate formation that requires coordinated burst of vesicles is also affected in *pi4kβ1β2* mutant (Lin et al., 2019). *pi4kβ1β2* mutants presents fewer but larger secretory vesicles still able to burst and reach the plasma membrane (Kang et al., 2011). This could indicate a role of PI4P in the control of secretion in the TGN/EE. A model could be that controlled secretion requires a burst of PI4P on SV, while the fusion of endocytic vesicles with the TGN requires a zone free of PI4P thanks to SAC7/RHD4, uncoupling secretion and endocytosis at the TGN.

The TGN is a dynamic platform that interconnects many compartments in the cells. Thus, the use of mutant might lead to compensatory effect or indirect consequences. To go further in the dissection of the role of PI4P at TGN/EE, a combination of fast inducible system to perturb PI4P synthesis or degradation and new live imaging microscopy approaches with better resolution will be needed.

Other membrane lipids have an important role for the function of the TGN/EE. In yeast, it has been hypothesized that the TGN displays lipid rafts that cluster proteins and lipids before secretion (Surma et al., 2011). In plants, no lipid raft has been observed at the

TGN so far. However, hydroxylated C24- and C26-acyl-chain sphingolipids are enriched in SV and necessary for proper PIN2 sorting, suggesting that lipids sorting coordinated with protein sorting might occur in plant TGN too (Ito et al., 2020; Wattelet-Boyer et al., 2016).

II- PI4Kα1 subunits are conserved among eukaryotes

In this study, we demonstrate that PI4Kα1 is not autonomously targeted to the plasma membrane but belongs to a heterotetrameric complex composed of NPG, HYC and EFOP proteins that define its localization. Using yeast-two-hybrid, we show that NPG proteins directly interact with PI4Kα1 and HYCCIN **(Results, Figure 2)**. Similar complexes exist in animal and yeast **(Figure 5)**. In yeast, Stt4 interacts directly with YPP1 that interacts in turn directly with efr3 (Baird et al., 2008; Chung et al., 2015; Wu et al., 2014). In animals, PI4KIIIα complex is centred on TTC7A/B that bridges EFR3A or B, FAM126A or B (also called hyccin) and PI4KIIIα (Baskin et al., 2016; Chung et al., 2015; Lees et al., 2017b; Wu et al., 2014). NPG, like YPP1 and TCC7B, is a TPR motif containing proteins allowing numerous protein-protein interactions **(Figure 6)**. Thus, NPG/TCC7/Ypp1 is the core protein that bridges the rest of complex together. In conformity with it, none of the HYCCIN and EFOP proteins were found in the yeast-two-hybrid screen using PI4Kα1 N-terminal part as bait.

The PI4Kinase complex is structurally conserved. To test to which extend this conservation is functional, we could try to complement yeast mutant with *Arabidopsis* protein and vice versa using the whole complex or only one subunit. This would test if the interaction domains are conserved.

In this study, we also show that EFOPs are recruiting the PI4Kα1 complex at the plasma membrane **(Results, Figure 7)**. We found that the N-terminal cysteines are necessary

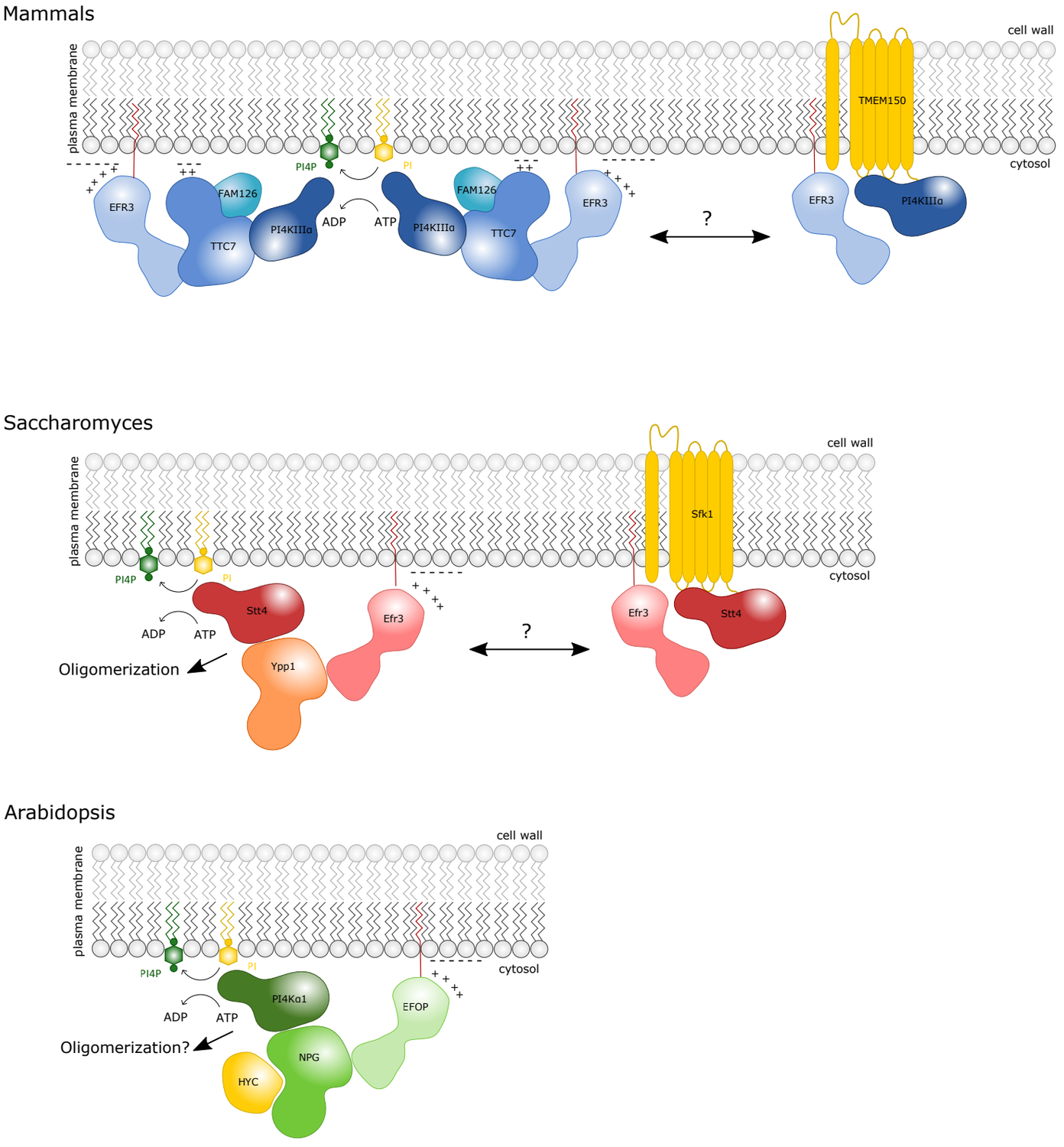

Figure 5. The plasma membrane PI4-Kinase complex in animal cell, yeast and Arabidopsis. The complex contains a catalytic unit (PI4KIIIα/Stt4/PI4Kα1), a structural unit that bridges all units together (TT7/Ypp1/NPG), a structural unit that targets the complex at the PM (EFR3/EFOP), and an additional unit (FAM126/HYC) in animal and plants. In animal and yeast, PI4KIIIα/Stt4 and EFR3 also interact with a transmembrane protein, TMEM150/Sfk1, independently of TT7/Ypp1.

and that a polybasic patch might be involved for the targeting at the plasma membrane. Moreover they are predicted to be S-acylated. Similar mechanism is found in yeast and animal cells. The mammal EFR3 is palmytoylated in N-terminal (Nakatsu et al., 2012). In yeast and mammals, positively charged amino acids in N-terminal of efr3 have been shown to form a electrostatic surface that mediates interactions with anionic lipids of the plasma membrane (Wu et al., 2014). The structure of the complex as well as the targeting mechanism to the plasma membrane is conserved among eukaryotes.

In animal, PI4KIIIα has been involved in cancer, Alzheimer disease and can also be hijacked by some human threatening viruses including hepatitis C (Clayton et al., 2013). Thus, the structures of the PI4KIIIαcomplex has been of particular interest and extensively studied for potential therapeutic solution. Notably, the cryo-EM structure of PI4KIIIα bound to TTC7B and HYCCIN/FAM126B have been obtained (Lees et al., 2017b). It revealed that PI4KIIIα complex form a dimer thanks to PI4KIIIα dimerization domain. In yeast, stt4 has not properly been shown to form dimer but to localize in patches containing around 30 Stt4 proteins suggesting an oligomerization mechanism (Baird et al., 2008). In this study, the possibility of PI4Kα1 to form dimer remains to be tested. However the patchy localization at the membrane suggest high concentration of PI4Kα1 complex that could be mediated by oligomerization as in animal cells or yeast **(Results, Figure 5 and 6)**.

Moreover, in animal, TTC7 N-terminal end and the kinase domain of PI4KIIIα form together a conserved surface composed of basic residues that interacts with the plasma membrane via electrostatic interactions (Lees et al., 2017b). This surface it thought to orient the kinase domain toward the membrane rather than participating to anchor the complex at the plasma membrane. Conserved basic residues are also found in the N-

terminal ends of NPG proteins **(Figure 6)**. It will also be interesting to test by directed mutagenesis if they influence the complex function, localization or the kinase turnover.

In animal cells and yeast, an additional protein, TMEM150/sfk1 has been shown to interact with EFR3 (Audhya and Emr, 2002; Chung et al., 2015). TMEM150/sfk1 is an integral membrane proteins composed of 7 transmembrane domains. In mammals' cells, EFR3 interaction with TMEM150 prevents its interaction with TTC7 (Chung, 2017). However, EFR3 somehow still localize PI4KIIIα at the plasma membrane when it interacts with TMEM50. This second mechanism of targeting of PI4KIIIα at the plasma membrane remains not well understood. Interaction with TTC7/FAM126 has been shown to increase the kinase activity of PI4KIIIα (Lees et al., 2017b). Thus, having a second targeting complex to the plasma membrane with TMEM150 might give another range of activity to PI4KIIIα allowing tight regulation of the amount of PI4P produced at the plasma membrane. In our study, we haven't been able to identify a good candidate to be the analogue of TMEM50. Nor our mass spectrometry analysis or blast analysis have allow us to find a potential analogue for TMEM50/sfk1. Thus, the existence of a second PI4Kα1 complex in *Arabidopsis* remains an open question. We can however expect PI4Kα1 bounds to NPG to behave differently at the plasma membrane than PI4Kα1 binding the potential analogue of TMEM50/Sfk1. So, we could study the dynamic of NPG protein and PI4Kα1 at the plasma membrane and see if they behave similarly or if we can distinguish two behaviours for PI4Kα1.

III- Post-translational regulation of the PI4Kα1 complex

PI4Kα1 targeting to the plasma membrane involved a large heterotetrameric complex. This high number of proteins localizing PI4Kα1 increases the complexity of the system and thus gives the possibility of a tight regulation of PI4P production. Indeed, the

regulation of PI4P production at the plasma membrane must not only take in account the transcription level, the mRNA maturation, the translational regulation, the protein degradation rate, the post translational modifications of PI4Kα1 but also the ones of NPG, HYCCIN and EFOP proteins.

PI4Kα1, NPG, EFOP and HYC are proteins of 225kDa, 77-83kDa, 110-114kDa and 39-48kDa, respectively. Together, PI4Kα1 complex is between 451-470kDa. Thus, the number of potential sites for posttranslational modifications is important making systematic directed mutagenesis to study them time consuming.

But posttranslational modifications, in particular phosphorylation are very likely regulating the PI4Kα1complex. In yeast, the C-terminal part of Efr3 is highly phosphorylated (Wu et al., 2014). These phosphorylations partially disturb the interaction with Ypp1, which results in mislocalization of Stt4 and in a decrease of around 10% of the total PI4P production in the cell. It is difficult from sequence alignment between EFOP and Efr3 to determine which amino acids could correspond on the *Arabidopsis* analogues. However, recently a new phosphoproteome of *Arabidopsis* have been published (Mergner et al., 2020). In this database, numerous phosphorylations are found for all members of the PI4Kα1 complex, including PI4Kα1 itself.

Interestingly, NPG proteins are found as highly phosphorylated at their N-terminus. In particular, one serine (S54/S62/S86 of NPG1, NPGR1, NPGR2, respectively) is predicted as phosphorylated in the three NPG and belongs to a region that is highly conserved among the NPG family **(Figure 6)**. Also western blot using anti-NPGR2 antibody often detected two bands indicating a possible posttranslational modifications **(Results, supplemental 2 and Figure 2)**.

Concerning HYC proteins some phosphorylation are found in the same region of the HYC domain that has a low conservation rate. However, most of the annotated phosphorylation sites are on the N-terminal end of HYC2 **(Figure 6)**. HYC1 is mainly constituted of a hyccin domain while HYC2 has an additional N-terminal sequence of low complexity. This N-terminal sequence is highly phosphorylated with a total of 17 phosphorylation sites annotated in the phosphoproteome. Although the short N-terminal end of HYC1 contains several serines, those are not annotated as phosphorylated. This suggests that different mechanisms could regulate HYC1 and HYC2 *in vivo*.

Altogether, a high number of regulatory mechanisms using phosphorylation might exist. It remains to be determined if these annotated phosphorylations exist *in vivo*, what are their effects on the PI4Kα1 complex and which kinases are responsible of them.

As mentioned before, EFOP proteins are S-acylated. S-acylation has the particularity to be a rapidly reversible lipid modification and thus can act as a molecular switch (Zaballa and Goot, 2018). It could be a regulatory mechanism of the synthesis of PI4P by recruiting or not the complex at the plasma membrane or to another compartments. Indeed, EFOP protein also localize in intracellular compartment that could correspond to plastids for instance **(Results, Figure 5)**. First, it would be interesting to confirm the S-acetylation of EFOP protein by S-acetylation assay (Hurst et al., 2017). Secondly, we could explore if the level of S-acetylation of EFOP changes upon environmental or developmental conditions. Looking for the protein responsible of the S-acylation of EFOP is difficult. Indeed, 24 putative Protein S-Acyl Transferases (PATs) are found in *Arabidopsis* and most of them have not been studied. No candidate has been found in a mass spectrometry analysis performed with EFOP2-mCt. We can note however that

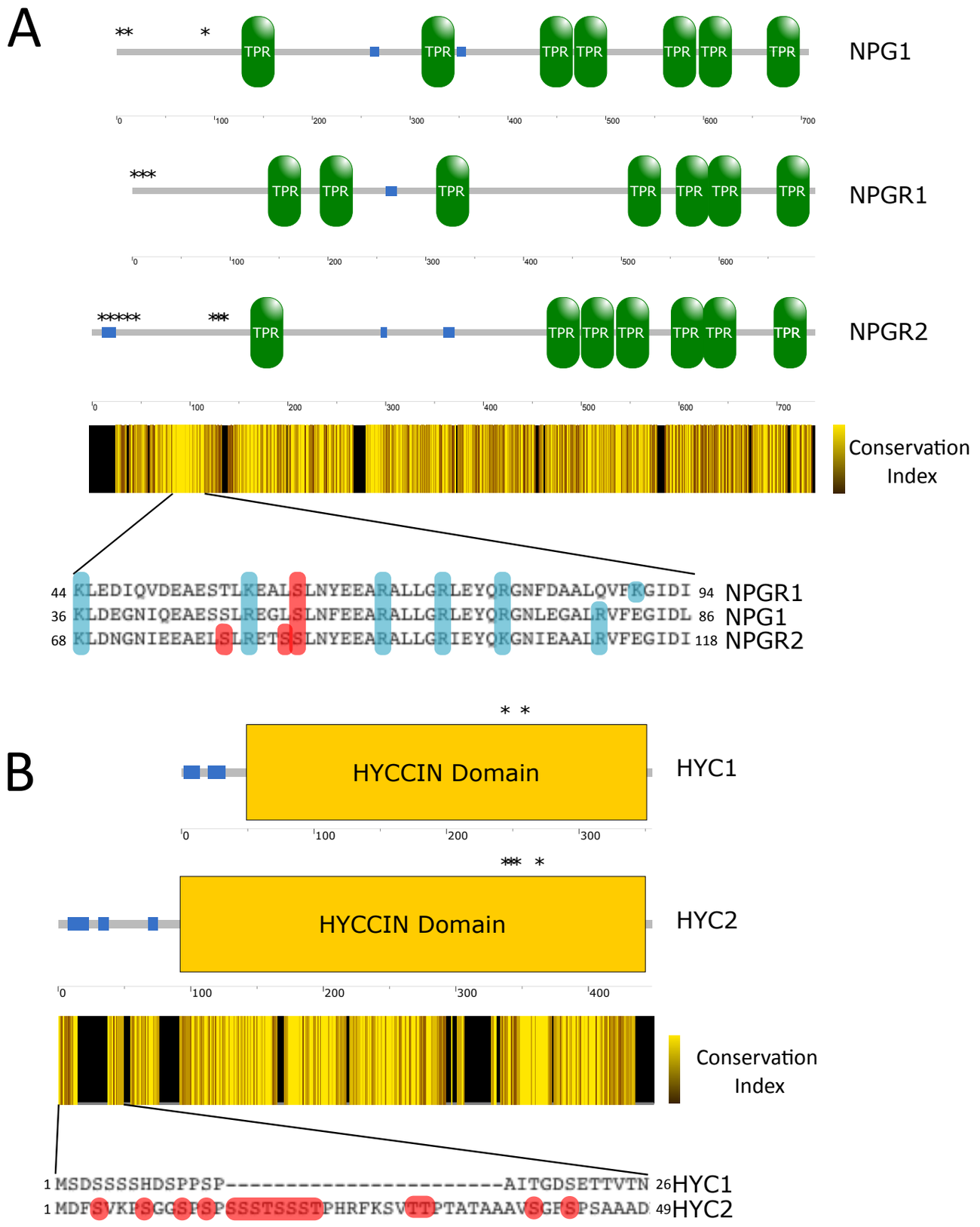

Figure 6. Protein domains and potential post-translational modifications of NPG and HYC proteins. Domains have been identified using the SMART (Simple Modular Architecture Research Tool) software. TPRs are represented in green, HYCCIN domain in yellow and low complexity regions are shown in blue. Amino acids mark in red and (*) indicate phosphorylation sites found in the phosphoproteome of Arabidopsis (PlantsP; http://plantsp.sdsc.edu). Sequence alignments have been performed using the Muscle WS software and edited with Jalview 2.0 software. Conservation index was obtained using Jalview 2.0 software. Conserved basic amino acids in the N-terminal ends of NPG proteins that might interact with the membrane to orientate the catalytic domain of PI4Kα1 are marked in blue.

PAT21 presents male gametophyte lethality with deformed pollen grains and localize at the plasma membrane (Li et al., 2019).

IV- Which strategy to study the role of PI4Kα1 complex on the membrane identity and plant development

To what extent does the PI4Kα1 complex is important for the production of PI4P at the plasma membrane (and the TGN) and on the PM identity? The male gametophyte lethality of PI4Kα1 limits the study by reverse genetic at the pollen grain. We could look at the PI4P and membrane surface charge (MSC) biosensor in mutant pollen grain. However the autofluorescence of the cell wall and the altered morphology of the pollen grains might make the observations difficult.

The role of the complex could be study by overexpressing it. However, the tag version of PI4Kα1 is not functional, as it does not complement the mutant. The untagged version is functional but cannot be monitor easily. In addition, the plant does not present any strong phenotype, which let us to think that it probably does not perturb the plasma membrane identity. Similarly, overexpression of the other subunits did not lead to any phenotype.

The PI4Kα1 complex has multiple isoforms for the structural subunits. NPG, HYC and EFOP present 2, 3 and 4 isoforms, respectively. A part of the work made during this thesis aimed to find expression pattern with tissue specificity using Gus reporter lines or phenotypic analysis. Indeed, a combination of mutant could lead to an easily observable tissue specific knockout of the PI4Kα1 complex avoiding the male gametophyte lethality. Concerning NPG protein, phenotypic analysis indicates that NPG1, NPGR1 and NPGR2 are important for pollen development **(Results, Figure 3 and Supplemental 3)**. NPG1 might have a more predominant role, as the single mutant is pollen lethal. Gus reporter

lines also indicate that the three isoforms are expressed in seedlings with a similar pattern **(data not shown)**. Only the triple mutant *npg1+/-npgr1-/-npgr2-/-* displays a sporophytic phenotype **(Results, Figure 4)**. Concerning HYC protein, phenotypic analysis indicates a specificity of HYC1 in the pollen grain and HYC2 in the sporophyte **(Results, Figure 3 and 4 and Supplemental 3 and 4)**. Both mutants are lethal. In the case of EFOP proteins, RNAseq data from efp browser indicate a specific expression of EFOP1 and EFOP3 in pollen grain while EFOP2 and EFOP4 should be broadly expressed. We found no pollen transmission *efop3efop4* and *efop1efop2efop3* mutant confirming the role of EFOP3 in pollen development and suggesting also expression of the three other isoforms **(Results, Figure 3 and Supplemental 3)**. We also noted that *EFOP1* (At5g21080) and *HYC1* (At5g21050) gene are close on the genome and might be under the control of common regulatory sequences. Altogether, a PI4Kα1/NPG1/HYC1/EFOP3 complex seems to predominate in *Arabidopsis* pollen. For the rest of the tissue however we haven't been able to determine any specific expression pattern for any of the subunits of the complex. Consequently, we were not able to find combination of mutant that has a phenotype strong and convenient for observation phenotype with the exception of the triple *npg* mutant, which might be a good tool in the future to study the developmental impact of PI4Kα1 complex loss.

An easy way to disturb the complex, that does not require genetic constructs or mutant, is the pharmacological approach. During my thesis, I tested two molecules PIK 93 and GSK-A1 that inhibits PI4KIIIβ and PI4KIIIα in human cell, respectively (Dornan et al., 2018). However, I did not observe any effect on PI4P or MSC biosensors in *Arabidopsis* epidermal root cell **(data not shown)**. The molecules might not inhibit the catalytic activity of the *Arabidopsis* enzymes or might not enter the cell due to the presence of a

cell wall. A screen for molecules able to inhibit specifically PI4Kα1 could be an interesting tool to know study the role of complex *in vivo*.

However, pharmacological approaches do not give the tissue specificity of genetic tools. We considered different genetically encoded system to knock down the PI4Kα1 complex. One of them was the design of artificial microRNA against PI4Kα1. This allows us to evaluate the impact of a partial loss of function of the kinase on the development of the sporophyte. We could conclude that the PI4Kα1 complex was critical not only for the development of the male gametophyte but also for the entire plant **(Results, Figure 4 and Supplemental 4)**. However, we did not observe any effect on the localization of PI4P or MSC biosensors upon induction of the artificial microRNA **(data not shown)**. It is likely due to the fact that the inhibition is not strong enough and that the remaining PI4Kα1 protein are sufficient to maintain a minimal pool of PI4P at the PM.

It might thus be required to obtained true inducible knock out of PI4Ka1. We discussed using other genetically encoded system, notably targeting the HYC subunit. Indeed, *hyc2* mutant is embryo lethal suggesting that HYC2 is fully required for the complex to function and that HYC1 is not express in the sporophyte to compensate the loss of HYC2 **(Results, Figure 4 and Supplemental 4)**. Inducible degron system, inducible tissue specific CrisPr as well as inducible rapamycin-dependent delocalization to the mitochondria has been considered, sometimes started and always dropped by lack of time because these are complex genetic strategies that are time consuming to build (Ali et al., 2020; Winkler et al., 2020).

V- PI4-Kinases and membrane patterning

1- How the PM pattern of PI4Kα1 is generated?

Our study suggests that PI4Kα1 complex localizes at the plasma membrane partly through electrostatic interactions between EFOP N-terminal end and anionic lipids. In *Arabidopsis*, the electrostatic field of the plasma membrane relies mostly on PI4P (Platre et al., 2018; Simon et al., 2016). Thus, PI4Kα1 might generate the lipid environment that allows the complex to be targeted at the plasma membrane, creating a positive feedback loop. As we observed that the PI4Kα1 complex was not homogenously localize at the plasma membrane but form a dotty pattern, we first wondered if this potential positive feedback could be the mechanism generating this pattern. However, using PAO treatment, that inhibits PI4-Kinase activity we did not see a delocalization or a loss of the patterning of EFOP2, HYC2 or NPGR2 **(Results, Figure 7)**. This suggests that the patterning relies on other protein (possibly actin or proteins of the EPCS as mention before) or lipid effectors. Indeed, S-acylated proteins have been associated with membrane raft enriched in sterol (Levental et al., 2010). For example, ROP6 is S-acylated upon activation and clustered into lipid rafts (Pan et al., 2019; Sorek et al., 2010, 2017). Thus, sterol could influence the nanodomain patterning of PI4Kα1 complex. This could be tested with complementary approaches using drug treatments (lovastatin, fenpropimorph) and mutants of the sterol pathway.

2- PI4P and PI4Kα1 dynamic at the membrane

Several questions remain about the localization of the complex at the plasma membrane. We show that the complex is clustered and do not diffuse laterally in the membrane **(Results, Figure 5 and 6)**. Moreover, it seems that the position of the PI4Kα1 subdomains are set but come for and back at the plasma membrane **(Results, Figure 6)**.

Do these subdomains correspond to a functional unit? A colocalization study with different markers including cytosqueleton, ER-PM contact site, plasmodesmata markers is on-going to determine a possible function of these subdomains.

Is PI4P also enriched is these subdomains? Crosses with PI4P biosensors will allow us to answer that question. Under normal condition, PI4P does not seem to form clusters. In addition, PI4Kα1 is inhibited by its substrate, which suggests that PI4P diffusion inside the membrane is needed for the catalytic activity to be maintained.

Is it changing depending of environmental cues, hormonal or physical cues? Is it modified during developmental processes? For instance, PS is forming immobile clusters into the plasma membrane (Platre et al., 2019). Upon auxin treatment these clusters become host ROP6, which activate its signalling pathway. PI(4,5)P_2 is also enriched in clusters at the plasma membrane (Fratini et al., 2020). Thus, it is possible that other anionic lipids change their membrane dynamics according to signals. In the case of PI4P, little is known. However, PI4P in combination with sterol is required for the nanoclustering of REM1.3 at the plasma membrane, suggesting that PI4P itself segregates into the membrane (maybe upon remorin activation) (Gronnier et al., 2017).

3- PI4Kβ: TGN membrane recognition through a +ALPS motif

PI4Kβ1 and 2 targeting to the TGN/EE is mediated by a mechanism of coincidence binding in which PI4Kβ directly interact with the membrane of the TGN/EE and also interact with RabA4b (Antignani et al., 2015; Kang et al., 2011; Preuss et al., 2006). PI4Kβ1 and PI4Kβ2 display a +ALPS (Amphipathic Lipid Packing Sensor) motif at the C-terminal end. ALPS motif forms an amphiphatic a-helice with a hydrophobic face and a hydrophilic face rich in serine and threonine (Platre et al., 2018). This last surface is able to recognize packing defects present in curved membrane. Upstream to this motif a

small sequence containing cationic residue can recognize anionic lipid. + ALPS motif targets curved and electrostatic membranes such as the TGN/EE membrane.

In N. benthamiana, depletion of this motif is sufficient to lose the TGN localization of PI4Kβ1 and this motif alone can localize at the TGN suggesting that this motif is necessary and sufficient for TGN localization (Platre et al., 2018). Preliminary data suggest that these results are reproducible in stable *Arabidopsis* lines. Observation of different constructs in the *pi4kβ1β2* double mutant T1 plants show that PI4Kβ_WT localize at the cell plate and in intracellular compartments that should correspond to the TGN/EE **(Figure 7)**. When the +ALPS motif was deleted (PI4Kβ1_Δ+ALPS), the protein became fully soluble. Moreover, single point mutation in the +ALPS helix (PI4Kβ1_L1102D) or mutation of the positive amino acids upstream the ALP motif (PI4Kβ1_+mut) seemed to reduce the association of PI4Kβ1 with the TGN but interestingly not with the cell plate. PI4Kβ1 cell plate localization might rely more on interactions with effectors than on the +ALPS. Reintroduction of PI4Kβ1_WT was able to complement the *pi4kβ1β2* growth phenotype in 50% of the T1 transformed plants. However, deletion of the +ALPS motif leads to 0% of complementation and mutated versions were not able to complement in most cases suggesting that the targeting of PI4Kβ through its +ALPS motif is necessary for its function. However, this is a preliminary analysis that should be reproduced quantitatively.

The +ALPS motif could be a common mechanism for targeting protein to the TGN/EE. For instance, the ARF-GAP proteins AGD6 and AGD7 seemed to also localize through this mechanism in *Arabidopsis* (Platre et al., 2018). Thus, screening for this motif could be a way to identify TGN/EE proteins in the future.

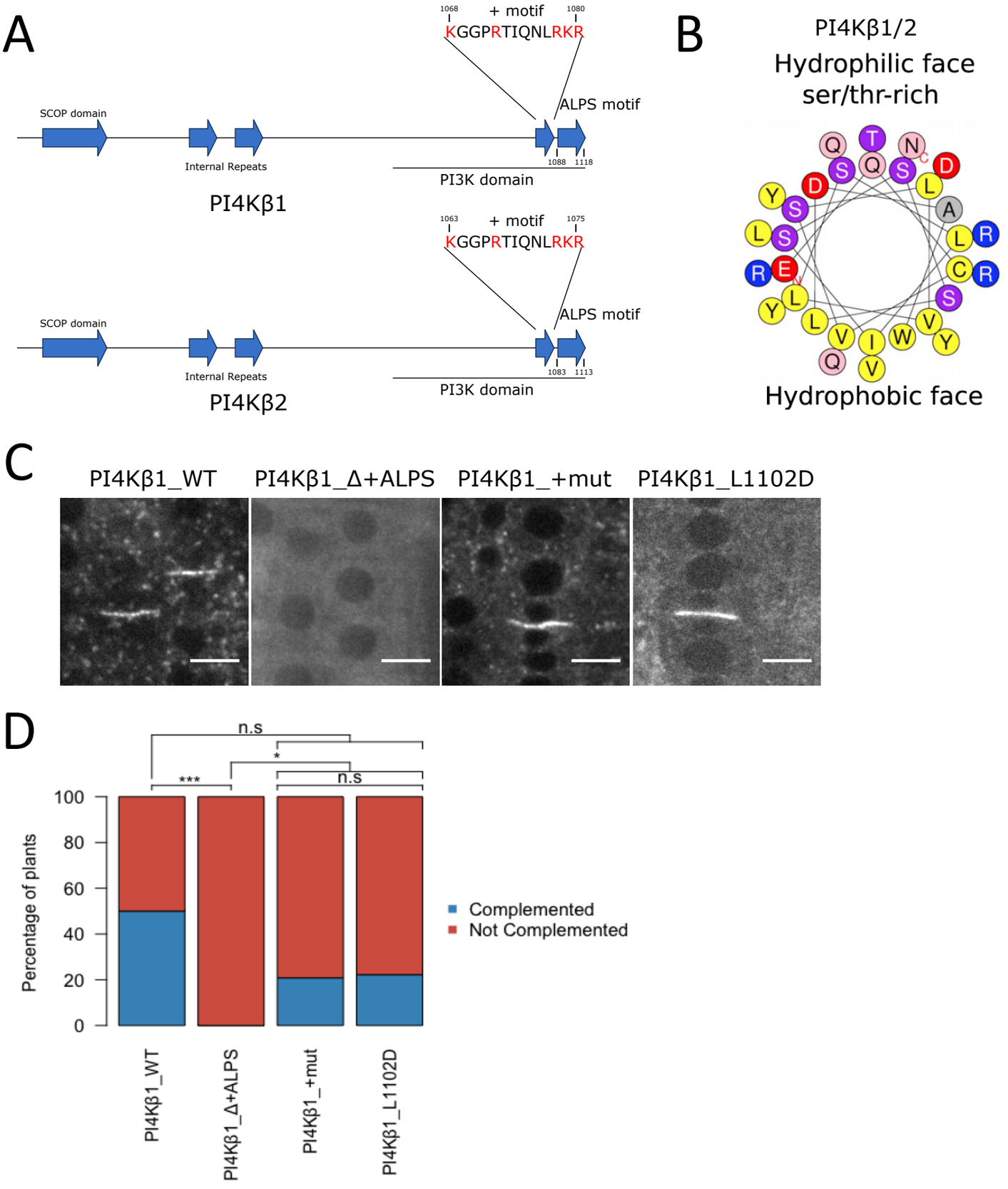

Figure 7. PI4Kβ membrane interaction (A) Schematic representation of PI4Kβ1 and PI4Kβ2 protein structure. The sequence of the +ALPS motif is indicated. Domains have been identified using the SMART (Simple Modular Architecture Research Tool) and the HELIQUEST software. **(B)** Helical wheel representation of the PI4Kβ1 or PI4Kβ2 ALPS motif using HELIQUEST software. **(C)** Confocal images in Arabidopsis root epidermal cells of PI4Kβ1_WT, PI4Kβ1_Δ+ALPS, PI4Kβ1_+mut and PI4Kβ1_L1102D fused to mCITRINE. **(D)** Percentages of complemented T1 plants expressing PI4Kβ1_WT, PI4Kβ1_Δ+ALPS, PI4Kβ1_+mut and PI4Kβ1_L1102D fused to mCITRINE under the control of the UBQ10prom. Statistics have been done using Fisher test.

VI- PI4Kα1 loss-of-function: What is going wrong?

Our phenotypic analysis of knock out and knock down reveals the critical importance of PI4Kα1 for plant development. However, our study did not allow us to precisely identify the reasons leading to male gametophyte lethality or the growth phenotype. As mentioned before, we cannot exclude indirect effect on other lipid homeostasis, notably PS and PI(4,5)P_2 which are intimately linked to PI4P.

1- Direct implication of PI4P on vesicular trafficking

Endocytosis, exocytosis or protein recycling at the plasma membrane could be affected in PI4Kα1 knockout or knockdown independently of PI(4,5)P_2. In yeast, PI4P is necessary for the recruitment of several proteins involved in clathrin-mediated endocytosis independently of PI(4,5)P_2 (Yamamoto et al., 2018). A direct role of PI4P in vesicular trafficking is also a possibility. First, the clusters form by the PI4Kα1 complex at the plasma membrane suggest that PI4Kα1 could be involved in specific processes at the plasma membrane **(Results, Figure 5 and 6)**. Furthermore, the yeast-two-hybrid screen performed with the N-terminal part of PI4Kα1 revealed possible interaction with proteins involved in trafficking. Here is the list of interesting potential interactions:

- **Dynamin related protein 1E (DRP1E)**

We found 2 independent clones of DRP1E. Dynamins and Dynamin related proteins are involved in trafficking as they form structures facilitating membrane tubulations. They can recruit various binding partners including proteins and lipids. DRP1E has been involved in several developmental processes including embryogenesis and reproduction, cold acclimation and cell death in response to powdery mildew (Kang et al., 2003; Tang et al., 2006). DRP1E seems to associate with mitochondria as well as with cell plate and plasma membrane. Interestingly, DRP1E forms a punctuated pattern that

corresponds to regions enriched in sterol and sphinglolipids at the plasma membrane (Minami et al., 2015). It has been hypothesized that these regions could correspond to CCP mediating endocytosis at the plasma membrane. DRP1E is also able to interact with PA and PI4P *in vitro* (Minami et al., 2015).

- **EHD1:**

One clone has been found in the yeast-two-hybrid screen. EHD1 localized in endosomes and at the plasma membrane (Bar et al., 2008). EHD1 is regulating the speed of internalization from the plasma membrane and has been involved in salt tolerance.

- **ROPGEF9:**

ROPGEF are regulators of ROP (Rho of plants), which act as molecular switch in many developmental processes including tip growth. Tip growth requires a coordination of exocytosis at the tip and endocytosis in the flank region. In pollen tube, several redundant ROP regulates polar growth by controlling actin dependant exocytosis downstream of the PRK2 receptor (Chang et al., 2013). ROPGEF9 in combination with other ROPGEF might be involved in the regulation of this process as the quadruple mutant *ropgef1,9,12,14* shows pollen tube growth defects (Chang et al., 2013).

- **EXO70H8:**

The exocyst complex tethers vesicles coming from the TGN to the plasma membrane during exocytosis. It is composed of eight subunits: SEC3, SEC4, SEC5, SEC6, SEC8, SEC10, EXO70 and EXO84. A plant particularity is the great amount of EXO70 paralogs compare to the unique EXO70 gene in animal or yeast. For instance, in *Arabidopsis* 23 different genes encode the EXO70 subunit (Li et al., 2010). It has first been thought that the high number of paralogs would be explained by tissue specificity. However, in many cells several exo70 paralogs are expressed. Recently, it has been shown that in tobacco pollen tube and in *Arabidopsis* trichomes, different Exo70 subunits are targeted to

different plasma membrane compartment according to their faculty to bind to PA, PS or PI(4,5)P_2 (Kubátová et al., 2019; Sekereš et al., 2017). We found two independent clones for interaction with EXO70H8. This paralog is pollen specific according to *efp* browser dataset. In addition, SEC3 was found by mass spec to interact with PI4Kα1.

Altogether, it is possible that the PI4Kα1 complex recruit or is recruited by one of those interactions specifically at endocytosis and exocytosis sites. A burst of PI4P could help curve the membrane thereby facilitating membrane deformation during those events. Uncoupling, the role of PI4P and PI(4,5)P_2 in trafficking is tricky. Only inducible system with fast response on the plasma membrane pool of PI4P can help us to unravel the direct importance of PI4P in trafficking.

2- Why is PI4Kα1 pollen lethal?

Pollen development takes place in the sporangia of the anthers (Borg and Twell, 2011) **(Figure 8)**. During pollen development numerous processes involving membrane trafficking occur in the pollen cells and in the maternal tissue surrounding the pollens, called tapetum. Indeed, first the mother pollen cells will expend and secrete a primary cell wall rich in cellulose. Then, during meiosis, this cell wall is replaced by a cell wall of callose. The tapetum cells specialize into polar secretion. After meiosis, each microspore synthesizes a cell wall containing callose and precursors of the intine and exine layers called primexine. The tapetum releases callase to free the microspores from the tetrad. Each microspore will generate many small vacuoles, which fuse to form one big vacuole at the macrospore stage. The nucleus will migrate in the opposite site of the aperture and the first asymmetric mitosis will occur giving the vegetative cell and the generative cell. The two cells will be separated by a cell wall enriched with callose. This cell wall will be degraded by secretion of degradation enzymes such as glucanase, allowing the

generative cell to migrate inside the vegetative cells. Two membranes next to each other separate the vegetative cell and the generative cell. From meiosis to the end of microspores development, the tapetum establishes the exine layers around the pollen grain by secreting sporopollenine, while the intine layer is synthesised by the pollen. The pollen maturation ends with the second mitosis of the generative cells giving two sperm cells.

pi4kα1, hyc1 and *efop3efop4* double mutant are male sterile according to the segregations and the reciprocal crosses performed. Many male sterile mutants have been identified in *Arabidopsis* and most of them are involved in pollen cell wall formation. This includes defects of secretion, biosynthesis or transport in the tapetal cells or microspores or callose and cellulose deposition by the microspores.

Scanning electron microscopy of *pi4kα1*, *hyc1* and *efop3efop4* pollens from heterozygous plants show that about 50% of the pollens are defectives and 50% have a normal morphology meaning that the mutation is recessive and only the mutant pollen are defective **(Results, Figure 1 and 3)**. They present a thicker an irregular intine layer. Thus, it is likely that the secretion of cell wall materials by the micropores is affected. The intine layer has a composition similar to a primary cell wall with cellulose, hemicellulose and pectin. *CESA1* and *CESA3* encode for subunit of the cellulose synthase complex (Mutwil et al., 2008). *cesa1* and *cesa3* mutants are pollen sterile with shrivelled pollen grains similar to *pi4kα1* mutant (Persson et al., 2007). In *cesa* mutants, a non-homogeneous deposition of intine is observed revealing the importance of cellulose

Figure 8. Pollen development

The different steps of pollen development involving membrane trafficking are described. The steps where PI4Kα1 complex might be necessary explaining the *pi4kα1*, *hyc1*, *efop2efop3* and *efop3efop4* mutant phenotype are indicated.

Microsporogenesis

Pollen Mother Cell

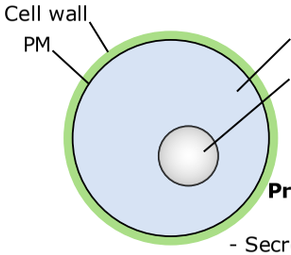

MEIOSIS

Primary cell wall degradation
- Secretion of degradation enzymes
- Cellulose synthase endocytosis

Primary cell wall apposition
- Cellulose Synthesis at the PM
- Vesicle secretion
- Cellulose synthase exocytosis

Tetrad

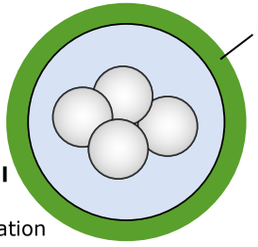

Cell wall of calose apposition
Calose synthase exocytosis

?
efop2efop3

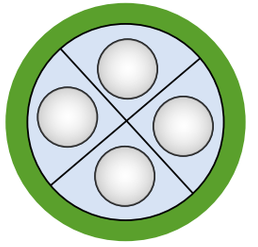

Cellularization
- Vesicule secretion from the TGN
- Vesicles fusion at the cell plate

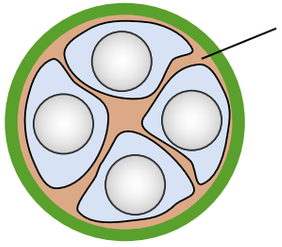

Primexine secretion
- Callose synthase exocytosis
- Secretion of vesicles containing intine and exine precursors
- Plasma membrane undulation

?
pi4ka1, hyc1, efop3efop4

Microspores

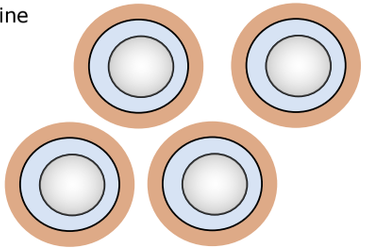

Microspore released
Callase complex (glucanase) secretion from the tapetum

Microgametogenesis

Unicellular

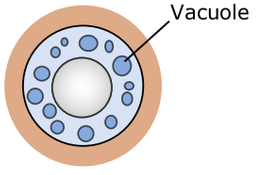

Vacuole formation
Scision of vesicles

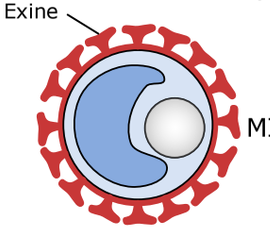

Vacuole fusion and nucleus migration

Exine formation
Secretion of sporospolenine precursors by the tapetum

?
efop2efop3

Bicellular

MITOSIS I

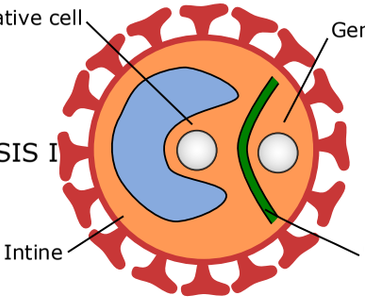

Cell division
- Secretion of vesicles from the TGN
- Vesicle fusion at the cell plate
- Callose deposition

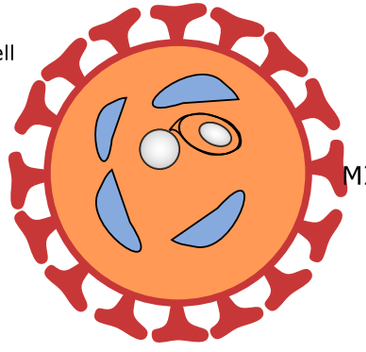

Cell wall degradation
Secretion of degradation enzymes (glucanase)

Tricellular

MITOSIS II

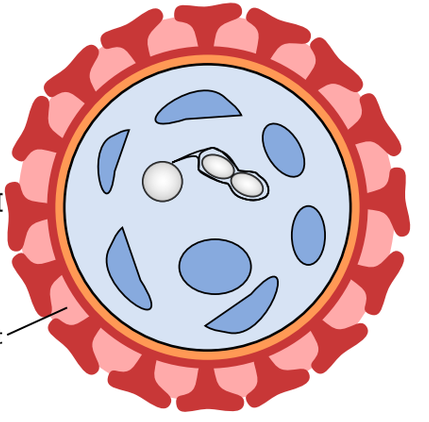

Pollen coat formation
Secretion of lipids by the tapetum

microfibrilles to guide intine deposition. Tplate complex has also been involved in pollen cell wall deposition (Van Damme et al., 2006). T-plate mutants are male sterile with shrivelled pollens due to abnormal deposition of callose in the intine layer. This could be explained by a missregulation of callose synthase endocytosis in *t-plate* mutant. It is possible that callose synthase endocytosis mediated by T-plate complex and/or cellulose deposition is also affected din *pi4kα1* complex mutant.

efop2efop3 mutant also presents pollen morphological defects **(Results, Figure 3 and Supp 3)**. Indeed, almost all the pollens from *efop2efop3* mutant are deformed. However, it was possible to obtain double homozygous plant indicating that the *efop2efop3* pollen grain is not lethal. Therefore, it is possible that the defect observed on the pollen grains do not come from the microspores but from a misregulation of the secretion of material by the tapetum. Another possibility is that the first steps of pollen development before meiosis are impaired in *efop2efop3* mutant.

Interestingly, during microspore development tapetal cells acquire a huge ER compartment that lay beneath the plasma membrane. Mutant involved in ER-Golgi transport such as *sec31b* that belongs to the COPII complex present similar phenotype that *efop2efop3* mutant with a combination of normal, deformed and collapse pollen grains (Zhao et al., 2016).

3- Maternal tissue, ovule and embryo: Why do you need your mother?

Animal, yeast and plant mutants for the PI4Kα1 complex are lethal suggesting that the cell cannot survive without it. However, in *Arabidopsis* the female gametophyte can still transmit the mutant allele for *pi4kα1* **(Results, Table 2)**. Similarly, while we assume that HYC1 was specifically express in pollen and HYC2 was broadly express in the rest of the tissue, *hyc2* mutant is still able to develop until the late globular stage **(Results,**

Figure 4). We wonder how the female gametophyte and the embryo still manage to develop in absence of the PI4Kα1 complex. The female gametophyte and the embryo have in common to be embedded in the maternal tissue. The maternal sporophyte is heterozygous and thus the PI4Kα1 complex is still present at the plasma membrane. Maternal tissue might be able to provide for the development of the female gametophyte. At the beginning of the female gametophyte development, numerous symplastic connections are present between the nucellus cells and the female gametophyte (Ingram, 2010). These connections persist at the chalazal pole of the megaspore. A little before or at the moment of fecundation, all symplastic connection between the maternal tissue and the female gametophyte disappear and the egg cell is isolated. PI4P or mRNA coding for PI4Kα1 could move through these symplastic connections.

hyc2 mutant seems to develop normally until globular/early heart stage. *HYC1* mRNA or HYC1 protein coming from the sperm cell after fecundation might be present in the early stage of embryo development and compensate for the *hyc2* knockout. After fecundation, the embryo and the suspensor develop and form a single symplast unit until globular/early heart stage (Ingram, 2010). This corresponds to the moment when hyc2 mutant stop its development and degenerate. The suspensor connects the embryo to the maternal tissue through active transport of nutrient and hormones (Jacob and Brian, 2020). It is also known for segregating protein and mRNA coming from the egg cell or the sperm cell. Thus, HYC1 mRNA or protein coming from the sperm cell after fecundation could segregate in the suspensor, explaining why the transition of globular to heart stage is critical for *hyc2* mutant.

V- Disregarded roles of PI4P in this study

The plasma membrane is part of the endomembrane system, which connects compartments through membrane continuity, vesicular trafficking or contact sites. However, PI4P can also be found in membranes that are not part of the endomembrane system (mitochondria and chloroplasts) or even not associated with membrane (Gerth et al., 2017a).

1- PI4P and PI4Kα1 in the nucleus

Inositol phosphates and phosphoinosites have been found at the nuclear envelope but also in the nucleoplasm. In animal and yeast, the nuclear phosphoinositides are involved in many nuclear processes including chromatin structure, DNA replication, transcription factor regulation, RNA processing, and transcription (Castano et al., 2019). Phosphoinositides present in the nucleoplasm could form micelle or lodge itself in hydrophobic pocket of proteins. For instance, PIP5K1A and PI(4,5)P_2 interact with the tumor suppressor protein p53 in animal cell which increases its stability (Choi et al., 2019). In animal cells, the entire PIP pathway has been described in the nucleus by localization of the PIP and the enzymes or presence of PIP activity *in vitro* (Gonzales and Anderson, 2006). Notably, PI4P localizes in nuclear speckles using PI4P antibody and PH^{Osh1} biosensors. PI4-Kinases including PI4KIIIα localized in the nucleus (Kakuk et al., 2006). In *Arabidospsis*, our knowledge so far relates mainly to PI(4,5)P_2. PI(4,5)P_2 is present in pits in the nuclei and accumulate with PA upon heat stress (Mishkind et al., 2009). Additionnaly, PI5K2 localize in the nucleus thanks to an NLS sequence and interact with importins implying that PI4P might be phosphorylated in the nucleus to produce PI(4,5)P_2 (Gerth et al., 2017b). PI4P could be transported or directly produced by PI4-Kinases inside the nucleus. Using immunolocalization, Gerth et al. revealed the

presence of PI4P in the nucleus, which favour the idea that PI4-Kinases must be present in nuclei (Gerth et al., 2017b).

In our study, we use PI4Kα1 antibody to localize the protein. In addition to the cytoplasmic and plasma membrane signal, we also observed a signal in the nucleoplasm suggesting that PI4Kα1 could localize in the nucleus **(Results, Figure 5)**. Three potential NLS sequence are predicted for PI4Kα1 **(Figure 9)**. However, only one is outside of the catalytic domain. Our reporter lines for PI4Kα1 (PI4Kα1-mCt, mCt-PI4Kα1 and PI4Kα1-2xmCherry) never showed a signal in the nucleus **(Results, Figure 5)**. Nevertheless, these constructs were not able to complement the *pi4kα1-1* mutant. It is possible that the fusion with a fluorescent protein hide the NLS sequence, which prevent the targeting to the nucleus and therefore the complementation of the mutant. Similarly, the fusion of PI4Kα1 with Lti6b, which localizes the protein at the PM, complemented *npg1-2* mutant but no transformant complementing *pi4kα1-1* was found **(Results, Figure 7)**. This data suggests that PI4Kα1 might have a role in the nucleus, independently of the other structural subunits of the complex that serve to target the kinase at the PM. To test this hypothesis, we are trying to artificially target PI4Kα1-mCt to the nucleus in order to complement the *pi4kα1-1* mutant and the *pi4kα1-1/PI4Kα1prom::PI4Kα1-mCt-Lti6b* line. We could also mutate the predicted NLS in PI4Ka1 to test their functionality.

In addition, several transcription factors (TEOSINTE BRANCHED 1/CYCLOIDEA/ PCF1 (TCP) transcription factors 20, 22 and 3) and chromatin-remodeling proteins (CHR11 and CHR17 that acts redundantly) were found in in the yeast-two-hybrid screen performed with the N-terminal part of PI4Kα1 (Huanca-Mamani et al., 2005).

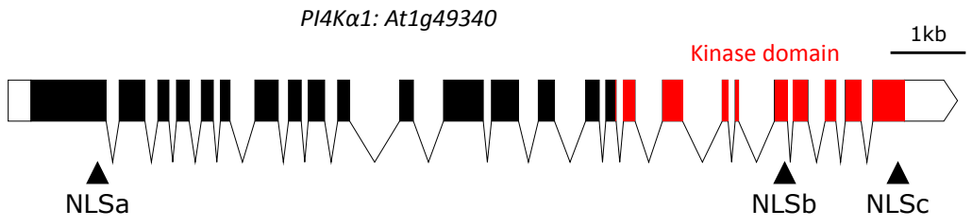

Name	Sequences (aa)	SeqNLS score	NLSmapper score
NLSa	^{322}KRQLQSMSAFLKSRKRDWNEQG^{343}	0.902	not predicted
NLSb	^{1701}RRAGIRRELEKIEMQGDDLYLPTAPNKLVRGI^{1732}	not predicted	5.5
NLSc	^{1976}RGDPIGNLRKRFHPE^{1990}	0.861	7.5

Figure 9. Potential NLS in PI4Kα1
Three potential NLS are predicted using SeqNLS or NLS mapper.

2- The importance of PI4P in the chloroplast

In our study we observed that an inhibition of PI4Kα1 induces a bleaching of the cotyledons followed by death of the seedlings when the seedlings are grown on MS medium non supplemented with sucrose **(Results, Supp1)**. Moreover, this phenotype is not observed anymore when sucrose is added to the medium. It suggests a photoautotrophic phenotype. PI4P is present in the envelope of chloroplast but its function in this compartment is still very elusive (Gerth et al., 2017b).

Recently, a sec14 like protein, called CPSFL1, has been described to co localize at the envelope of the chloroplast with PI4P (García-Cerdán et al., 2020). CPSFL1 can complement the *sec14* yeast mutant and is able to transfer PI4P from one liposome to another, *in vitro*. The *cpsfl1* mutant presents photoautotrophic phenotype due to a lack of chloroplastic vesicles. These vesicles have been suggested to play a role in thylakoids growth and de novo formation. It is not known if thylakoid membranes are formed via the fusion of vesicles coming from the envelope, membrane contact sites between the envelope and the thylakoid membrane or lipid transfer protein. This study suggests that PI4P plays a central role in chloroplast vesicular trafficking. Another paper shows that a knockdown of PI4Kα1 is sufficient to remove PI4P from chloroplast (Okazaki et al., 2015). However, the absence of PI4P increases chloroplast division in this case, which is difficult to compute with our own observations.

Conclusion

In this study, we uncovered some of the main molecular actors of the production of PI4P at the plasma membrane. The PI4Kα1 complex is likely responsible for the main production of PI4P at the plasma membrane. In the near future, we need to investigate how thee complex is regulated and what is the functional relevance of its specific localization into nanodomains. One of the main topic to delve into will be to study what are the interplays between PI4P or the PI4Kα1 complex and the other membrane lipid pathways.

References

Ali, Z., Mahfouz, M.M., and Mansoor, S. (2020). CRISPR-TSKO: A Tool for Tissue-Specific Genome Editing in Plants. Trends in Plant Science *25*, 123–126.

Antignani, V., Klocko, A.L., Bak, G., Chandrasekaran, S.D., Dunivin, T., and Nielsen, E. (2015). Recruitment of PLANT U-BOX13 and the PI4Kβ1/β2 Phosphatidylinositol-4 Kinases by the Small GTPase RabA4B Plays Important Roles during Salicylic Acid-Mediated Plant Defense Signaling in Arabidopsis. Plant Cell *27*, 243–261.

Audhya, A., and Emr, S.D. (2002). Stt4 PI 4-Kinase Localizes to the Plasma Membrane and Functions in the Pkc1-Mediated MAP Kinase Cascade. Developmental Cell *2*, 593–605.

Audhya, A., Foti, M., and Emr, S.D. (2000). Distinct Roles for the Yeast Phosphatidylinositol 4-Kinases, Stt4p and Pik1p, in Secretion, Cell Growth, and Organelle Membrane Dynamics. Mol Biol Cell *11*, 2673–2689.

Baird, D., Stefan, C., Audhya, A., Weys, S., and Emr, S.D. (2008). Assembly of the PtdIns 4-kinase Stt4 complex at the plasma membrane requires Ypp1 and Efr3. J Cell Biol *183*, 1061–1074.

Balla, A., and Balla, T. (2006). Phosphatidylinositol 4-kinases: old enzymes with emerging functions. Trends Cell Biol. *16*, 351–361.

Balla, A., Tuymetova, G., Barshishat, M., Geiszt, M., and Balla, T. (2002). Characterization of type II phosphatidylinositol 4-kinase isoforms reveals association of the enzymes with endosomal vesicular compartments. J. Biol. Chem. *277*, 20041–20050.

Balla, A., Tuymetova, G., Tsiomenko, A., Várnai, P., and Balla, T. (2005). A Plasma Membrane Pool of Phosphatidylinositol 4-Phosphate Is Generated by Phosphatidylinositol 4-Kinase Type-III Alpha: Studies with the PH Domains of the Oxysterol Binding Protein and FAPP1. MBoC *16*, 1282–1295.

Bar, M., Aharon, M., Benjamin, S., Rotblat, B., Horowitz, M., and Avni, A. (2008). AtEHDs, novel Arabidopsis EH-domain-containing proteins involved in endocytosis. The Plant Journal *55*, 1025–1038.

Baskin, J.M., Wu, X., Christiano, R., Oh, M.S., Schauder, C.M., Gazzerro, E., Messa, M., Baldassari, S., Assereto, S., Biancheri, R., et al. (2016). The leukodystrophy protein FAM126A/Hyccin regulates PI4P synthesis at the plasma membrane. Nat Cell Biol *18*, 132–138.

Bayer, E.M., Sparkes, I., Vanneste, S., and Rosado, A. (2017). From shaping organelles to signalling platforms: the emerging functions of plant ER-PM contact sites. Curr. Opin. Plant Biol. *40*, 89–96.

Borg, M., and Twell, D. (2011). Pollen: Structure and Development. In ELS, (American Cancer Society), p.

Brault, M.L., Petit, J.D., Immel, F., Nicolas, W.J., Glavier, M., Brocard, L., Gaston, A., Fouché, M., Hawkins, T.J., Crowet, J.-M., et al. (2019). Multiple C2 domains and transmembrane region proteins (MCTPs) tether membranes at plasmodesmata. EMBO Reports *0*, e47182.

Castano, E., Yildirim, S., Fáberová, V., Krausová, A., Uličná, L., Paprčková, D., Sztacho, M., and Hozák, P. (2019). Nuclear Phosphoinositides—Versatile Regulators of Genome Functions. Cells *8*.

Chang, F., Gu, Y., Ma, H., and Yang, Z. (2013). AtPRK2 Promotes ROP1 Activation via RopGEFs in the Control of Polarized Pollen Tube Growth. Molecular Plant *6*, 1187–1201.
Choi, S., Chen, M., Cryns, V.L., and Anderson, R.A. (2019). A nuclear phosphoinositide kinase complex regulates p53. Nature Cell Biology *21*, 462–475.

Chung, J., Nakatsu, F., Baskin, J.M., and De Camilli, P. (2015). Plasticity of PI4KIIIα interactions at the plasma membrane. EMBO Rep *16*, 312–320.

Clayton, E.L., Minogue, S., and Waugh, M.G. (2013). Mammalian phosphatidylinositol 4-kinases as modulators of membrane trafficking and lipid signaling networks. Progress in Lipid Research *52*, 294–304.

De Matteis, M.A., and Godi, A. (2004). PI-loting membrane traffic. Nature Cell Biology *6*, 487–492.

Delage, E., Ruelland, E., Guillas, I., Zachowski, A., and Puyaubert, J. (2012). Arabidopsis Type-III Phosphatidylinositol 4-Kinases β1 and β2 are Upstream of the Phospholipase C Pathway Triggered by Cold Exposure. Plant Cell Physiol *53*, 565–576.

Despres, B., Bouissonnié, F., Wu, H.-J., Gomord, V., Guilleminot, J., Grellet, F., Berger, F., Delseny, M., and Devic, M. (2003). Three SAC1-like genes show overlapping patterns of expression in Arabidopsis but are remarkably silent during embryo development. The Plant Journal *34*, 293–306.

Dornan, G.L., Dalwadi, U., Hamelin, D.J., Hoffmann, R.M., Yip, C.K., and Burke, J.E. (2018). Probing the Architecture, Dynamics, and Inhibition of the PI4KIIIα/TTC7/FAM126 Complex. J. Mol. Biol. *430*, 3129–3142.

Foti, M., Audhya, A., and Emr, S.D. (2001). Sac1 Lipid Phosphatase and Stt4 Phosphatidylinositol 4-Kinase Regulate a Pool of Phosphatidylinositol 4-Phosphate That Functions in the Control of the Actin Cytoskeleton and Vacuole Morphology. MBoC *12*, 2396–2411.

Fratini, M., Krishnamoorthy, P., Stenzel, I., Riechmann, M., Bacia, K., Heilmann, M., and Heilmann, I. (2020). Plasma membrane nano-organization specifies phosphoinositide effects on Rho-GTPases and actin dynamics in tobacco pollen tubes. BioRxiv 2020.08.12.248419.

Galvão, R.M., Kota, U., Soderblom, E.J., Goshe, M.B., and Boss, W.F. (2008). Characterization of a new family of protein kinases from Arabidopsis containing

phosphoinositide 3/4-kinase and ubiquitin-like domains. Biochem. J. *409*, 117–127.

García-Cerdán, J.G., Schmid, E.M., Takeuchi, T., McRae, I., McDonald, K.L., Yordduangjun, N., Hassan, A.M., Grob, P., Xu, C.S., Hess, H.F., et al. (2020). Chloroplast Sec14-like 1 (CPSFL1) is essential for normal chloroplast development and affects carotenoid accumulation in Chlamydomonas. PNAS *117*, 12452–12463.

Gerth, K., Lin, F., Menzel, W., Krishnamoorthy, P., Stenzel, I., Heilmann, M., and Heilmann, I. (2017a). Guilt by Association: A Phenotype-Based View of the Plant Phosphoinositide Network. Annual Review of Plant Biology *68*, 349–374.

Gerth, K., Lin, F., Daamen, F., Menzel, W., Heinrich, F., and Heilmann, M. (2017b). Arabidopsis phosphatidylinositol 4-phosphate 5-kinase 2 contains a functional nuclear localization sequence and interacts with alpha-importins. The Plant Journal *92*, 862–878.

Gonzales, M.L., and Anderson, R.A. (2006). Nuclear phosphoinositide kinases and inositol phospholipids. Journal of Cellular Biochemistry *97*, 252–260.

Gronnier, J., Crowet, J.-M., Habenstein, B., Nasir, M.N., Bayle, V., Hosy, E., Pierre Platre, M., Gouguet, P., Raffaele, S., Martinez, D., et al. (2017). Structural basis for plant plasma membrane protein dynamics and organization into functional nanodomains. ELife *6*.

Hammond, G.R.V., Schiavo, G., and Irvine, R.F. (2009). Immunocytochemical techniques reveal multiple, distinct cellular pools of PtdIns4P and PtdIns(4,5)P2. Biochem J *422*, 23–35.

Hammond, G.R.V., Machner, M.P., and Balla, T. (2014). A novel probe for phosphatidylinositol 4-phosphate reveals multiple pools beyond the Golgi. J Cell Biol *205*, 113–126.

Huanca-Mamani, W., Garcia-Aguilar, M., León-Martínez, G., Grossniklaus, U., and Vielle-Calzada, J.-P. (2005). CHR11, a chromatin-remodeling factor essential for nuclear proliferation during female gametogenesis in Arabidopsis thaliana. PNAS *102*, 17231–17236.

Hurst, C.H., Turnbull, D., Plain, F., Fuller, W., and Hemsley, P.A. (2017). Maleimide scavenging enhances determination of protein S-palmitoylation state in acyl-exchange methods. BioTechniques *62*, 69–75.

Ingram, G.C. (2010). Family life at close quarters: communication and constraint in angiosperm seed development. Protoplasma *247*, 195–214.

Ito, Y., Esnay, N., Platre, M.P., Noack, L.C., Menzel, W., Claverol, S., Moreau, P., Jaillais, Y., and Boutté, Y. (2020). Sphingolipids mediate polar sorting of PIN2 through phosphoinositide consumption at the trans-Golgi Network. BioRxiv 2020.05.12.090399.

Jacob, D., and Brian, J. (2020). The short and intricate life of the suspensor. Physiologia Plantarum *169*, 110–121.

Janda, M., Šašek, V., and Ruelland, E. (2014). The Arabidopsis pi4kIIIβ1β2 double mutant is salicylic acid-overaccumulating: a new example of salicylic acid influence on plant stature. Plant Signaling & Behavior *9*, e977210.

Kakuk, A., Friedländer, E., Vereb Jr., G., Kása, A., Balla, A., Balla, T., Heilmeyer Jr., L.M.G., Gergely, P., and Vereb, G. (2006). Nucleolar localization of phosphatidylinositol 4-kinase PI4K230 in various mammalian cells. Cytometry Part A *69A*, 1174–1183.

Kang, B.-H., Rancour, D.M., and Bednarek, S.Y. (2003). The dynamin-like protein ADL1C is essential for plasma membrane maintenance during pollen maturation. The Plant Journal *35*, 1–15.

Kang, B.-H., Nielsen, E., Preuss, M.L., Mastronarde, D., and Staehelin, L.A. (2011). Electron Tomography of RabA4b- and PI-4Kβ1-Labeled Trans Golgi Network Compartments in Arabidopsis. Traffic *12*, 313–329.

Kim, Y.J., Guzman-Hernandez, M.-L., Wisniewski, E., and Balla, T. (2015). Phosphatidylinositol-Phosphatidic Acid Exchange by Nir2 at ER-PM Contact Sites Maintains Phosphoinositide Signaling Competence. Developmental Cell *33*, 549–561.

Kubátová, Z., Pejchar, P., Potocký, M., Sekereš, J., Žárský, V., and Kulich, I. (2019). Arabidopsis trichome contains two plasma membrane 3 domains with different lipid composition which 4 attract distinct EXO70 subunits. Int. J. Mol. Sci. 15.

Lee, E., Vanneste, S., Pérez-Sancho, J., Benitez-Fuente, F., Strelau, M., Macho, A.P., Botella, M.A., Friml, J., and Rosado, A. (2019). Ionic stress enhances ER–PM connectivity via phosphoinositide-associated SYT1 contact site expansion in Arabidopsis. PNAS *116*, 1420–1429.

Lee, E., Vila Nova Santana, B., Samuels, E., Benitez-Fuente, F., Corsi, E., Botella, M.A., Perez-Sancho, J., Vanneste, S., Friml, J., Macho, A., et al. (2020). Rare earth elements induce cytoskeleton-dependent and PI4P-associated rearrangement of SYT1/SYT5 ER-PM contact site complexes in Arabidopsis. Journal of Experimental Botany eraa138.

Lees, J.A., Messa, M., Sun, E.W., Wheeler, H., Torta, F., Wenk, M.R., Camilli, P.D., and Reinisch, K.M. (2017a). Lipid transport by TMEM24 at ER–plasma membrane contacts regulates pulsatile insulin secretion. Science *355*.

Lees, J.A., Zhang, Y., Oh, M.S., Schauder, C.M., Yu, X., Baskin, J.M., Dobbs, K., Notarangelo, L.D., Camilli, P.D., Walz, T., et al. (2017b). Architecture of the human PI4KIIIα lipid kinase complex. PNAS *114*, 13720–13725.

Levental, I., Grzybek, M., and Simons, K. (2010). Greasing Their Way: Lipid Modifications Determine Protein Association with Membrane Rafts. Biochemistry *49*, 6305–6316.

Levine, T.P., and Munro, S. (1998). The pleckstrin homology domain of oxysterol-binding protein recognises a determinant specific to Golgi membranes. Current Biology *8*, 729–739.

Levine, T.P., and Munro, S. (2002). Targeting of Golgi-Specific Pleckstrin Homology Domains Involves Both PtdIns 4-Kinase-Dependent and -Independent Components. Current Biology *12*, 695–704.

Li, S., van Os, G.M.A., Ren, S., Yu, D., Ketelaar, T., Emons, A.M.C., and Liu, C.-M. (2010). Expression and Functional Analyses of EXO70 Genes in Arabidopsis Implicate Their Roles in Regulating Cell Type-Specific Exocytosis1[W][OA]. Plant Physiol *154*, 1819–1830.

Li, Y., Li, H.-J., Morgan, C., Bomblies, K., Yang, W., and Qi, B. (2019). Both male and female gametogenesis require a fully functional protein S-acyl transferase 21 in Arabidopsis thaliana. The Plant Journal *100*, 754–767.

Lin, F., Krishnamoorthy, P., Schubert, V., Hause, G., Heilmann, M., and Heilmann, I. (2019). A dual role for cell plate-associated PI4Kβ in endocytosis and phragmoplast dynamics during plant somatic cytokinesis. EMBO J. *38*.

Löfke, C., T, I., S, K., S, F., and I, H. (2008). Alternative metabolic fates of phosphatidylinositol produced by phosphatidylinositol synthase isoforms in Arabidopsis thaliana. Biochem J *413*, 115–124.

Manford, A.G., Stefan, C.J., Yuan, H.L., MacGurn, J.A., and Emr, S.D. (2012). ER-to-Plasma Membrane Tethering Proteins Regulate Cell Signaling and ER Morphology. Developmental Cell *23*, 1129–1140.

Marhava, P., Aliaga Fandino, A.C., Koh, S.W.H., Jelínková, A., Kolb, M., Janacek, D.P., Breda, A.S., Cattaneo, P., Hammes, U.Z., Petrášek, J., et al. (2020). Plasma Membrane Domain Patterning and Self-Reinforcing Polarity in Arabidopsis. Developmental Cell *52*, 223-235.e5.

Mergner, J., Frejno, M., List, M., Papacek, M., Chen, X., Chaudhary, A., Samaras, P., Richter, S., Shikata, H., Messerer, M., et al. (2020). Mass-spectrometry-based draft of the Arabidopsis proteome. Nature *579*, 409–414.

Minami, A., Tominaga, Y., Furuto, A., Kondo, M., Kawamura, Y., and Uemura, M. (2015). Arabidopsis dynamin-related protein 1E in sphingolipid-enriched plasma membrane domains is associated with the development of freezing tolerance. Plant J *83*, 501–514.

Mishkind, M., Vermeer, J.E.M., Darwish, E., and Munnik, T. (2009). Heat stress activates phospholipase D and triggers PIP accumulation at the plasma membrane and nucleus. Plant J. *60*, 10–21.

Moreau, P., Sturbois, B., Morré, D.J., and Cassagne, C. (1994). Effect of low temperatures on the transfer of phospholipids with various acyl-chain lengths to the plasma membrane of leek cells. Biochim. Biophys. Acta *1194*, 239–246.

Moreau, P., Bessoule, J.J., Mongrand, S., Testet, E., Vincent, P., and Cassagne, C. (1998). Lipid trafficking in plant cells. Progress in Lipid Research *37*, 371–391.

Mueller-Roeber, B., and Pical, C. (2002). Inositol Phospholipid Metabolism in Arabidopsis. Characterized and Putative Isoforms of Inositol Phospholipid Kinase and Phosphoinositide-Specific Phospholipase C. Plant Physiol *130*, 22–46.

Mutwil, M., Debolt, S., and Persson, S. (2008). Cellulose synthesis: a complex complex. Current Opinion in Plant Biology *11*, 252–257.

Nagashima, S., Tábara, L.-C., Tilokani, L., Paupe, V., Anand, H., Pogson, J.H., Zunino, R., McBride, H.M., and Prudent, J. (2020). Golgi-derived PI(4)P-containing vesicles drive late steps of mitochondrial division. Science *367*, 1366–1371.

Nakatsu, F., Baskin, J.M., Chung, J., Tanner, L.B., Shui, G., Lee, S.Y., Pirruccello, M., Hao, M., Ingolia, N.T., Wenk, M.R., et al. (2012). PtdIns4P synthesis by PI4KIIIα at the plasma membrane and its impact on plasma membrane identity. J Cell Biol *199*, 1003–1016.

Okazaki, K., Miyagishima, S., and Wada, H. (2015). Phosphatidylinositol 4-Phosphate Negatively Regulates Chloroplast Division in Arabidopsis[OPEN]. Plant Cell *27*, 663–674.

Omnus, D.J., Manford, A.G., Bader, J.M., Emr, S.D., and Stefan, C.J. (2016). Phosphoinositide kinase signaling controls ER-PM cross-talk. Mol Biol Cell *27*, 1170–1180.

Omnus, D.J., Cadou, A., Thomas, F.B., Bader, J.M., Soh, N., Chung, G.H.C., Vaughan, A.N., and Stefan, C.J. (2020). A heat-sensitive Osh protein controls PI4P polarity. BMC Biology *18*, 28.

Pan, X., Fang, L., Liu, J., Senay-Aras, B., Lin, W., Zheng, S., Zhang, T., Manor, U., Chen, W., and Yang, Z. (2019). Auxin-induced nanoclustering of membrane signaling complexes underlies cell polarity establishment in Arabidopsis. BioRxiv 734665.

Pérez-Sancho, J., Vanneste, S., Lee, E., McFarlane, H.E., Valle, A.E. del, Valpuesta, V., Friml, J., Botella, M.A., and Rosado, A. (2015). The Arabidopsis Synaptotagmin1 Is Enriched in Endoplasmic Reticulum-Plasma Membrane Contact Sites and Confers Cellular Resistance to Mechanical Stresses. Plant Physiology *168*, 132–143.

Persson, S., Paredez, A., Carroll, A., Palsdottir, H., Doblin, M., Poindexter, P., Khitrov, N., Auer, M., and Somerville, C.R. (2007). Genetic evidence for three unique components in primary cell-wall cellulose synthase complexes in Arabidopsis. PNAS *104*, 15566–15571.

Platre, M.P., and Jaillais, Y. (2016). Guidelines for the use of protein domains in acidic phospholipid imaging. Methods Mol Biol *1376*, 175–194.

Platre, M.P., Noack, L.C., Doumane, M., Bayle, V., Simon, M.L.A., Maneta-Peyret, L., Fouillen, L., Stanislas, T., Armengot, L., Pejchar, P., et al. (2018). A Combinatorial Lipid Code Shapes the Electrostatic Landscape of Plant Endomembranes. Dev. Cell *45*, 465-480.e11.

Platre, M.P., Bayle, V., Armengot, L., Bareille, J., Marquès-Bueno, M. del M., Creff, A.,

Maneta-Peyret, L., Fiche, J.-B., Nollmann, M., Miège, C., et al. (2019). Developmental control of plant Rho GTPase nano-organization by the lipid phosphatidylserine. Science *364*, 57–62.

Preuss, M.L., Schmitz, A.J., Thole, J.M., Bonner, H.K.S., Otegui, M.S., and Nielsen, E. (2006). A role for the RabA4b effector protein PI-4Kβ1 in polarized expansion of root hair cells in Arabidopsis thaliana. J Cell Biol *172*, 991–998.

Roy, A., and Levine, T.P. (2004). Multiple Pools of Phosphatidylinositol 4-Phosphate Detected Using the Pleckstrin Homology Domain of Osh2p. J. Biol. Chem. *279*, 44683–44689.

Rubilar-Hernández, C., Osorio-Navarro, C., Cabello, F., and Norambuena, L. (2019). PI4KIIIβ Activity Regulates Lateral Root Formation Driven by Endocytic Trafficking to the Vacuole. Plant Physiology *181*, 112–126.

Saravanan, R.S., Slabaugh, E., Singh, V.R., Lapidus, L.J., Haas, T., and Brandizzi, F. (2009). The targeting of the oxysterol-binding protein ORP3a to the endoplasmic reticulum relies on the plant VAP33 homolog PVA12. The Plant Journal *58*, 817–830.

Sekereš, J., Pejchar, P., Šantrůček, J., Vukašinović, N., Žárský, V., and Potocký, M. (2017). Analysis of Exocyst Subunit EXO70 Family Reveals Distinct Membrane Polar Domains in Tobacco Pollen Tubes. Plant Physiol. *173*, 1659–1675.

Shimada, T.L., Betsuyaku, S., Inada, N., Ebine, K., Fujimoto, M., Uemura, T., Takano, Y., Fukuda, H., Nakano, A., and Ueda, T. (2019). Enrichment of Phosphatidylinositol 4,5-Bisphosphate in the Extra-Invasive Hyphal Membrane Promotes Colletotrichum Infection of Arabidopsis thaliana. Plant and Cell Physiology pcz058.

Simon, M.L.A., Platre, M.P., Marquès-Bueno, M.M., Armengot, L., Stanislas, T., Bayle, V., Caillaud, M.-C., and Jaillais, Y. (2016). A PtdIns(4)P-driven electrostatic field controls cell membrane identity and signalling in plants. Nature Plants *2*, nplants201689.

Sorek, N., Segev, O., Gutman, O., Bar, E., Richter, S., Poraty, L., Hirsch, J.A., Henis, Y.I., Lewinsohn, E., Jürgens, G., et al. (2010). An S-Acylation Switch of Conserved G Domain Cysteines Is Required for Polarity Signaling by ROP GTPases. Current Biology *20*, 914–920.

Sorek, N., Poraty, L., Sternberg, H., Buriakovsky, E., Bar, E., Lewinsohn, E., and Yalovsky, S. (2017). Corrected and Republished from: Activation Status-Coupled Transient S-Acylation Determines Membrane Partitioning of a Plant Rho-Related GTPase. Molecular and Cellular Biology *37*.

Stefan, C.J., Manford, A.G., Baird, D., Yamada-Hanff, J., Mao, Y., and Emr, S.D. (2011). Osh proteins regulate phosphoinositide metabolism at ER-plasma membrane contact sites. Cell *144*, 389–401.

Stenzel, I., Ischebeck, T., König, S., Hołubowska, A., Sporysz, M., Hause, B., and Heilmann, I. (2008). The Type B Phosphatidylinositol-4-Phosphate 5-Kinase 3 Is Essential for Root

Hair Formation in Arabidopsis thaliana. Plant Cell *20*, 124–141.

Stevenson, J.M., Perera, I.Y., and Boss, W.F. (1998). A Phosphatidylinositol 4-Kinase Pleckstrin Homology Domain That Binds Phosphatidylinositol 4-Monophosphate. J. Biol. Chem. *273*, 22761–22767.

Stevenson-Paulik, J., Love, J., and Boss, W.F. (2003). Differential Regulation of Two Arabidopsis Type III Phosphatidylinositol 4-Kinase Isoforms. A Regulatory Role for the Pleckstrin Homology Domain. Plant Physiol *132*, 1053–1064.

Sun, E.W., Guillén-Samander, A., Bian, X., Wu, Y., Cai, Y., Messa, M., and Camilli, P.D. (2019). Lipid transporter TMEM24/C2CD2L is a Ca2+-regulated component of ER–plasma membrane contacts in mammalian neurons. PNAS *116*, 5775–5784.
Surma, M.A., Klose, C., Klemm, R.W., Ejsing, C.S., and Simons, K. (2011). Generic Sorting of Raft Lipids into Secretory Vesicles in Yeast. Traffic *12*, 1139–1147.

Tang, D., Ade, J., Frye, C.A., and Innes, R.W. (2006). A mutation in the GTP hydrolysis site of Arabidopsis dynamin-related protein 1E confers enhanced cell death in response to powdery mildew infection. The Plant Journal *47*, 75–84.

Thole, J.M., Vermeer, J.E.M., Zhang, Y., Gadella, T.W.J., and Nielsen, E. (2008). ROOT HAIR DEFECTIVE4 Encodes a Phosphatidylinositol-4-Phosphate Phosphatase Required for Proper Root Hair Development in Arabidopsis thaliana. Plant Cell *20*, 381–395.

Uemura, T., Suda, Y., Ueda, T., and Nakano, A. (2014). Dynamic behavior of the trans-golgi network in root tissues of Arabidopsis revealed by super-resolution live imaging. Plant Cell Physiol. *55*, 694–703.

Van Damme, D., Coutuer, S., De Rycke, R., Bouget, F.-Y., Inzé, D., and Geelen, D. (2006). Somatic Cytokinesis and Pollen Maturation in Arabidopsis Depend on TPLATE, Which Has Domains Similar to Coat Proteins. Plant Cell *18*, 3502–3518.

Viotti, C., Bubeck, J., Stierhof, Y.-D., Krebs, M., Langhans, M., van den Berg, W., van Dongen, W., Richter, S., Geldner, N., Takano, J., et al. (2010). Endocytic and Secretory Traffic in Arabidopsis Merge in the Trans-Golgi Network/Early Endosome, an Independent and Highly Dynamic Organelle[W]. Plant Cell *22*, 1344–1357.

Wang, P., Hawes, C., and Hussey, P.J. (2016a). Plant Endoplasmic Reticulum–Plasma Membrane Contact Sites. Trends in Plant Science *0*.

Wang, P., Richardson, C., Hawkins, T.J., Sparkes, I., Hawes, C., and Hussey, P.J. (2016b). Plant VAP27 proteins: domain characterization, intracellular localization and role in plant development. New Phytologist *210*, 1311–1326.

Wang, Y.J., Wang, J., Sun, H.Q., Martinez, M., Sun, Y.X., Macia, E., Kirchhausen, T., Albanesi, J.P., Roth, M.G., and Yin, H.L. (2003). Phosphatidylinositol 4 Phosphate Regulates Targeting of Clathrin Adaptor AP-1 Complexes to the Golgi. Cell *114*, 299–310.

Wattelet-Boyer, V., Brocard, L., Jonsson, K., Esnay, N., Joubès, J., Domergue, F., Mongrand,

S., Raikhel, N., Bhalerao, R.P., Moreau, P., et al. (2016). Enrichment of hydroxylated C24- and C26-acyl-chain sphingolipids mediates PIN2 apical sorting at trans-Golgi network subdomains. Nature Communications *7*, 12788.

Wei, Y.J., Sun, H.Q., Yamamoto, M., Wlodarski, P., Kunii, K., Martinez, M., Barylko, B., Albanesi, J.P., and Yin, H.L. (2002). Type II phosphatidylinositol 4-kinase beta is a cytosolic and peripheral membrane protein that is recruited to the plasma membrane and activated by Rac-GTP. J. Biol. Chem. *277*, 46586–46593.

Winkler, J., Mylle, E., Meyer, A.D., Pavie, B., Merchie, J., Grones, P., and Damme, D.V. (2020). Rapamycin-dependent delocalization as a novel tool to reveal protein-protein interactions in plants. BioRxiv 2020.03.09.983270.

Wu, H., Carvalho, P., and Voeltz, G.K. (2018). Here, there, and everywhere: The importance of ER membrane contact sites. Science *361*, eaan5835.

Wu, X., Chi, R.J., Baskin, J.M., Lucast, L., Burd, C.G., De Camilli, P., and Reinisch, K.M. (2014). Structural Insights into Assembly and Regulation of the Plasma Membrane Phosphatidylinositol 4-Kinase Complex. Dev Cell *28*, 19–29.

Xue, H.-W., Pical, C., Brearley, C., Elge, S., and Müller-Röber, B. (1999). A Plant 126-kDa Phosphatidylinositol 4-Kinase with a Novel Repeat Structure CLONING AND FUNCTIONAL EXPRESSION IN BACULOVIRUS-INFECTED INSECT CELLS. J. Biol. Chem. *274*, 5738–5745.

Yamamoto, W., Wada, S., Nagano, M., Aoshima, K., Siekhaus, D.E., Toshima, J.Y., and Toshima, J. (2018). Distinct roles for plasma membrane PtdIns(4)P and PtdIns(4,5)P2 during receptor-mediated endocytosis in yeast. J Cell Sci *131*.

Zaballa, M.-E., and Goot, F.G. van der (2018). The molecular era of protein S-acylation: spotlight on structure, mechanisms, and dynamics. Critical Reviews in Biochemistry and Molecular Biology *53*, 420–451.

Zewe, J.P., Miller, A.M., Sangappa, S., Wills, R.C., Goulden, B.D., and Hammond, G.R.V. (2020). Probing the subcellular distribution of phosphatidylinositol reveals a surprising lack at the plasma membrane. J Cell Biol *219*.

Zhao, B., Shi, H., Wang, W., Liu, X., Gao, H., Wang, X., Zhang, Y., Yang, M., Li, R., and Guo, Y. (2016). Secretory COPII Protein SEC31B Is Required for Pollen Wall Development. Plant Physiology *172*, 1625–1642.

ANNEXES

Transient gene expression as a tool to monitor and manipulate the levels of acidic phospholipids in plant cells

Lise C. Noack[1], Přemysl Pejchar[2,3], Juraj Sekereš[2,3], Yvon Jaillais[1*], Martin Potocký[2,3*]

[1] Laboratoire Reproduction et Développement des Plantes, Université de Lyon, ENS de Lyon, UCB Lyon 1, CNRS, INRA, Lyon 69342, France

[2] Institute of Experimental Botany v. v. i.; Academy of Sciences of the Czech Republic; Prague, Czech Republic

[3] Department of Experimental Plant Biology, Faculty of Science, Charles University, Prague, Czech Republic

*Corresponding authors: e-mail: potocky@ueb.cas.cz and yvon.jaillais@ens-lyon.fr

Running head: Exploring phospholipid signalling in plant cells using transient gene expression

Abstract

Anionic phospholipids represent only minor fraction of cell membranes lipids but they are critically important for many membrane-related processes, including membrane identity, charge, shape, the generation of second messengers and the recruitment of peripheral proteins. The main anionic phospholipids of the plasma membrane are phosphoinositides phosphatidylinositol 4-phosphate (PI4P), phosphatidylinositol 4,5-bisphosphate ($PI4,5P_2$), phosphatidylserine (PS), and phosphatidic acid (PA). Recent insights in the understanding of the nature of protein–phospholipid interactions enabled the design of genetically-encoded fluorescent molecular probes that can interact with various phospholipids in a specific manner allowing their imaging in live cells. Here, we describe the use of transiently transformed plant cells to study phospholipid-dependent membrane recruitment.

Keywords: Microscopy, *Nicotiana benthamiana*, *Nicotiana tabacum*, phosphoinositides, phospholipid-binding domains, pollen tube, transient expression

1. Introduction

All living cells are surrounded by membranes, which help to define their spatial identity and create the semipermeable boundary between intra- and extra-cellular space [**1**]. Typical cellular membrane is composed of a bilayer of lipids and proteins, whose organization and interactions are crucial for its function as organizing platforms for cellular processes. Historically, cellular membrane studies were once dominated by a protein-centric view, where proteins executed majority of membrane-related functions and the membrane lipids were often regarded only as passive players whose role was to provide structural support for bilayer formation [**2**]. It is now generally accepted that both lipids and proteins play indispensable active roles in the various functions of cellular membranes [**3**].

Among plant plasma membrane lipids, negatively-charged (anionic) phospholipids, phosphoinositides like phosphatidylinositol 4-phosphate (PI4P) and phosphatidylinositol 4,5-bisphosphate ($PI4,5P_2$), together with phosphatidylserine (PS) and phosphatidic acid (PA), constitute low-abundant but essential component [**4**-**6**]. They possess many important roles, which include defining membrane identity, generation of downstream signalling molecules, generating membrane negative charge, modulating membrane curvature and creating binding sites for the targeting of effector proteins [**7**-**12**].

The realization of the important roles of anionic phospholipids has created a need for methods that would enable their non-invasive spatio-temporal monitoring in living cells. The identification and characterization of protein modules that specifically bind to various anionic phospholipids led to the idea that these protein modules might be used to detect phospholipids in living cells. This resulted in the development of genetically-encoded phospholipid sensors that consist of the specific phospholipid-binding domains (either single or in tandem) fused with various fluorescent proteins, enabling the live cell imaging of phospholipid dynamics [**13**-**15**]. Especially in the past decade, this approach has been successfully used in plants to generate sensors for a wide variety of phospholipids including PI4P [**16**-**18**], $PI4,5P_2$ [**17**, **19**, **20**], PA [**21**, **22**] and PS [**17**, **22**]. Concomitantly, many enzymes involved in the production and degradation of anionic lipids were identified and the phenotypes of their knockout or overexpressing mutant lines described (for plants see e.g. Refs **23**, **24**). This also led to the development of tools allowing the manipulation of phospholipid levels in the cell upon generic or targeted overexpression of phospholipid-modifying enzymes [**25**].

The recruitment of phospholipid-binding peripheral proteins to cell membranes is essential for many cellular processes. The targeting of proteins to specific phospholipids or to the membranes of particular lipid compositions, mediated by lipid-binding domains, allows their recruitment to be precisely controlled in spatio-temporal fashion. Despite the manifold biological consequences associated with the targeted recruitment of peripheral protein to their target membranes, only a basic understanding of the interactions of proteins with membrane surfaces exists because these questions are inaccessible by commonly used structural techniques [**26**, **27**]. Therefore, the selective colocalization of peripheral proteins (or individual protein domains, protein deletions, point mutations etc.) with the particular lipid marker together with its relocalization after coexpression with corresponding phospholipid-modifying enzymes may bring valuable informations about the nature of protein-membrane interface. Transient gene expression approaches are particularly beneficial, since they enable quick screening of many proteins or protein variants and allow easy manipulation of expression level. Here, we describe the protocols allowing transient coexpression of proteins of interest with genetically-encoded lipid markers or phospholipid-modifying enzymes in two different plant cell types: biolistics-mediated transformation of growing tobacco pollen tubes (that show spatially-separated plasma membrane domains enriched with distinct phospholipids, Refs **21**, **22**), and agroinfiltration of *Nicotiana benthamiana* leaf epidermal cells (where high transformation efficiency can be achieved).

2. Materials

Prepare all solutions using ultrapure water and store at room temperature (RT), unless stated otherwise.

2.1 Particle bombardment solutions

1. **Gold particles**: resuspend 30 mg of 1.6 μm gold microcarriers (Bio-Rad, #1652264, **Note 1**) in 1 ml absolute ethanol, vortex vigorously for 3 min and spin down at table top centrifuge (1 min, maximum speed). Wash twice with H_2O and resuspend in 1 ml of 50% glycerol (sterile). Store at 4 °C.

2. **2.5 M $CaCl_2$**: Dissolve 3.675 g $CaCl_2 \cdot 2H_2O$ (Sigma, #C7902) in 10 ml H_2O. Filter sterilize and keep 1 ml aliquots at -20 °C. Working aliquot can be kept at 4 °C for several months.

3. **Protamine**: Dissolve 10 mg of protamine sulfate (Sigma, #P4505) in 10 ml H_2O. Filter sterilize and keep 0.5 ml aliquots at -20 °C. Working aliquot can be kept at 4 °C for several weeks.

2.2 DNA

1. For tobacco pollen particle bombardment, dilute DNA stock with H_2O to 0.25-1 μg/μl working solution. In order to achieve good transformation frequency and expression levels, target construct expression must be driven by promoters active in pollen (typically LAT52p or UBQ10p). 35S promoter is not recommended. Usually, clean miniprep is enough for several transformations. Store at -20 °C.

2. For *N. benthamiana* leaves infiltration, use DNA plasmid concentrated at 0.25-1 μg/μl to transform *Agrobacterium*. Expression of the construct is usually driven by *UBQ10* or *35S* promoters.

2.3. Biological material

1. **Pollen:** Flowers of outdoor- or glasshouse-grown tobacco plants (*Nicotiana tabacum* cv. Samsun) are collected in warm and dry weather conditions before opening; anthers are taken out and kept in laboratory conditions on a filter paper for one day to let anthers open and dehydrate (anthers might be surface sterilized and dried in the laminar box to harvest sterile pollen). Dried pollen grains are sifted through to remove anthers. Harvested pollen can be kept frozen at −20 °C without apparent loss of the germination capacity for several years. 1 mg of pollen is usually used per transformation.

2. ***N. benthamiana* leaves:** Use tobacco leaves from 2-3 weeks old plants. For infiltration, select leaves that are heart shaped. If the plant has already flowered, it is too late to perform the infiltration.

3. **Agrobacterium:** The electrocompetent *A. tumefaciens* C58pmp90 strain is used for tobacco leaves infiltration.

2.4 Cultivation Media

1. **2x pollen tube medium (2xPTM)**: 10% w/v sucrose, 25% w/v PEG-6000, 2 mM $CaCl_2$, 2 mM KCl, 1.6 mM $MgSO_4$, 3.2 mM H_3BO_3, 60 μM $CuSO_4$, 0.06% w/v casein

acid-hydrolysate, 0.6% w/v MES, pH 5.9. Prepare 10x stock solution for salts (1470 mg/l $CaCl_2 \cdot 2H_2O$, 746 mg/l KCl, 1972 mg/l $MgSO_4 \cdot 7H_2O$, 989 mg/l H_3BO_3, 75 mg/l $CuSO_4 \cdot 5H_2O$) and 50x stock for casein hydrolysate (1.5% w/v). Store the stocks at -20 °C. Dissolve appropriate amounts of sucrose, MES, salt and casein hydrolysate stocks in H_2O, adjust pH to 5.9 with 4 M KOH, add PEG-6000 and make up to the final volume with H_2O. Store 50 ml aliquots at -20 °C.

2. **Solid pollen tube medium**: 1xPTM solidified with 0.25% Phytagel (**Note 2**). Thaw 50 ml aliquot of 2xPTM and warm it in water bath to at least 60 °C. Prepare 0.5% Phytagel (Sigma, #P8169) solution: weigh 0.25 g of Phytagel into 50 ml H_2O and resuspend. Dissolve Phytagel by carefully heating up to the boiling point while stirring. Mix 2xPTM and Phytagel solutions and keep the 1xPTM/0.25% Phytagel medium in hot water bath. In laminar box, prepare plates with solidified medium by rapid pouring of 4 ml of hot PTM/Phytagel solution onto 5 cm Petri dishes. Let dry and store up to one month at 4 °C.

3. **LB medium:** Agrobacterium are grown on LB liquid medium (Difco™ LB Broth, Lennox, #240230, 20 g/l) and LB plate (Difco™ LB Broth, Lennox, #214010, 20 g/l, 15% w/v agar, Difco™ Bacto Agar).

4. **Infiltration medium:** 10 mM MES (Sigma-Aldrich, #D8250-250G), 10 mM $MgCl_2$ (Sigma-Aldrich, #M2670), 0.15 mM acetosyringone (Sigma-Aldrich, #D134406). Prepare a stock solution of 100 mM MES. Weight and dissolve the appropriate amount of MES in H_2O and adjust the pH to 5.7 using KOH solution. Autoclave the MES solution for 30 min and store it at RT. Prepare a stock solution of acetosyringone at 100 mM in EtOH and store it at -20 °C. Just before performing the infiltration, dilute the MES solution in H_2O, add the $MgCl_2$ and the acetosyringone to a final concentration of 10 mM and 0.15 mM, respectively.

3. Methods

Carry out all procedures at RT unless otherwise specified (**Note 3**).

3.1 DNA macrocarrier preparation for pollen particle bombardment

Add following to the 1.5 ml microcentrifuge tube to prepare one macrocarrier (the sample should be mixing continuously, keep sequence and timing): 25 µl of gold particles suspension, vortex 1 min, add 2.5-7 µl of plasmid DNA (~1-10 µg, **Note 4**), 25 µl of 2.5 M

$CaCl_2$ and 10 µl of protamine (1 mg/ml) solution. Vortex vigorously for at least 3 min. Spin down in tabletop centrifuge for 30 s at max speed. Remove the supernatant carefully using yellow pipette tip or vacuum and discard it. Resuspend the pellet completely (**Note 5**) in 200 µl of absolute ethanol and vortex for 3 min. Spin down again and discard the supernatant. Resuspend the pellet in 18 µl of absolute ethanol, vortex for 1 min and load the suspension on the macrocarrier (Bio-Rad, #1652335). Keep the suspension dispersed by constant pipetting. For future manipulations, it is better to have macrocarrier fitted in the steel macrocarrier holder (Bio-Rad, #1652322) before loading. Let the macrocarrier dry in a vibration-free environment. One should obtain evenly distributed layer of gold particles without any visible clumps. Although dried macrocarriers can be stored in dry chamber at RT for several hours, it is better to perform the transformation immediately after preparation.

3.2 Pollen plating

For one transformation, resuspend 1 mg of tobacco pollen per 5 ml of 1xPTM. Pour the suspension on the prewetted nylon 47 mm (0.8 µm) filter disc (Whatman, #Z746282) placed on filtration apparatus (e.g. Millipore, #XX1004720) and remove medium using vacuum. Transfer the pollen to the solidified PTM by placing the filter disc upside-down briefly. Repeat for the next DNA sample and/or proceed to the particle bombardment immediately (**Note 6**).

3.3 Particle bombardment

Set up the PDS-1000/He system (Bio-Rad, #1652257) according to the instruction manual using standard settings. Put the rupture disc (1100 psi, Bio-Rad, #1652329) in place and tighten gently with the screwdriver. Assemble macrocarrier and stopping screen (Bio-Rad, #1652336) into microcarrier launch assembly and insert it into the uppermost position. Use the second free slot from above for the pollen plated on solidified medium. Evacuate the chamber to 28 inHg and perform the bombardment. Release the vacuum immediately, seal the sample plate with parafilm and store it at RT.

3.4 Agrobacterium transformation

Transform each construct in Agrobacterium. To do so, add 1 µl of DNA plasmid into 50 µl of electrocompetent Agrobacterium on ice. Transfer the Agrobacterium into cold 1 mm wide

electroporation chamber (Eurogentec, #CE00150). Put the electroporation chamber into the MicropulserTM (Bio-Rad, #165-2100) and give a pulse of 2 kV, 335 Ω, 15 µF, for 5 ms. Add 1 ml of liquid LB medium and transfer the bacteria into a new tube and incubate them at 29 °C for at least 2 h. Plate the Agrobacterium onto LB plates containing the appropriate antibiotics to select the Agrobacterium strain (gentamycin 20 µg/ml and rifampicin 50 µg/ml) and the target construct. Incubate the plate at 29 °C for 48 h.

3.5 *Nicotiana benthamiana* infiltration

Prepare the infiltration medium as indicated in the "cultivation media" part. Scoop transformed Agrobacterium from the transformation plate with a tip and resuspend the bacteria into 2 ml infiltration medium by pipetting. Measure the OD_{600} using a spectrophotometer (Biophotometer, Eppendorf). Adjust the OD_{600} to 1 by adding infiltration medium. For co-infiltration of several constructs, mix the same quantity of each transformed Agrobacterium to obtain a final OD_{600} of 1. Using 1 ml syringe (Terumo, #125162229), press the infiltration solution with the Agrobacterium onto the abaxial side of the chosen tobacco leaf keeping your finger on the other side of the leaf. The solution must spread into the leaf (**Note 7**). Mark the place where the infiltration has been made with a permanent marker. Put the plant back to the growth chamber for 2-3 days.

3.6 Data acquisition, analyses and quantification

Images can be exported from the microscope-specific acquisition software and analyzed with suitable analysis software. We use Fiji for this purpose, which is a distribution of well-known software ImageJ [**28**, **29**], bundling a lot of plugins which facilitate scientific image analysis, and which is freely available at https://fiji.sc/. A number of basic and advanced tools are available within this software, including subtraction of background, and measurements of intensities, both based on the definition of a region of interest.

1. **Particle-transformed pollen tubes**:

For the initial evaluation of protein overexpression on pollen tube growth and polarity, observe the cells 12-24 h after transformation with 5-10x lenses. Identify transformed cells based on FP fluorescence and take images using the same acquisition settings. Mean pollen tube length, pollen tube width, tip swelling and cell "curviness" (calculated as the ratio of the

distance between the pollen grain/pollen tube tip and the pollen tube length, is close to 1 for straight pollen tubes) are good parameters for the initial quantitative assessment.

Several simple measures can be used to monitor the binding of protein of interest to the plasma membrane, e.g. measuring of the membrane- and cytoplasmic-associated intensities from the line scan (**Figure 1**, see also Refs **21**, **30**) and calculating the ratio as a proxy for membrane recruitment index, and/or measuring the length of membrane signal (in case of asymmetric localizations, see **Figure 1**). For the quantitative assessment of colocalization, Pearson or Spearman rank correlation coefficients can be calculated from the data (e.g. with Coloc 2 plugin available in Fiji).

2. Confocal observation of *N. benthamiana* leaves

Cut 5 mm^2 regions of the leaf that surround the place where the infiltration has been made. Place the piece of leaf into water between slide and coverslip with the abaxial side of the leaf facing the coverslip. It may be convenient to tape the slide and coverslip together to maintain the coverslip on the slide as the leaf sample is thick. Using the appropriate wavelength, an epifluorescent microscope and the smallest objective (10X), screen the surface of the leaf to find the transformed cells. Then, switch to confocal microscope and 63X objective to look at the subcellular localization of the fluorescent protein.

3. Analysis of the effect of PM-targeted phosphatases on anionic phospholipid localization

In order to perturb anionic phospholipid production with subcellular accuracy, it is possible to target an isolated phosphatase (or kinase) domain to a specific organelle. For example, Simon et al., targeted the 4-phosphatase SAC domain of the yeast Sac1p protein to the PM using a Myristoylation and Palmitoylation anchor (MP) (see **Figure 2**). This MP-Sac1 construct was fused to a mTurquoise2 (mTu2) protein to monitor protein localization (MP-mTu2-Sac1) in order to verify that this synthetic enzyme was indeed efficiently targeted to the PM. Co-transfection with genetically encoded anionic phospholipid sensors allowed to determine the effect of the 4-phosphatase activity on the production of a given phospholipid. Quantification of the effect of the phosphatase activity may be performed using the analyses mentioned above for pollen tubes. Typically, three behaviours may be anticipated for the biosensors following co-expression with an organelle targeted phosphatase: i) no effect, ii)

redistribution of the sensor from a membrane to a cytosolic pool, and iii) redistribution of the sensor to a different organelle. For example, MP-Sac1 expression induced the redistribution of PI4P biosensors from the PM to endosomes (**Figure 2**, see also Refs **18**, **22**, **31**). This can be quantified qualitatively, as a percentage of cell with endosomal labelling by the PI4P sensor, as compared to the total number of cells analyzed. It can also be quantified by making a ratio of membrane vs soluble signal, but this later quantification methods is difficult given the reduced cytoplasm of *N. benthamiana* leaf cells. Once validated, such heterologous transient assay may be used to probe the importance of a given lipid for targeting a protein. It may also be used to validate *in vivo* catalytic activity of a phosphoinositide phosphatase of unknown specificity.

4. Notes

1. Different sizes of particles (0.6 or 1.0 μm) may be also used, this will however affect the amount of coatable DNA. Alternatively, cheaper tungsten particles may be used, their size distribution is however much more variable, resulting in yet greater variability in expression levels.

2. Do not use agar or agarose as they would cause the precipitation of pollen tube medium.

3. For the details of PDS-1000/He assembly and operation, consult the PDS-1000/He Particle Delivery System Instruction Manual and watch the YouTube tutorial.

4. When transforming with more than one construct, premix the DNA before coating. Use only small amount (0.5-1 μg of plasmids expressing phospholipid markers to prevent the perturbation of phospholipid signalling due to overexpression of lipid-binding domain).

5. This is crucial for obtaining good transformation frequency. The more DNA is added the longer it takes to resuspend the pellet completely.

6. We routinely transform up to 12 plates in a row. If more transformations are needed, split the plating/bombardment into batches of 10.

7. The infiltration might not work if the stomata are closed. To get around this problem, make small holes with a needle.

Acknowledgment

Research in the Prague lab is supported by the Czech Science Foundation (grants no. 17-27477S and and 18-18290J) and by the Ministry of Education Youth and Sport of the Czech Republic (project no. NPUI LO1417). Y.J. is funded by ERC no. 3363360-APPL under FP/2007-2013 and L.C.N is funded by a fellowship from the French Ministry of Higher Education.

References

1. Bernardino de la Serna, J., Schütz, G.J., Eggeling, C., and Cebecauer, M. (2016). There Is No Simple Model of the Plasma Membrane Organization. Frontiers in Cell and Developmental Biology 4:106.
2. Singer,SJ, and Nicolson GL (1972) The Fluid Mosaic Model of the Structure of Cell Membranes. Science 175:720–731.
3. Nicolson GL (2014). The Fluid—Mosaic Model of Membrane Structure: Still relevant to understanding the structure, function and dynamics of biological membranes after more than 40 years. Biochimica et Biophysica Acta (BBA) - Biomembranes 1838:1451–1466.
4. Devaiah SP, Roth MR, Baughman E, Li M, Tamura P, et al. (2006) Quantitative profiling of polar glycerolipid species from organs of wild-type Arabidopsis and a PHOSPHOLIPASE Dα1 knockout mutant. Phytochemistry 67:1907–1924.
5. Mosblech A, König S, Stenzel I, Grzeganek P, Feussner I, et al. (2008) Phosphoinositide and Inositolpolyphosphate Signalling in Defense Responses of Arabidopsis thaliana Challenged by Mechanical Wounding. Molecular Plant 1:249–261.
6. Furt F, Simon-Plas F, Mongrand S (2011) Lipids of the Plant Plasma Membrane. In The Plant Plasma Membrane, A.S. Murphy, B. Schulz, and W. Peer, eds. (Berlin, Heidelberg: Springer Berlin Heidelberg), pp. 3–30.
7. Balla T (2013) Phosphoinositides: Tiny Lipids With Giant Impact on Cell Regulation. Physiological Reviews 93:1019–1137.
8. Kay JG, Grinstein S (2013) Phosphatidylserine-Mediated Cellular Signaling. In Lipid-Mediated Protein Signaling, D. Capelluto, ed. (Springer, Dordrecht), pp. 177–193.
9. Sekereš, J, Pleskot, R, Pejchar, P, Žárský, V, and Potocky, M (2015). The song of lipids and proteins: dynamic lipid-protein interfaces in the regulation of plant cell polarity at different scales. Journal of Experimental Botany 66:1587–1598.

10. Noack, LC, and Jaillais, Y (2017). Precision targeting by phosphoinositides: how PIs direct endomembrane trafficking in plants. Current Opinion in Plant Biology 40:22–33.

11. Pokotylo, I, Kravets, V, Martinec, J, and Ruelland, E (2018). The phosphatidic acid paradox: Too many actions for one molecule class? Lessons from plants. Progress in Lipid Research 71:43–53.

12. Tanguy, E, Kassas, N, and Vitale, N (2018). Protein–Phospholipid Interaction Motifs: A Focus on Phosphatidic Acid. Biomolecules 8:20.

13. Vermeer, JEM, and Munnik, T (2010). Imaging Lipids in Living Plants. In Lipid Signaling in Plants, T. Munnik, ed. (Berlin, Heidelberg: Springer Berlin Heidelberg), pp. 185–199.

14. Platre, MP, and Jaillais, Y (2016). Guidelines for the Use of Protein Domains in Acidic Phospholipid Imaging. In Lipid Signaling Protocols, M.G. Waugh, ed. (New York, NY: Springer New York), pp. 175–194.

15. Várnai, P, Gulyás, G, Tóth, DJ, Sohn, M, Sengupta, N, et al. (2017). Quantifying lipid changes in various membrane compartments using lipid binding protein domains. Cell Calcium 64:72–82.

16. Vermeer, JEM, Thole, JM, Goedhart, J, Nielsen, E, Munnik, T, et al. (2009). Imaging phosphatidylinositol 4-phosphate dynamics in living plant cells. The Plant Journal 57:356–372.

17. Simon, MLA, Platre, MP, Assil, S, van Wijk, R, Chen, WY, et al. (2014). A multi-colour/multi-affinity marker set to visualize phosphoinositide dynamics in Arabidopsis. The Plant Journal 77:322–337.

18. Simon, MLA, Platre, MP, Marquès-Bueno, MM, Armengot, L, Stanislas, T, et al. (2016). A PtdIns(4)P-driven electrostatic field controls cell membrane identity and signalling in plants. Nature Plants 2:16089.

19. Kost, B, Lemichez, E, Spielhofer, P, Hong, Y, Tolias, K, et al. (1999). Rac Homologues and Compartmentalized Phosphatidylinositol 4, 5-Bisphosphate Act in a Common Pathway to Regulate Polar Pollen Tube Growth. The Journal of Cell Biology 145:317–330.

20. van Leeuwen, W, Vermeer, JEM, Gadella, TWJ, and Munnik, T (2007). Visualization of phosphatidylinositol 4,5-bisphosphate in the plasma membrane of suspension-cultured tobacco BY-2 cells and whole Arabidopsis seedlings. The Plant Journal 52:1014–1026.

21. Potocký, M, Pleskot, R, Pejchar, P, Vitale, N, Kost, B, et al. (2014). Live-cell imaging of phosphatidic acid dynamics in pollen tubes visualized by Spo20p-derived biosensor. New Phytologist 203:483–494.

22. Platre, MP, Noack, LC, Doumane, M, Bayle, V, Simon, MLA, et al. (2018). A Combinatorial Lipid Code Shapes the Electrostatic Landscape of Plant Endomembranes. Developmental Cell 45:465-480.

23. Heilmann, I (2016). Phosphoinositide signaling in plant development. Development 143:2044–2055.

24. Yao, H-Y, and Xue, H-W (2018) Phosphatidic acid (PA) plays key roles regulating plant development and stress responses. Journal of Integrative Plant Biology in press, doi:10.1111/jipb.12655

25. Idevall-Hagren, O, and De Camilli, P (2015). Detection and manipulation of phosphoinositides. Biochimica et Biophysica Acta (BBA) - Molecular and Cell Biology of Lipids 1851:736–745.

26. Pu, M., Orr, A., Redfield, A.G., and Roberts, M.F. (2010). Defining Specific Lipid Binding Sites for a Peripheral Membrane Protein in Situ Using Subtesla Field-cycling NMR. Journal of Biological Chemistry 285, 26916–26922.

27. Pleskot, R., Cwiklik, L., Jungwirth, P., Žárský, V., and Potocký, M. (2015). Membrane targeting of the yeast exocyst complex. Biochimica et Biophysica Acta (BBA) - Biomembranes 1848, 1481–1489.

28. Schindelin, J, Arganda-Carreras, I, Frise, E, Kaynig, V, Longair, M, et al. (2012). Fiji: an open-source platform for biological-image analysis. Nature Methods 9:676–682.

29. Schneider, CA, Rasband, WS, and Eliceiri, KW (2012). NIH Image to ImageJ: 25 years of image analysis. Nature Methods 9:671–675.

30. Sekereš, J, Pejchar, P, Šantrůček, J, Vukašinović, N, Žárský, V, et al. (2017). Analysis of Exocyst Subunit EXO70 Family Reveals Distinct Membrane Polar Domains in Tobacco Pollen Tubes. Plant Physiology 173:1659–1675.

31. Gronnier, J., Crowet, J.-M., Habenstein, B., Nasir, M.N., Bayle, V., et al. (2017). Structural basis for plant plasma membrane protein dynamics and organization into functional nanodomains. eLife, e26404.

Figure legends

Figure 1. Elevation of PI4,5P$_2$ levels by the overexpression of the CFP-tagged PI4P-5 kinase (PI4P5K) results in increased NtSEC3a:YFP recruitment to the plasma membrane in tobacco pollen tubes. Pollen tubes with comparably low expression level of NtSEC3a:YFP were selected. For co-expression with PI4P5K, cells expressing high levels of PI4P5K:CFP (not shown) and displaying characteristic PI4PK5-overexpression phenotype were selected. White dashed lines mark the site of intensity profiles and yellow dotted lines indicate length of the membrane fluorescence signal. Micrographs are shown using a color intensity code in order to display local enrichment of the YFP fluorescence. See Sekereš et al. (2017) for more details.

Figure 2. Organelle-targeted phosphatase as a way to locally interfere with acidic phospholipids. a) The top panel represents a schematic representation of a possible construct for organelle-specific targeting of a lipid modifying enzyme. Such system include an organelle-specific targeting anchor/protein (which may be at the N- or C-terminal end of the synthetic chimeric protein), a fluorescent protein to verify localization specificity, and the isolated catalytic domain of a lipid modifying enzyme. An important criteria for the use of the catalytic domain is that it should be free of any endogenous targeting capacity. The bottom panel represent an example of construct for the specific depletion of PI4P at the plasma membrane (i.e. MP-Sac1). b) Schematic representation of MP-Sac1 action at the PM but not endosome and c) effect of MP-Sac1 on PI4P accumulation. In the control condition (left, for example with expression of a catalytically dead MP-Sac1 enzyme), there is much more PI4P at the PM than in endosomes and as a result, a PI4P biosensor such as P4M is localized preferentially at the PM. Upon expression of MP-Sac1 (right), the pool of PI4P at the PM is reduced, which triggers the redistribution of the P4M PI4P sensor to both PM and endosomes.

Figure 1.

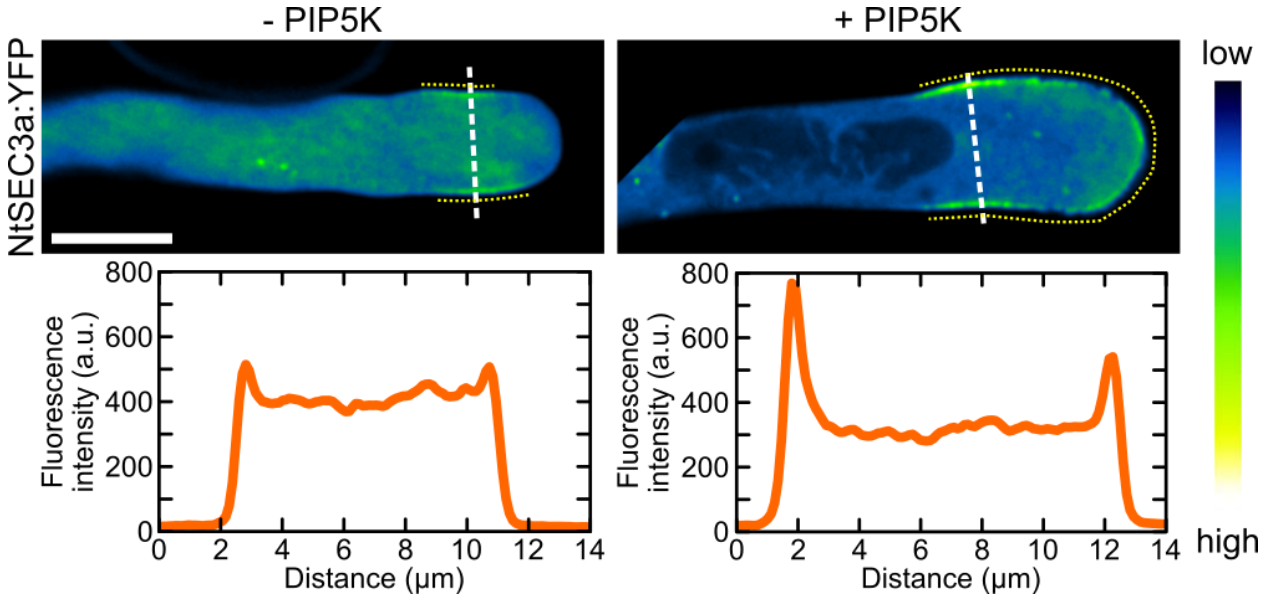

Figure 2

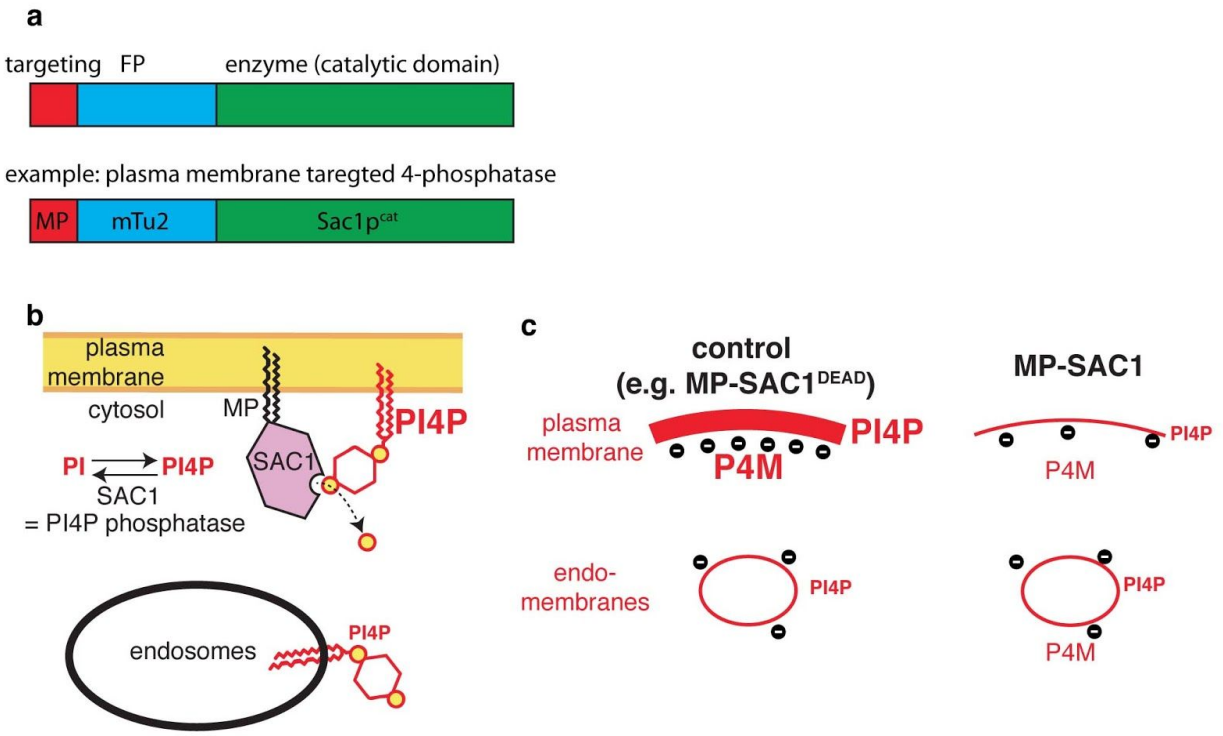

Platre MP, Noack LC, Doumane M, Bayle V, Simon MLA, Maneta-Peyret L, Fouillen L, Stanislas T, Armengot L, Pejchar P, Caillaud MC, Potocký M, Čopič A, Moreau P, Jaillais Y. A Combinatorial Lipid Code Shapes the Electrostatic Landscape of Plant Endomembranes. Dev Cell. 2018 May 21;45(4):465-480.e11. doi: 10.1016/j.devcel.2018.04.011. Epub 2018 May 10. PMID: 29754803.

https://doi.org/10.1016/j.devcel.2018.04.011